1-1-2012

From Bacteria to Human: Biophysical Studies of Inward Rectifying Potassium Channels

Wayland Cheng
Washington University in St. Louis

WASHINGTON UNIVERSITY IN ST. LOUIS

Division of Biology and Biomedical Sciences

Molecular Cell Biology

Dissertation Examination Committee:
Colin Nichols, Chair
Jianmin Cui
Alex Evers
Katherine Henzler-Wildman
Christopher Lingle
Joe Henry Steinbach

From Bacteria to Human: Biophysical Studies of Inward Rectifying Potassium Channels

by

Wayland Wing-Lun Cheng

A dissertation presented to the
Graduate School of Arts and Sciences
of Washington University in
partial fulfillment of the
requirements for the degree
of Doctor of Philosophy

May 2012

Saint Louis, Missouri

ABSTRACT OF THE DISSERTATION

From Bacteria to Human: Biophysical Studies of Inward Rectifying Potassium Channels

by

Wayland Wing-Lun Cheng

Doctor of Philosophy in Biology and Biomedical Sciences

Molecular Cell Biology

Washington University in St. Louis, 2012

Professor Colin Nichols, Chairperson

Inward rectifying potassium (Kir) channels are important in regulating cellular excitability in organs such as the heart, brain and pancreas. Prokaryotic KirBac channels are structurally similar to eukaryotic Kir channels, but distantly related and of unknown function. The goal of this thesis has been to investigate the functional properties of KirBac1.1 and to relate these findings to eukaryotic Kir channels. The approach was to use recombinantly-expressed, purified K^+ channels—KirBac1.1, KcsA, Kir2.1 and Kir2.2—in order to integrate findings from functional studies, using liposomal flux assays and patch-clamping, with high-resolution crystal structures. By reconstituting KirBac1.1 into giant liposomes for patch-clamping, I show that this channel is an inward rectifier, sensitive to spermine block when a pore-lining residue, 138, is mutated to an aspartate. However, unlike eukaryotic Kir channels, KirBac1.1 is inhibited by PIP_2 and single channel currents exhibit multiple conductance states. These findings inform the use of KirBac1.1 as a structural model for eukaryotic Kir channels. A general feature of Kir channels is that K^+-selectivity is dependent on the integrity of a highly conserved salt

bridge behind the selectivity filter. To explore the role of this interaction further, I examined the prokaryotic K^+ channel, KcsA, and found that the E71A mutation, which disrupts an equivalent molecular interaction, reduces K^+-selectivity by maintaining a conductive selectivity filter in the presence of Na^+ and absence of K^+. By reconstituting purified KirBac1.1 and human Kir2.1 and Kir2.2 proteins into liposomes, I definitively and quantitatively show that PIP_2 directly regulates human in addition to bacterial Kir channels. These findings demonstrate an absolute requirement of Kir2.1 and Kir2.2 activity for PIP_2 as well as a non-specific secondary requirement for anionic phospholipids. The secondary requirement represents a distinct mode of lipid regulation implying that phosphatidylinositol phosphates (PIPs) can have dual regulatory effects on channel activity. Comparing functional properties of bacterial and human inward rectifying potassium channels not only informs the structural basis of these properties but raises new hypotheses about how these properties may have evolved.

ACKNOWLEDGEMENTS

I would like to acknowledge my wife, Sherah, and my parents, Daniel and Christina, for their unconditional love and support. I am grateful to Colin Nichols for his mentorship and his diligence in teaching me about scientific thinking and writing. I am also indebted to Decha Enkvetchakul, Nazzareno D'Avanzo, and Shizhen Wang for helpful discussions and critical reading of this dissertation.

For their contributions to the work reported in this dissertation, I would like to acknowledge Decha Enkvetchakul for identifying the I131C/I138D mutant and its sensitivity to spermine by flux assay, Jason McCoy for determining the crystal structure of KcsA [E71A] in Na^+, Ameer Thompson for lipid bilayer recordings of Na^+ block in KcsA [E71A], Crina Nimigean for aid in writing the KcsA [E71A] manuscript, and Nazzareno D'Avanzo for determining the expression and purification protocol of Kir2.1 and Kir2.2 and equal contribution in characterizing the lipid dependence of activity for these channels.

Finally, I would like to acknowledge the American Heart Association for granting me a pre-doctoral fellowship for two years (0810196Z).

TABLE OF CONTENTS

LIST OF TABLES AND FIGURES

CHAPTER 1

INTRODUCTION AND BACKGROUND

I. INWARD RECTIFYING POTASSIUM CHANNELS: FUNCTION AND STRUCTURE

Potassium (K^+) channels are membrane proteins that form selective pores for conduction of K^+ ions across cell membranes. At cellular ionic conditions (high intracellular K^+, low extracellular K^+), the reversal potential of K^+ is very negative (~ -70 mV) making K^+ currents the primary repolarizing force in most excitable cells. The basic pore structure of all K^+ channels consists of a four-fold assembly of a P-loop (pore helix and selectivity filter) and two transmembrane (TM) helices (1). Unlike voltage-gated K^+ channels, most of which are comprised of the 2TM/P-loop pore-forming structure and a 4-TM voltage sensor, and unlike 2P K^+ channels, which are a dimer of two P-loops with four transmembrane domains, inward rectifying K^+ (Kir) channels are composed of the basic 2TM/P-loop pore-forming structure with a large cytoplasmic domain (1). The focus of this dissertation is on the functional properties of Kir channels, as well as a prokaryotic K^+ channel, KcsA, which is also a 2-TM K^+ channel.

IA. PHYSIOLOGICAL ROLES OF KIR CHANNELS

Mammalian Kir channels are a family of 16 K^+-selective channels, grouped into 7 subfamilies (i.e. KirX.Y, where X denotes the subfamily), that play many physiological roles in organs such as the heart, pancreas, brain, kidney and skeletal muscle (2-5). Kir2.x

(six members) and heterotetramers of Kir3.1 and Kir3.4 make up the predominant inward rectifier currents in the heart (I_{K1} and I_{KAch}, respectively), and function in maintaining the resting membrane potential, repolarizing of the action potential and regulating heart rate (6). The K_{ATP} channel, which is composed of the pore-forming subunit Kir6.2 and the accessory subunit SUR and is inhibited by ATP, is actually the most highly expressed inward rectifier in the heart but is minimally open in normal physiological conditions, and its exact role in cardiac physiology remains unclear (7). In the pancreas, however, Kir6.2 plays a critical role in regulating insulin secretion by responding to the metabolic state of the β cell (8).

The physiological roles of Kir channels have become particularly apparent with the identification Kir channelopathies; monogenic diseases that result in gain- or loss-of-function (GOF or LOF) of channel activity and often present as a syndrome. LOF mutations in Kir1.1 result in Bartter's syndrome, a renal tubular disorder that presents with hypokalemia and metabolic alkalosis (9); LOF mutations in Kir2.1 result in Anderson-Tawil syndrome, which presents with ventricular arrhythmias (long QT syndrome 7) and physical deformities such as micrognathia (10); and GOF mutations in Kir6.2 result in DEND syndrome, which presents with developmental delay, muscle weakness, epilepsy and neonatal diabetes (11). These monogenic diseases not only highlight the physiological roles of these channels; the mutations also provide structural insights into channel function and regulation. Many Anderson-Tawil mutations have been proposed to disrupt PIP_2 activation of Kir2.1 by altering the lipid binding site (12), and DEND mutations shift the ATP sensitivity of inhibition in Kir6.2 by disrupting ATP

binding or transduction (13, 14). Thus, an understanding of the structural determinants of Kir channel function is relevant to physiology and disease. Mutagenesis and molecular modeling studies of Kir channels have made significant advances in understanding their pore and gating properties since the first high resolution crystal structures of K^+ channels were solved (15, 16). Next, I will introduce two prokaryotic potassium channels, since their crystal structures serve as important models for inward rectifiers and K^+ channels in general.

IB. KCSA: STRUCTURE OF A K^+ CHANNEL

KcsA is a prokaryotic K^+ channel identified in *Streptomyces lividans*. It has highest sequence identity to voltage-gated K^+ channels such as Shaker channels (64% for P-loop and 23% for TM1 for ShC1), and poorer identity to inward rectifiers (40% for P-loop and 14% for TM1 for ROMK1) (17). This prokaryotic membrane protein is a functional K^+-selective channel that is activated by low pH and exhibits a pH-dependent inactivation (18-20). In 1998, a crystal structure of KcsA was solved at a resolution of 3.2 Å, marking the first high resolution structure of a recombinantly expressed alpha-helical membrane protein (15). The structure, which was a truncated transmembrane-only construct of KcsA, provided vivid confirmation and new insights into decades of structure-function and modeling studies (21, 22). The structure revealed a tetrameric assembly surrounding an asymmetric pore with a narrow selectivity filter on the extracellular end and a wide aqueous pore on the intracellular end (Figure 1.1A and 1.1B). Each subunit is composed of two transmembrane helices (TM1 and TM2), and the

P-loop consisting of a tilted re-entrant helix (pore helix) that spans half the membrane on the extracellular side and the selectivity filter (Figure 1.1A). In the selectivity filter, formed by the K^+ channel signature sequence, TXGYG, the backbone carbonyls face the pore forming a series of four binding/coordination sites (S1-S4 from outside to inside) for dehydrated K^+ ions, and the side chains interact with aromatic and charged amino acids behind the filter to maintain its structural integrity (23) (Figure 1.1C). The narrow selectivity filter represents the catalytic site of the channel where ion selectivity is achieved (24) by the structure and chemistry of the coordinating ligands, and rapid conduction is achieved by single file multi-ion occupancy of the binding sites (25) (see IIIA: selectivity filter).

Intracellular to the selectivity filter, the conducting pore opens into a 10 Å aqueous inner cavity that is lined by hydrophobic side chains from TM2 and is just below the C-terminal end of the pore helix. K^+ ions remain hydrated in this cavity and are stabilized by the negative electrostatic potential from the pore helix dipole such that the transmembrane electric field remains low in the cavity and is focused in the short 12 Å selectivity filter (15, 26, 27). The inner transmembrane helices (TM2) are tilted 25^o to the normal and the bottom of these helices form an occlusion to the permeation path called the “bundle crossing” such that the overall shape of KcsA is an “inverted tepee” (Figure 1.1A). The bundle crossing and the selectivity filter are thought to represent two gates for the channel (28): the bundle crossing forms the ligand- or pH-dependent gate (29, 30) and the selectivity filter forms the inactivation gate (20).

KcsA is considered the archetype of K^+ channel structure and has been a robust model channel to study using functional, biochemical, crystallographic and computational modeling techniques. Homology models of Kir channels have been made using the KcsA structure (31, 32), and while these may approximate the transmembrane region of Kir channels, they are missing the cytoplasmic domain, which plays an important role in ligand-mediated gating and the voltage-dependence of block by polyamines (see II: inward rectification). Furthermore, there are notable differences between the transmembrane regions of KcsA and Kir channels. Using yeast genetic screens of mutant Kir2.1 channels, Minor et al correctly identified, before any high resolution structures, that the transmembrane helices of Kir channels are arranged differently from KcsA. In Kir channels, TM1 interacts with two TM2 helices from the same and adjacent subunits (Figure 1.2B), whereas in KcsA, TM1 interacts only with TM2 of the same subunit (33) (Figure 1.1B). The P-region and especially the structure of the extracellular turret is also likely to be different since, just like voltage-gated K^+ channels (34), a mutant of KcsA is sensitive to the scorpion toxin, agitoxin2 (35), which binds at the extracellular entrance, but Kir channels do not show the same sensitivity to agitoxin2 and related peptide toxins (36).

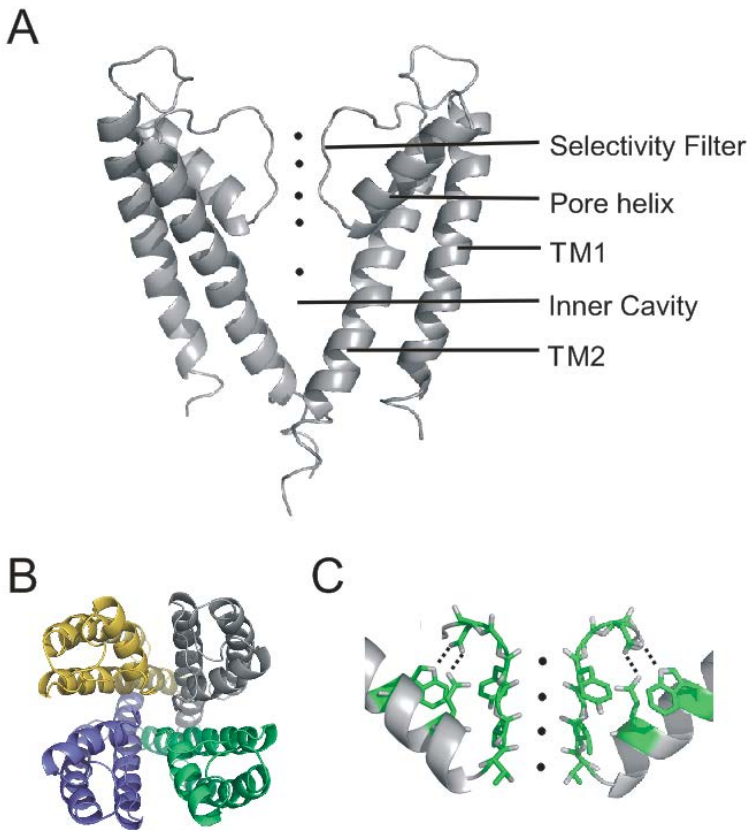

Figure 1.1: Structures of the transmembrane domain of the KcsA K^+ channel. (A) Two out of four subunits from a 3.2 Å crystal structure of KcsA (1BL8). Black dots represent K^+ ions: four in the selectivity filter and one in the inner cavity. TM1 and TM2 are the two transmembrane helices. The bottom of TM2, called the "bundle crossing", forms a steric occlusion of the pore. (B) Structure of KcsA (1BL8) viewed from the extracellular side showing four symmetrical subunits surrounding a central pore. TM1 (outer helix) makes contacts only with TM2 (pore-lining helix) of the same subunit. (C) Selectivity filter and pore helix from two out of four adjacent subunits of KcsA (1K4C). In the selectivity filter, four K^+ ions (black dots) are coordinated by backbone carbonyls (S1-S4) and the threonine side chains of T75 (S4). Behind the filter, polar and aromatic

side chains (shown are W67, E71, Y78 and D80) form important H-bond interactions (dotted lines) that maintain the structure of the selectivity filter.

IC. KIRBAC1.1: STRUCTURE AND FUNCTION

In 2001, a family of prokaryotic genes was identified based on sequence similarity to eukaryotic Kir channels (37). These genes products, called KirBacs, are unique in that they have sequences similar to the cytoplasmic domains of Kir channels. Still, there are many sequence differences between KirBacs and eukaryotic Kir proteins, and KirBacs are closer in primary sequence to Kv channels or KcsA in the P-loop and TM2 than to Kir channels (e.g. KirBacs have an aspartate after the filter consensus sequence, TVGYGD, like KcsA and unlike eukaryotic Kirs which have an arginine in that position which forms an important salt-bridge interaction). Kir7.1 is the closest match in sequence with KirBac1.1 and still shows only 28% sequence identity and 55% similarity (38). Thus, KirBacs are likely to be rather distant ancestral precursors to eukaryotic Kir channels (37).

In 2002, the cytoplasmic domain of Kir3.1 was solved at a resolution of 1.8 Å revealing a predominantly beta sheet structure that was predicted to extend the length of the channel pore to 60 Å (39). Soon after, the structure of full length KirBac1.1 was solved at 3.65 Å showing transmembrane and cytoplasmic domains similar to KcsA (except for the differences in helix packing and extracellular turret structure noted above) and Kir3.1 structures, respectively, and a pore length of 88 Å (16) (Figure 1.2A and 1.2B)—a long pore is thought to be an important structural feature of steep voltage-

dependent block (see II: inward rectification). The cytoplasmic domain is formed primarily by the C-terminus with a small contribution from the N-terminus. The transmembrane and cytoplasmic domains are linked by “flexible” linkers in both the N- and C-terminal ends, and the N-terminal linker is followed by a helix parallel to the membrane interface called the “slide helix” (Figure 1.2A). The slide helix and its interactions with the cytoplasmic domain and transmembrane helices were hypothesized to be involved in gating (16), and indeed, numerous slide helix mutations in different Kir channels have marked effects on gating (10, 40-42). Like KcsA, KirBac1.1 is in a closed state featuring a hydrophobic residue (F146) at the bundle crossing of TM2 that occludes the pore (Figure 1.2A). Unlike KcsA, the selectivity filter of KirBac1.1 shows only three K^+ ion densities (S1-S3) (Figure 1.2A), but how this relates to ion occupancy during conduction is unknown.

The structure of KirBac1.1 has now been used extensively as a model for eukaryotic Kir channels (43-45) and for molecular simulation studies of permeation and gating (46-51). However, the validity of these modeling studies depends on whether KirBac1.1 is a functional channel that behaves like an inward rectifier. Prior to the onset of this project, studies of recombinant, purified KirBac1.1 reconstituted in liposomes showed, using $^{86}Rb^+$ flux assay, that KirBac1.1 is a functional K^+-selective channel that is blocked by Ba^{2+} and inhibited by low pH (52)—features characteristic of Kir channels. However, while all Kir channels are activated by PIP_2, KirBac1.1 is potently inhibited by PIP_2 (53). Thus, functionally, there are similarities and at least one interesting difference between KirBac1.1 and eukaryotic Kir channels, and many other functional features such

as polyamine sensitivity remained uncharacterized in this prokaryotic channel at the onset of this work.

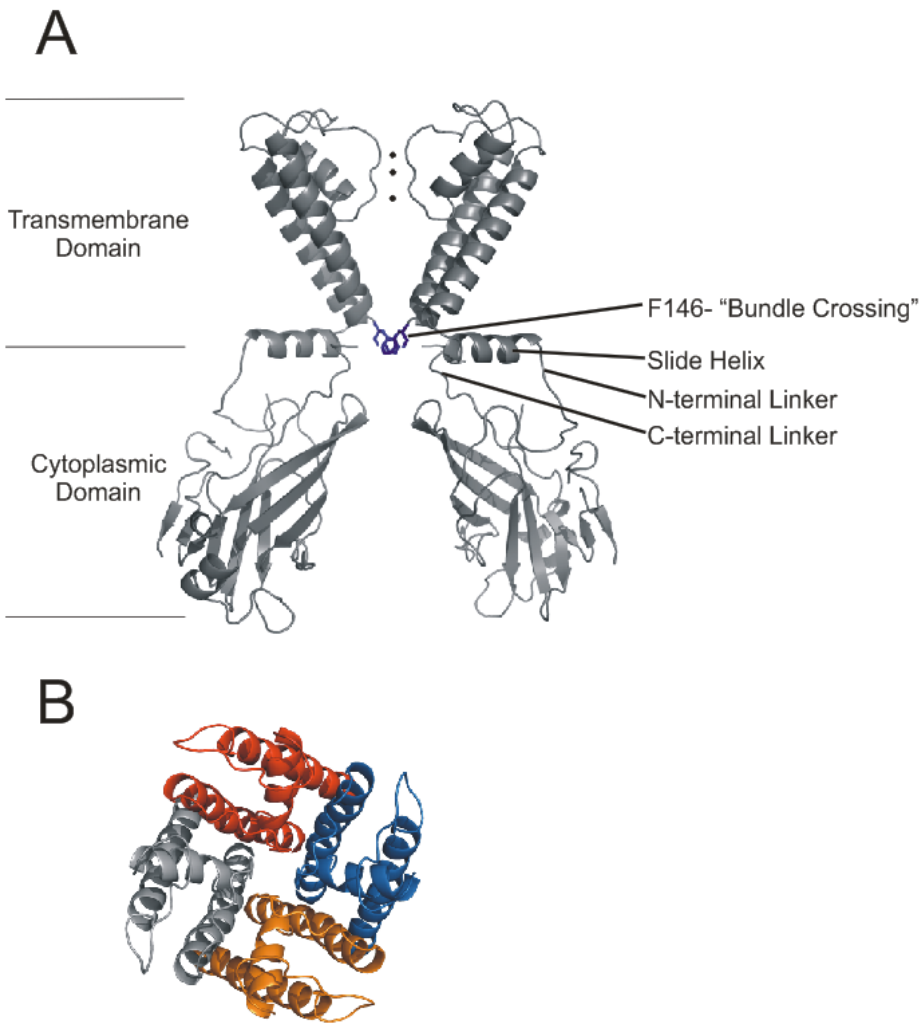

Figure 1.2: Crystal structure of KirBac1.1. (A) Two out of four subunits from the 3.65 Å structure of KirBac1.1 (1P7B) showing the transmembrane and cytoplasmic domains. For clarity of the central pore, the transmembrane domains are from two subunits and cytoplasmic domains from the other two subunits. F146 forms the "bundle crossing" at the bottom of TM2 that occludes the pore. Three K^+ ion densities (black dots) are located in the selectivity filter. (B) Structure of KirBac1.1 (1P7B) viewed from the extracellular side showing four symmetrical subunits surrounding a central pore. TM1 (outer helix)

makes contacts with TM2 (pore-lining) helices of both the same subunit and adjacent subunit.

ID. OTHER KIRBAC AND KIR CHANNEL STRUCTURES

In addition to KirBac1.1, the structure of three other full length KirBac or Kir channels have been reported during the course of this project including a Kir3.1-KirBac1.3 chimera (54), KirBac3.1 (55), and chicken Kir2.2 (56). These structures provide additional insight into the structure and function of Kir channels. For the Kir3.1-KirBac1.3 chimera, two different structures have been solved, revealing a “dilated” and “constricted” conformation at the G-loop (54), which is a second constriction below the bundle crossing formed by a cytoplasmic loop and originally identified in Kir2.1 (57). These conformations have been taken as suggestive that the G-loop may form a functionally relevant gate in Kir channels (54). The chimera structures also show a detergent-like density bound to the intracellular interface, which is perhaps indicative of a lipid binding site in Kir channels (54) (see IVC. PIP_2 binding site in Kir channels). For KirBac3.1, a series of structures reveal subtle but correlated changes between the structure of cytoplasmic domain and the position of ion densities in the selectivity filter (55). These findings have led to speculations that gating in the intracellular side of the channel (bundle crossing or G-loop) is coupled to gating at the selectivity filter (55). The structure of Kir2.2 shows a large extracellular turret, quite distinct from KcsA or KirBac channels, that may explain why Kir channels are relatively insensitive to scorpion toxins (56). Both the Kir2.2 and Kir3.1-KirBac1.3 chimera structures show multiple ion densities, not only in the selectivity filter and inner cavity, but also in the cytoplasmic pore, leading the authors to suggest that displacement of these ions by polyamines

underlies the steep voltage-dependence of rectification in Kir channels (56) (see IIB: Voltage-dependence of polyamine block).

IE. DEVELOPMENT OF THESIS

Until the structure of chicken Kir2.2 was solved in 2009, only structures of KcsA and KirBac channels were available as structural models of eukaryotic Kir channels. At the onset of my thesis work, very little was known about the function of KirBac1.1—particularly, whether it behaves as an inward rectifier. To address this problem, I developed the technique to reconstitute KirBac1.1 in giant liposomes for voltage-clamp analysis and determined that KirBac1.1 currents exhibit strong inward rectification and are K^+-selective (Chapter 3). In eukaryotic Kir channels, disruption of a putative salt bridge behind the selectivity filter invariably reduces K^+-selectivity. Since the KirBac1.1 structure shows a H-bond interaction (E106-D115) at the equivalent position, I tested the effects of this interaction on K^+-selectivity. Preliminary experiments in KirBac1.1 indicated that the E106A mutation has no effect on selectivity, but that the equivalent mutation in KcsA, E71A, profoundly affects selective permeation of Na^+. This led me to investigate the mechanism by which E71A reduces selectivity in KcsA (Chapter 4). By reconstituting KirBac1.1 in liposomes, lipid regulation of channel activity can be studied quantitatively in a pure system. Having shown that PIP_2 directly inhibits KirBac1.1, I also reconstituted human Kir2.1 and Kir2.2 to characterize the lipid dependence of activity for these channels. Since all eukaryotic Kir channels are activated by PIP_2, I began by assessing the effects of various phospholipid headgroups on channel function

(Chapter 5). Before presenting the results of these studies, I will first review the current understanding for the molecular basis of inward rectification, K^+-selectivity, and phospholipid regulation of Kir channels.

II. INWARD RECTIFICATION

Inward rectification describes a conduction phenomenon in Kir channels where the flow of K^+ ions is greater in the inward direction than in the outward direction. It was originally called "anomalous" rectification because rectification is in the opposite direction to that predicted by electrodiffusion given the K^+ concentration gradient in cells (58) (Figure 1.3A). The physiological relevance of strong inward rectification is most apparent in the heart, where Kir2.x channels (IK1) maintain the cardiac resting membrane potential and contribute to repolarization at the end of the action potential, but are blocked during the depolarized plateau phase of the action potential (6). The voltage-dependence of conductance in Kir channels can be described by fitting the distribution of non-conductive to conductive channels (current or conductance in the presence of blocker relative to control, G_{rel}) versus voltage (ΔV) with a Boltzmann function:

$$G_{rel} = \frac{A}{1 + e^{(F/RT)\cdot\delta z\cdot(\Delta V - V_{1/2})}}$$

where A is amplitude, δz or equivalent valence is the product of the effective charge of the blocker and the relative distance traversed by the blocker through the electric field, ΔV is the voltage difference between membrane voltage and E_K, $V_{1/2}$ is the voltage of half-maximal current (relative conductance), and F, R and T have their usual meanings.

Fitting this distribution for strong inward rectifiers yields a high δz of ~4-5 for the steepest component of rectification, similar to voltage-dependent gating of outward rectifying K^+ channels (1, 59) (Figure 1.3A). However, unlike outward rectifying currents, the current-voltage relationship of inward rectifier currents shifts to more positive voltages with increasing $[K^+]_{ext}$: $V_{1/2}$ (voltage of half-maximal current) shifts in parallel with E_K (equilibrium potential for K^+) (60) (Figure 1.3A). Also, increasing $[K^+]_{ext}$ speeds up the rate of "activation" when pulsing from positive to negative voltages (61). The $[K]_{ext}$-dependence of $V_{1/2}$ and rate of "activation" effect suggests that inward rectification is due to intracellular voltage-dependent block of the channel, as increasing extracellular K^+ might displace or "knock-off" the blocking cation (62). Indeed, intracellular Mg^{2+} blocks Kir channels (63, 64), but a steeply-voltage dependent inward rectification remains in Kir currents even after removal of Mg^{2+} ions that cannot be accounted for by other mono or divalent cations (65-67). The molecular basis of strong inward rectification was subsequently shown to be due to intracellular block by polyamines such as spermine, spermidine and putrescine (68-69)(68-70). Since this discovery, two questions have predominated in the field: 1) what are the structural determinants or the binding site(s) of polyamines in the Kir channel pore and 2) what is the mechanism of the steep voltage dependence of block?

IIA. STRUCTURAL DETERMINANTS OF POLYAMINE BLOCK

Not all inward rectifiers are equally sensitive to block by Mg^{2+} and polyamines—those that are relatively insensitive, weak inward rectifiers, include Kir1.1 (ROMK) and

Kir6.2 (KATP). Strong inward rectifiers include Kir2.1 (IRK1) and Kir3.1 (GIRK- the G-protein coupled Kir channel). All strong inward rectifiers have a negatively-charged pore-lining aspartate in the inner cavity whereas the equivalent residue in weak inward rectifiers is neutral (e.g. D172 in Kir2.1 and N160 in Kir6.2) (Figure 1.3B). Mutation of this residue in weak inward rectifiers to an aspartate or glutamate (i.e. N171D in Kir1.1 and N160D in Kir6.2) confers strong inward rectification as seen by voltage dependent block by Mg^{2+} or spermine (71, 72). Mutations to neutral or positively-charged residues do not have the same effect suggesting that this residue interacts with blockers by an electrostatic interaction (71). This pore-lining residue has been called the "rectification controller" residue, and its position in the inner cavity defines the general region of the polyamine binding site (Figure 1.3B). The rectification controller, however, does not constitute the whole story of polyamine block, since mutations of D172 in Kir2.1, which is the archetypal inward rectifier, to a neutral residue do not entirely abolish inward rectification (73). Furthermore, diamines of different chain length block Kir2.1 and longer diamines block with higher efficacy, suggesting that hydrophobic interactions also play an important role in blocker interactions with the pore (73, 74).

The first descriptions of polyamine block of Kir channels found that the extent of block at steady state versus voltage shows two components: a low affinity component with shallow voltage dependence (δz ~0.4) and a high affinity component with steep voltage dependence (δz ~4-5) (59, 75). Several models have been proposed to account for this observation including two polyamines in the pore (59), two independent polyamine binding sites (75), or two sequential binding sites (59, 76). A careful account of the

current data suggests that the shallow and steep voltage-dependent components of block result from two sequential binding sites: an outer site mediated by acidic residues in the cytoplasmic pore and a deep site further in the pore (76-78). Charge screening of acidic residues in the cytoplasmic pore of Kir2.1 (E224, D255, D259, and E299; Figure 1.3B) (57) by polyamines reduces single channel conductance, which can account for the low affinity, shallow voltage-dependent component of block (76). Neutralizing these residues reduces the shallow component of block and slows the kinetics of block (76, 79). The contributions of these residues to the deep polyamine binding site(s), however, has been controversial. Mutations of E224 and E299, along with the "rectification controller" residue, D172, have been reported to reduce the affinity and voltage-dependence of the steep component of block (80, 81), but mutations of the more outer/intracellular residues, D255 and D259, do not (79) (Figure 1.3B). Mutating the equivalent of E224 in the weak inward rectifier, Kir1.1 (G223E), does not affect polyamine sensitivity, but substituting the entire C-terminus of Kir1.1 with that of Kir2.1 does confer strong inward rectification (82, 83). Thus, although there is general agreement that the shallow polyamine binding site is at the outer cytoplasmic pore, the exact location of the deep binding site has remained the subject of continued controversy.

Two contrasting locations have been proposed for the deep polyamine binding site. One proposal is that polyamines such as spermine bind with the tail amine anchored at the level of the bundle crossing (M183) interacting with acidic residues in the cytoplasmic pore (E224 and E299), and the leading amine at the rectification controller position (D172 in Kir2.1) (73, 78, 84) (Figure 1.3C). This hypothesis is based on the

effect of mutating these key residues on the affinity and voltage-dependence of block by diamines of varying length (85). For example, the double mutant, E224G/E299S, reduces the affinity of diamines equally at all lengths, whereas the D172N mutation reduces the affinity of longer diamines more than shorter ones, which could be consistent with the idea that the tail amine of these blockers interact with E224/E299 and longer blockers stretch up towards D172 (73).

An alternative proposal for the polyamine binding site is that the tail amine binds at the rectification controller position and the polyamine stretches up to the selectivity filter (Figure 1.3C). In the weak rectifier, Kir6.2, introduction of glutamate to any pore-lining position in the inner cavity confers strong inward rectification. The efficacy of block is enhanced for shorter diamines when the glutamate is nearer to the selectivity filter and for longer diamines when the glutamate is nearer to the bundle crossing, consistent with the diamine binding above the rectification controller residue (N160) (77). Furthermore, when these same pore-lining residues are mutated to cysteine in the polyamine-sensitive mutant, Kir6.2[N160D], or strong inward rectifier, Kir2.1, modification of residues above the rectification controller position by MTS reagents reduces the efficacy and voltage-dependence of polyamine block, whereas modification of residues below the rectification controller slows polyamine unblock without affecting efficacy (86-88). Similarly, polyamine block in Kir2.1 prevents MTS modification of residues above the rectification controller residue, but only slows modification of residues below (89). These studies provide uncontested evidence that the deep site of polyamine block is above the rectification controller in strong and weak inward rectifiers.

The conflicting conclusions of Lu colleagues may have resulted from the complications of interpreting the effects of mutating key charged residues in the pore (e.g. D172N), which may substantially alter blocking behavior and perhaps shift the blocking site. Indeed, modeling studies suggest that charged or polar residues up make significant contributions to the electrostatic free energy of K^+ ion and blocker interactions up to 40 Å away from the relevant regions of the pore (51). Thus, neutralization of basic residues in the inner cytoplasmic pore of Kir2.1, such as E224, are predicted to have a significant destabilizing effect on cations in the inner cavity (51).

IIB. VOLTAGE DEPENDENCE OF POLYAMINE BLOCK

Voltage dependence of block was first described by Woodhull as resulting from movement of the charged blocker across the electric field in the membrane (i.e. the blocker binding site is located in the electric field) (90). Using a Boltzmann function to describe the distribution of blocked and unblocked channels, the voltage-dependence of block is reported as δz (i.e. the product of the electrical distance of the binding site and the charge of the blocker). Polyamine block of Kir channels exhibits steep voltage dependence (δz ~4-5). The fact that δz exceeds the charge of the blocker cannot be reconciled with the simple Woodhull model, but can be explained by displacement of K^+ ions by the blocker in a multi-ion pore (1, 91). Indeed, the equivalent valence of block by diamines in Kir2.1 increases with increasing length of the blocker (from ~1.5 for 2 methylene groups to ~5 for 10 methylene groups), suggesting that these blockers displace K^+ ions across the electric field with longer diamines being more effective (73, 74).

Furthermore, the equivalent valence of block by quaternary ammonium ions in Kir1.1 is highly dependent on intracellular and extracellular permeant ion concentrations, with larger δz at higher K^+ concentrations, suggesting that block is coupled to K^+ ion movement (92).

The long cytoplasmic pore revealed by the crystal structure of the Kir3.1 cytoplasmic domain led Nishida et al to hypothesize that a column of K^+ ions extending even in the cytoplasmic pore is pushed by polyamines to the extracellular solution (39). The exact location of the polyamine binding site is important in determining how polyamine block is coupled to K^+ ion movement. If polyamines bind below the rectification controller residue, then the charge of the blocker itself would not contribute to the valence of block (most of the electric field across the membrane is at the selectivity filter), and the high valence of block would mean strict displacement of at least five K^+ ions, without any "leak" (85), from the long and wide aqueous pore through the narrow selectivity filter. A recent crystal structure of the Kir3.1 cytoplasmic domain revealed five K^+ ion densities coordinated along the cytoplasmic pore axis by acidic residues, although the presence of five densities does not imply a total occupancy of five K^+ ions in these sites (85) (Figure 1.3D). Deletion of a potentially constrictive loop at the intracellular end of the pore significantly decreased δz (4.3 to 2.5), suggesting that this loop forms a "gasket" that prevents backflow of K^+ ions around the blocker (85) (Figure 1.3D). Such a mechanism need not be true if polyamines bind above the rectification controller residue near the selectivity filter where blocker would be more effective in displacing K^+ ions and may move partially through the electric field itself, depending on

how far it enters the filter. To better elucidate the mechanism of steeply voltage-dependent polyamine block, more structural and computational simulation studies are needed to clarify the distribution of K^+ ions in the pore, the distribution of the electric field in the pore, and the exact binding site of deep polyamine block. KirBac1.1 has been used as a structural model to simulate the binding of polyamines in a Kir channel pore (87), but it remains unknown whether the KirBac1.1 pore is even sensitive to block by polyamines. This problem provides the rationale for the experiments in Chapter 3.

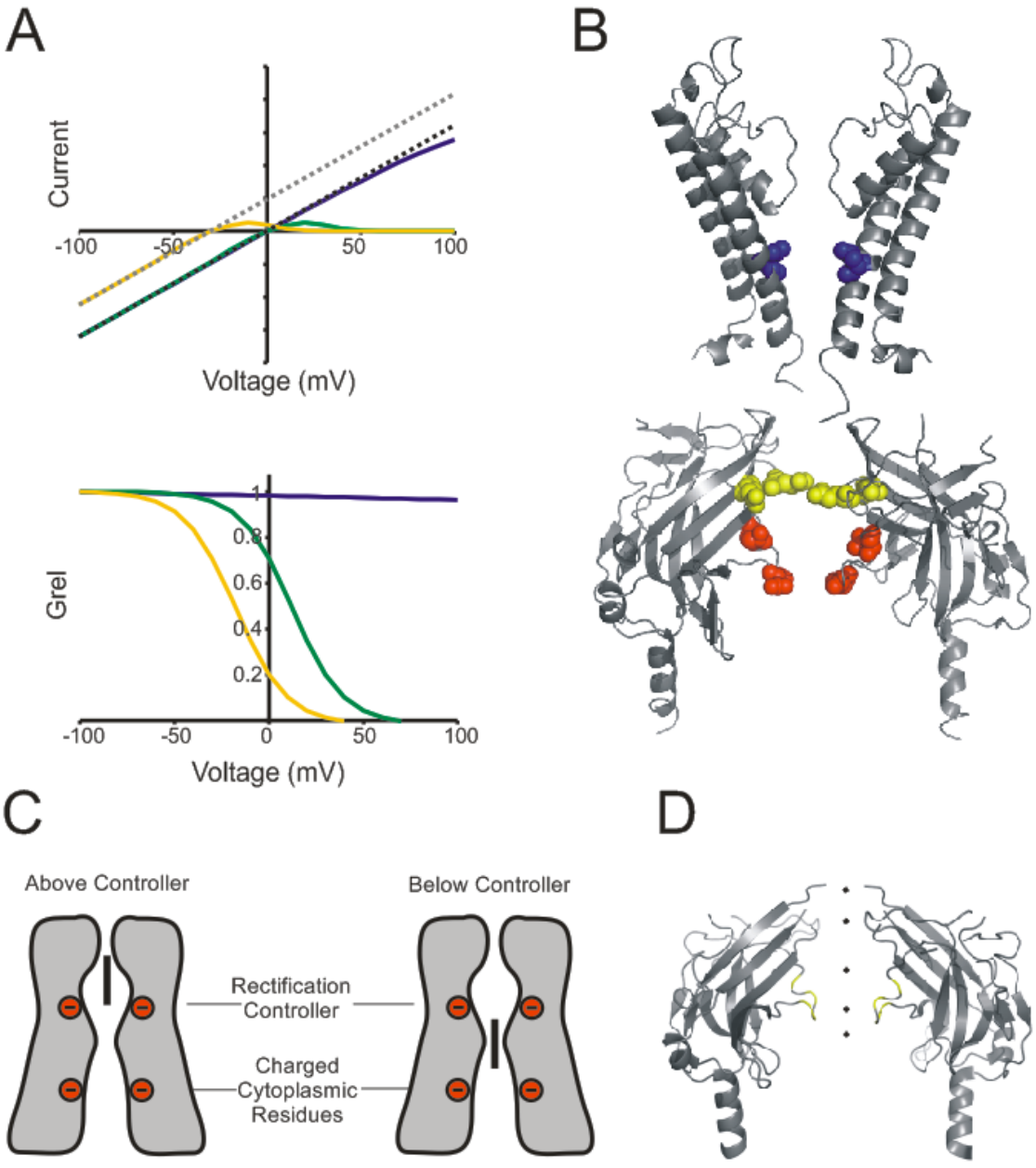

Figure 1.3: The structural basis of strong inward rectification. (A) *Top*: Hypothetical current-voltage plots showing strong (green) and weak inward rectification (blue) in symmetrical K^+. If the voltage dependence of block is steep, a negative slope conductance is often apparent in strong rectifiers (green). Yellow curve shows the effect

of a -30 mV shift in E_K (e.g. decrease in external K^+) on the voltage dependence of the strong rectifier I-V curve. The green and yellow curves illustrate a "crossover effect". When extracellular K^+ accumulates in the heart, this "cross-over" effect leads to an increase in Kir2.x (IK1) conductance and shortening of the action potential (93, 94). *Bottom*: Plot of relative conductance (Grel) versus voltage of the I-V curves above. These curves can be fit with a Boltzman equation to obtain $V_{1/2}$ and δz. (B) Kir2.2 crystal structure (3JYC) highlighting the equivalent Kir2.1 residues, D172 (blue), E224 and E299 (yellow), and D255 and D259 (red). (C) Cartoons diagramming two hypotheses for the deep polyamine binding site: above or below the rectification controller. Adapted from Kurata et al (86). (D) Kir3.1 cytoplasmic domain crystal structure (3K6N) showing five K^+ ion densities in the cytoplasmic pore. Yellow indicates the cytoplasmic loop thought to form a gasket against K^+ "leak".

III. SELECTIVITY IN POTASSIUM CHANNELS

Ion selectivity is a broad term that refers to differential permeation of ions such as K^+ over Na^+ through a channel. Selectivity can be defined experimentally in terms of several different measurements including permeability ratios from reversal potential measurements, conductance ratios, binding affinity determined by the concentration dependence of conductance or block, punch-through of impermeant/blocking ions, and heat of binding. Most of these measurements examine non-equilibrium phenomena (i.e. ion flux/permeation), except for blocker competition measurements (e.g. monitoring the K^+ or Na^+ dependence of Ba^{2+} block) (95, 96) or ionic binding measurements using isothermal titration calorimetry (97). Recently, many studies on the mechanism of K^+-selectivity have utilized K^+ channel crystal structures and full-atom molecular dynamics (MD) simulations. However, the microsecond time scale of ion permeation has made MD simulations of full permeation events prohibitive until recently (98), and most theoretical treatments have considered selectivity in terms of selective partitioning of ions from solution into the channel pore at equilibrium.

However it has been assessed, KcsA is at least 150-fold more selective for K^+ over Na^+ (19). Similar to other K^+ channels, KcsA is estimated to exhibit a free energy difference for binding K^+ over Na^+ of ~5-6 kcal/mol (personal communication from Miller and colleagues (96)). No Na^+ currents have yet been reported; however, Na^+ does enter the pore and block the channel with mM affinity showing fast “flicker” and slow blocking components as well as punch-through at high voltages (99).

IIIA. THE SELECTIVITY FILTER- COORDINATION BY CARBONYLS

The narrow 12 Å-long extracellular region of the pore in KcsA called the selectivity filter consists of four K^+ binding sites (S1-S4) coordinated by backbone carbonyls from the residues, TXGYG, that make up a signature sequence present in all K^+ channels (Figure 1.1A and 1.4A) (15). At high K^+ concentrations, each binding site has an occupancy of ~0.5 implying that 2 K^+ ions occupy the filter simultaneously, and molecular simulations suggest that the most favorable configurations are S1/S3 or S2/S4 (100, 101). This structural interpretation is consistent with decades of electrophysiological findings, which had suggested that K^+ channels consist of a single file multi-ion pore (91) with four K^+ binding sites (95, 96). The structure and occupancy of K^+ ions in the filter (100) also point to a "knock-on" mechanism for conduction, originally proposed by Hodgkin and Keynes (25). Using molecular dynamics free energy perturbation (MD FEP) calculations, Roux and colleagues show that rapid conduction is a consequence of the four K^+ binding sites being nearly energetically equivalent and is dependent on electrostatic repulsion from an incoming K^+ ion (101, 102) (Figure 1.4B). Simulations where K^+ is "alchemically" changed into Na^+ show that K^+ binding is favored over Na^+ with each coordination site showing different selectivity (102, 103). S2 is the most selective with a free energy difference between K^+ and Na^+ of ~6 kcal/mol consistent with experimental data (96), S1 and S3 show intermediate selectivity, and S4 is nearly non-selective (104).

How is this selectivity achieved? Because Na^+ is smaller than K^+, selectivity for K^+ over Na^+ cannot be achieved by a sieve-like size exclusion mechanism. Classically,

two other mechanisms have been proposed: the “snug-fit” (105) and the “field strength” (106) hypotheses. These mechanisms assume that ions must be completely dehydrated to enter the channel pore. The snug-fit hypothesis proposes that the pore consists of coordination “cages” for K^+ that are narrow and rigid, and cannot collapse to accommodate the smaller Na^+ ion (105). The field strength hypothesis proposes that the field strength or partial charge of the coordinating ligand(s) in the pore accounts for discriminate binding of ions, where ligands of low field strength bind large ions (which have a lower density of charge) more favorably and high field strength smaller ions (106). According to this theory, a ligand(s) of low field strength reproduces the typical cation selectivity sequence of K^+ channels ($K^+ \sim Rb^+ > Cs^+ >> Na^+ \sim Li^+$).

The crystal structures of KcsA have revived these old theories using all-atom simulations to seek a microscopic understanding of selective permeation. Initial inspection of the selectivity filter might suggest a snug fit mechanism because the static structure shows eight carbonyl ligands ideally positioned to interact with K^+ and too far apart to coordinate Na^+ (15). This is in contrast to the Na^+-dependent leucine transporter, LeuT, which binds Na^+ with five oxygen-containing ligands, permitting a smaller, more suitable binding site (107) (Figure 1.4C). This “cavity size” mechanism has been challenged by Roux and colleagues who argue that, despite the relative rigidity of the filter, thermal fluctuations estimated from the B-factors of the structure are ~1 Å, which far exceeds the difference in ionic radius between K^+ and Na^+ (0.38 Å) (104). MD FEP simulations suggest that the carbonyls are highly flexible, and that K^+ selectivity, in a similar vein as Eisenman’s field strength theory, results from the high partial charge of

carbonyls relative to water. Coordination of Na^+ by carbonyls requires a smaller geometry which is unfavorable primarily because of strong carbonyl-carbonyl repulsion (104). If this repulsion is "turned off", KcsA becomes non-selective even if the entire channel except for the backbone atoms of the filter is frozen (104). These data suggest that the chemistry of the coordinating ligands, not the structure, is the primary determinant of a K^+-selective pore. The argument can be further generalized by simulating a "toy model" where different types (carbonyls or water molecules) and number of ligands are permitted to freely fluctuate within 3.5 Å around a K^+ or Na^+ ion. Even these highly flexible models favor coordination of K^+ over Na^+ unless most of the carbonyl ligands are replaced with water (108). Thus, one explanation for why S2 is the most selective site is that it is the least accessible to water (109, 110).

Selective ion permeation is not simply determined by differential partitioning of ions into the pore at equilibrium, but also the energy barriers associated with permeating the pore. Electrophysiological and crystallography studies suggest that Na^+ and Li^+ block KcsA from the intracellular side by binding in the filter between S3 and S4 (in plane with the T75 carbonyl) and even punch through the channel at high voltages (99, 111). However, the free energy profile for intracellular Na^+ to enter a multi-ion pore (2 K^+ ions in S1 and S3) calculated by MD simulations suggests that a large energy barrier, due to electrostatic repulsion from K^+ ions, prohibits it from progressing to the planar site between S3 and S4 (111). For Na^+ entering from the extracellular side, the multi-ion free energy profile also shows stable energy wells near S0 and S1, and a significant energy barrier that would prevent movement into S2 (110). Thus, both the mechanism of

selective partitioning and the kinetics of the entire permeation event in a multi-ion pore are important aspects of understanding selectivity in K^+ channels.

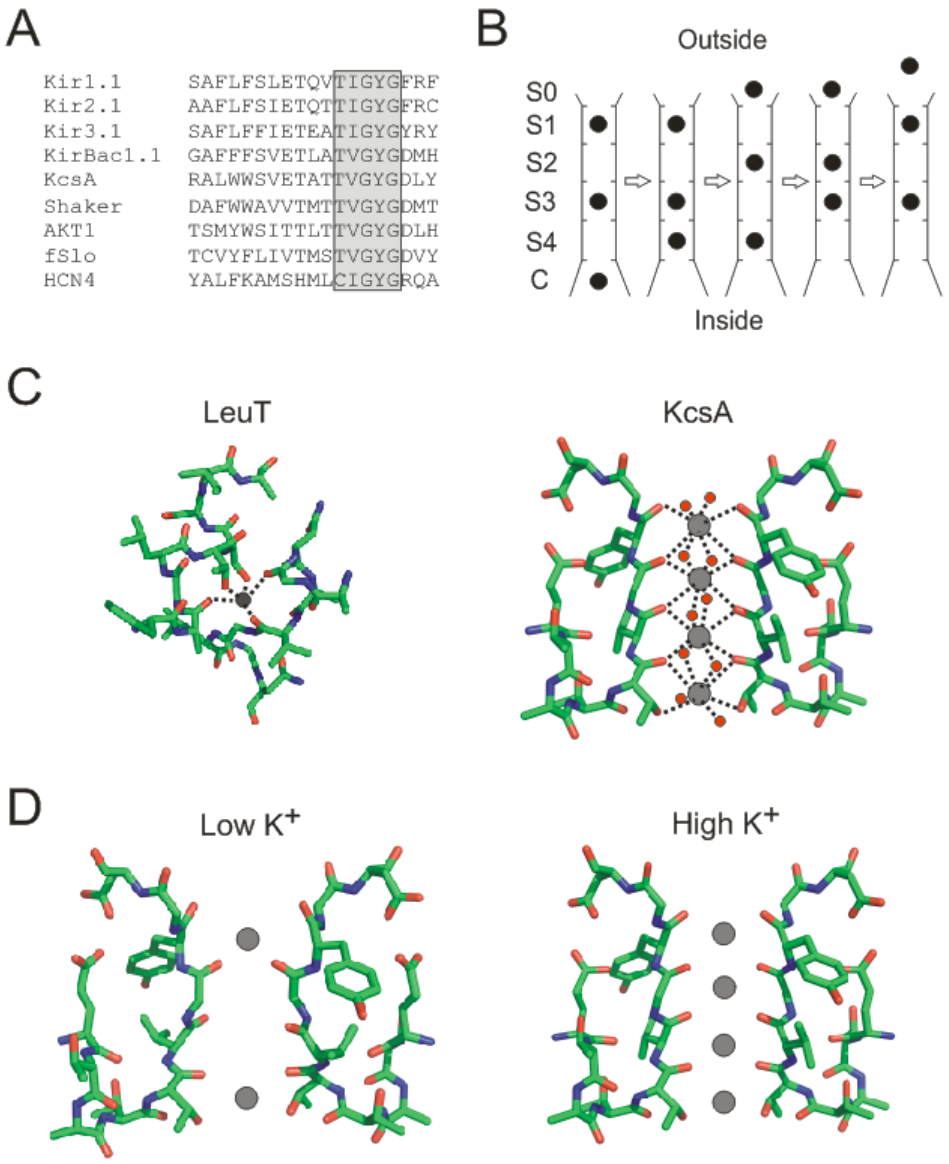

Figure 1.4: Mechanisms of ion selectivity and conduction in K^+ channels. (A) Sequence alignment of the P-loop (selectivity filter and pore helix) of K^+ channels. Shaker is a voltage-gated K^+ channel cloned from *Drosophila*. AKT1 is a plant inward rectifier, fSlo is a Ca^{2+}-activated K^+ channel from *Drosophila*, and HCN4 is a hyperpolarization-activated cyclic nucleotide-gated channel that has weak K^+ selectivity. Despite variable selectivity among these channels, they all contain the GYG signature

sequence. (B) Schematic of classic “knock-on” mechanism (25) for outward K^+ conduction based on the configurations identified by Berneche et al (102). MD free energy calculations suggest that certain ion configurations are more K^+-selective than others (102, 112). (C) Pentameric coordination site of Na^+ in the Na^+-dependent leucine transporter LeuT with an average Na^+-O distance of 2.28 Å (2A65), and octameric coordination site of K^+ in KcsA with an average K^+-O distance of 2.84 Å (1K4C). Adapted from Gouaux and MacKinnon (107) (D) Selectivity filter structures of KcsA comparing the collapsed low K^+ structure (1K4D) and the patent high K^+ structure (1K4C).

IIIB. STRUCTURAL DETERMINANTS OUTSIDE THE SELECTIVITY FILTER

Among K^+ channels, all of which contain the selectivity filter signature sequence, TXGYG, selectivity for K^+ over Na^+ varies by more than two orders of magnitude (1) (Figure 1.4A). Even hyperpolarization-activated cyclic nucleotide-gated cation (HCN) channels, which are nearly non-selective for cations (P_{Na}/P_K ~0.3) contain a similar signature sequence (CIGYG) (113) (Figure 1.4A). In voltage-gated K^+ channels, conformational changes associated with inactivation alter selectivity (114, 115), and mutations outside of the signature sequence are known to alter both inactivation and selectivity (116, 117). Thus, the backbone carbonyls that form the selectivity filter cannot be the only determinants of selectivity in K^+ channels.

In Kir channels, several mutagenesis studies have shown that structural features outside of the selectivity filter can decrease or increase K^+-selectivity. All inward rectifiers contain a conserved glutamate and arginine residue before and after the selectivity filter sequence, respectively, that form a salt bridge interaction (56, 118). Mutations of residues in this salt bridge in Kir2.1, Kir3.1/3.4 and Kir1.1 alter K^+-selectivity, and in some cases, completely abolish selectivity against Na^+ permeation (118-120). In more recent studies, mutations that alter selectivity in Kir3.2 were identified using a yeast genetic screen. Mutations of S177 (particularly S177W), which is found in the upper half of TM2 near the bottom of the selectivity filter, do not support yeast growth in low K^+ because they abolish K^+-selectivity (121). On a S177W background, a second screen identified seven mutants that restored selectivity, located throughout the channel in TM1, TM2 and the pore helix (122). The exact mechanism by

which these mutations restore selectivity is unclear, but the mutations show that structural changes more than 10 Å away from the filter can alter selectivity. One of these mutations, N184D, is located in TM2 facing the inner cavity (the "rectification controller" residue for Kir3.2) (123). Interestingly, only mutations to acidic residues at N184 or at other pore lining residues above and below this position in TM2 restore selectivity on the S177W background, suggesting an electrostatic mechanism whereby these residues stabilize K^+ in the inner cavity (123). A kinetic model can explain this increase in selectivity (112). The model shows that stabilization of K^+ in the cavity concurrently stabilizes certain K^+ ion configurations in the selectivity filter—configurations which favor K^+ permeation over Na^+ (Figure 1.4B). Thus, without altering the structure of the selectivity filter, stabilization of K^+ in the cavity by N184D may "amplify" selectivity by altering the kinetics of permeation (112).

Molecular modeling studies also demonstrate that structural forces outside of the selectivity filter are necessary to achieve selective partitioning. Since the proposal by Roux and colleagues that freely fluctuating carbonyls are sufficient to maintain a K^+-selective binding site (108), others have argued, using a different force field to perform simulations or using quantum chemical calculations, that coordination by eight water ligands is also K^+-selective and that Roux et al's "toy models" do not actually reflect an unrestrained liquid-like environment (124, 125). What makes the selectivity filter K^+-selective compared to aqueous solution is the high (octameric) coordination number of the carbonyls in contrast to the lower coordination numbers observed in aqueous solution (<7) (124-126). This "over-coordinated" state is maintained or, rather, tuned by the

surrounding protein structure of KcsA, which provides a “quasi-liquid” environment that is flexible but contains no nearby H-bond donors, unlike the aqueous phase. H-bond donors would interact with carbonyls in the filter, and thus lower the average coordination number (125), as may be the case with the water-filled cavities in the filter of the non-selective NaK channel (109, 127), or the S177W mutation in Kir3.2 which introduces a potential H-bond donor at the base of the selectivity filter (122).

To summarize, the current picture of how selectivity is achieved in K^+ channels is incomplete and multi-faceted. Mechanisms for K^+-selectivity include theories about 1) selective partitioning into the filter at equilibrium and 2) the complete free energy profile of the pore that determines the kinetics of permeation and the configurations of multiple ions in the pore. Selective partitioning is likely determined by the field strength of the carbonyls and the high coordination numbers in the filter maintained by the surrounding protein structure (128), rather than the exact cavity size of the K^+ binding sites. Theoretical studies of K^+ channels with different structures or degrees of selectivity will further test the relative contributions of these hypotheses (129, 130). In my thesis work, I determine that the E71A mutant in KcsA reduces K-selectivity (Chapter 4) and this raises the opportunity to test how structural changes in this mutant may account for reduced selectivity by any one of the above proposed mechanisms (Chapter 6 IIB).

IIIC. SELECTIVE EFFECTS OF IONS ON CHANNEL FUNCTION AND STRUCTURE

There is extensive electrophysiological, biochemical and structural evidence that the interaction of ions within the pore of K^+ channels can have significant effects on channel function (e.g. selectivity, conduction) and structure (e.g. oligomeric stability). This adds another dimension to our understanding of selectivity: K^+ channels not only select for and against different cations, but the structure and function of these channels is selectively modulated by interaction with different cations. Armstrong and colleagues were the first to observe that K^+ currents in squid axon irreversibly decay in the absence of intra- and extracellular K^+, but that this loss of current is prevented in the presence extracellular K^+, Cs^+, NH_4^+ or Rb^+ but not Na^+ and Li^+ (131). Later studies in Shaker channels found that this loss of current results from evacuation of K^+ from the pore of open channels (132) such that the channel enters a long-lasting "defunct" or non-conductive state (133). Several lines of evidence suggest that the "defunct" state involves a closure or deformation at the selectivity filter. First, in the absence of extracellular K^+ but presence of intracellular K^+, intracellular TEA makes squid axon K^+ channels defunct at depolarizing potentials, suggesting that the critical K^+ binding sites being evacuated are external to the TEA binding site in the inner cavity (134). Second, as Shaker channels become defunct, they enter a "dilated" state where the channels become transiently less selective and permeable to Na^+ (135). Third, Shaker mutants that do not exhibit C-type inactivation, which is thought to occur through gating at the selectivity filter (20, 115), are also immune to becoming defunct (133). Thus, for K^+ channels to remain conductive and selective, they require interactions with permeant ions in the filter.

These electrophysiological findings have been complemented by structural and biochemical studies of KcsA. High resolution structures of KcsA in Na^+ with low K^+ (< 3 mM) or no K^+ reveal a collapsed and putatively non-conductive filter where the backbone carbonyl of G77 pinches the conduction pathway closed and abrogates the S2 binding site (23) (Figure 1.4D). Only two K^+ ion densities are present in S1 and S4 with a total occupancy of 1 (23, 97) (Figure 1.4D). Isothermal titration calorimetry experiments measuring the heat of binding different cations with KcsA show that only the relatively permeant cations, K^+, Rb^+, and Cs^+, but not Na^+, release significant heat upon binding to the channel in the presence of Li^+ and it has been proposed that this change in enthalpy is associated with conformational changes of the filter transitioning from a collapsed to conductive structure (97). In support of the structural changes in the filter being associated with the heat of K^+ binding, the mutant M96V maintains a conductive filter in low K^+ and does not exhibit the same change in enthalpy with the addition of K^+ (97). In a similar vein, the crystal structure of a KcsA mutant, where residue A77 is substituted with D-alanine, also shows a conductive filter in low K^+, and the channel, although still selective in the presence of K^+, shows significant Na^+ conduction in the absence of K^+ (136, 137). As proposed by Mackinnon and colleagues, KcsA and perhaps K^+ channels in general, exhibit two "layers of selectivity": selectivity for K^+ over Na^+ in the presence of K^+, and selectivity against Na^+ conduction in the absence of K^+ because the selectivity filter is collapsed (136). This mechanism cannot apply to all K^+ channels, however, since MthK, a prokaryotic K^+ channel that is similar to voltage- and Ca^{2+}-dependent BK

channels, does not exhibit a collapsed filter in the absence of K^+, and consequently remains permeable to Na^+ (138).

Cations also affect K^+ channel quaternary structure by stabilizing the channel tetramer. Detergent-solubilized KcsA is highly stable, running as a tetramer in SDS-PAGE, and denatures to the monomeric form only after prolonged, harsh treatments with heat or high pH (139, 140). The tetramer stability of KcsA is dependent on cations, being highly stable in the presence of the permeant cations K^+, Rb^+ and Tl^+, less stable in Cs^+ and NH_4^+, and even less so in Na^+ and Li^+ (141). The fact that this pattern of tetramer stability matches the selectivity sequence of KcsA, and the fact that only certain mutations near the selectivity filter disrupt tetramer stability (139, 142), suggests that this effect is mediated by interactions with cations in the selectivity filter. Indeed, Ba^{2+}, which has a higher affinity for K^+ channels than K^+ itself (95) and blocks K^+ channels by binding in the selectivity filter at S4 (95, 143), is the most effective cation for stabilizing the KcsA tetramer (141), and the only cation that stabilizes the tetramer of KirBac1.1 in SDS-PAGE (144). Furthermore, mutation of T75, which forms S4 in KcsA with its side chain and backbone carbonyl, to a cysteine destabilizes the KcsA tetramer in K^+ and Ba^{2+}, but increases stability in Na^+ (145).

Given the functional and structural effects that K^+ and other cations have on K^+ channels, it is clear that cations bound to the channel pore function as essential cofactors (141), and modulators of channel function such as selective permeation. Differential effects of cations on the structure of the selectivity filter or the stability of the channel tetramer may point to the nature of the interactions between cations and K^+ channels that

make these channels selective. As one example, collapse of the selectivity filter in the absence of K^+ and presence of Na^+ may point to one structural mechanism by which K^+ channels select against Na^+ or gate as in the case of slow C-type inactivation and fast flicker closures (20, 146, 147). In Chapter 4, I investigate this mechanism of selectivity in KcsA by testing whether the E71A mutant responds differently from the WT channel to the absence of K^+ and presence of Na^+.

IV. PHOSPHOLIPID REGULATION OF POTASSIUM CHANNELS

Ion channels are embedded in a heterogeneous and dynamic lipid bilayer and lipids play an important role in maintaining and regulating channel function. $PI(4,5)P_2$ or PIP_2 is one of the best studied lipid regulators of ion channels and all eukaryotic Kir channels are activated by PIP_2 (148). It is conceivable that local and rapid fluctuations of PIP_2 in the cell membrane may function as a second messenger to regulate excitability through Kir channels, although these hypotheses remain untested and there are few instances where a physiological role for PIP_2 regulation of K^+ channels (e.g. GPCR-mediated hydrolysis of PIP_2 inhibiting the activity of KCNQ channels or M current) is known (148-150). Regardless of its physiological importance, PIP_2 regulation of Kir channels has been the subject of numerous biophysical studies aimed at understanding the nature of interaction between lipid and channel. Before addressing the topic of lipid regulation of K^+ channels, and in particular, PIP_2 regulation of Kir channels, I will first review the structure and function of lipids in cell membranes.

IVA. STRUCTURE AND FUNCTION OF CELLULAR LIPIDS: FOCUS ON ANIONIC PHOSPHOLIPIDS

The lipids of cellular membranes exhibit remarkable diversity as well as heterogeneity in their spatial organization. The number of lipid species in a single cell is at least on the order of thousands with variations in lipid type (e.g. glycerophospholipids, sphingolipids, sterols), headgroups (e.g. choline, serine), acyl chains (e.g. number, length, saturation), and the diacyl ester structure (e.g. plasmalogens) (151, 152). In eukaryotic cells, 1,2-diacyl glycerophospholipids are the primary membrane lipid species along with cholesterol, sphingomyelin and glycosphingolipids (Table 1) (153). 1,2- diacyl glycerophospholipids (hereafter referred to as phospholipids) are composed of a glycerol backbone with two fatty acid acyl chains esterified at the *sn-1* and *sn-2* positions, and a phosphate esterified at the *sn-3* position with different headgroups bound to the phosphate (Figure 1.5A). The phospholipid phosphatidic acid (PA), consisting of just the phosphate group at the *sn-3* position, is anionic (-1), and can be modified by the addition of headgroups that make it zwitterionic (PC- phosphatidylcholine, PE- phosphatidylethanolamine) or anionic (PS- phosphatidylserine, PG- phosphatidylglycerol, CL- cardiolipin or diphosphatidylglycerol, PI- phosphatidylinositol) (Figure 1.5A). PI can also be phosphorylated at the 3, 4, and 5 positions of the inositol ring in any combination, to generate seven different phosphatidylinositol phosphates (PIPs). The lipid compositions of mammalian cell membranes are generally similar, but quite different from prokaryotic membranes. Both PC and PE make up the bulk of phospholipids (40-70 mole% of total lipid) in the plasma

membrane of mammalian cells (154-156), whereas PE is the only neutral phospholipid in *E. coli* (75 mole% of total lipid) (157) (Table 1). For anionic phospholipids, PS (~5-10%) and PI (~10%) are the predominant species in the mammalian plasma membrane, whereas PG is the predominant species in *E. coli* and other prokaryotes (Table 1). Cardiolipin, an important lipid cofactor of respiratory chain enzymes complexes (e.g. cytochrome c oxidase) in the mitochondria (158, 159), is primarily found in the inner mitochondrial membrane (15-20%) (160), and is also present in prokaryotic membranes (Table 1).

In addition to phospholipids, three other types of lipid are significant components of eukaryotic membranes: cholesterol (25-50%), sphingomyelin (10-20%) and glycosphingolipids (~10%) (Table 1) (153). Both sphingomyelin and glycosphingolipids are sphingolipids consisting of a sphingosine backbone linked by an amide bond to a fatty acid (e.g. ceramide) and by a primary hydroxyl to a variety of headgroups. Headgroups range from a phosphocholine group for sphingomyelin (Figure 1.1B), to complex glycans for glycosphingolipids. Sphingomyelin is neutral, but modifications to the headgroup can generate charged lipids, which can have important regulatory effects on ion channels. For example, sphingomyelinase D converts sphingomyelin to ceramide 1-phosphate (-1 charge), which activates the voltage-gated K^+ channel Kv2.1 (161).

Among the major lipid types mentioned above, there are additional levels of complexity in their organization in a cell. First, there are significant differences in lipid content between the plasma membrane and the membranes of intracellular organelles. Both cholesterol and sphingomyelin are much less abundant in intracellular membranes

compared to the plasma membrane, and glycosphingolipids reside almost exclusively in the plasma membrane, forming a thick extracellular oligosaccharide matrix called the glycocalyx (151, 162). Intracellular membranes also vary in anionic phospholipid content, which are most abundant in the plasma membrane (total ~11-15%), although high levels of PI are present in the outer mitochondrial membrane and Golgi (~10%) (151, 153). Not only is PI(4,5)P_2 present exclusively in the plasma membrane, but other PIPs are specifically distributed throughout intracellular organelles and vesicles and play an important role in vesicle trafficking by interacting with peripheral effector proteins involved in vesicle movement, tethering, endocytosis or exocytosis (163). PI(3)P is particularly abundant in early endosomes, PI(3,5)P_2 in late endosomes, and PI(4)P in the Golgi (163). PI(4,5)P_2 and PI(4)P are the primary PIPs in the plasma membrane present at comparable but highly variable amounts (164).

A second level of complexity is that glycerophospholipids and sphingolipids are asymmetrically distributed between the inner and outer leaflet of the plasma membrane. This asymmetry is maintained by lipid translocases/transporters and is critical for the physical stability of the membrane and certain cell functions (165). In mammalian cells, sphingomyelin, glycosphingolipids and PC are predominantly in the outer leaflet, whereas PE and anionic phospholipids such as PS and PI are in the inner leaflet (166). By contrast, in prokaryotes such as *B. megaterium*, where PE makes up 70% of total phospholipid and PG 30%, PG is nearly exclusively localized to the outer leaflet (167). The anionic phospholipids PS and PI (particularly PIPs) are bioactive lipids, and their predominance in the inner leaflet is consistent with their cellular functions. PI(4,5)P_2 is

the most abundant PI derivative in the eukaryotic plasma membrane (~1%), and is the substrate for generating three intracellular second messengers (i.e. cleavage by phospholipase C into diacylglycerol and inositol triphosphate, phosphorylation by 3-kinase to PIP_3) (1). PIP_2 also interacts with and regulates numerous effector proteins such as regulatory proteins of the actin cytoskeleton (168). PS is also a lipid cofactor for various protein effectors such as protein kinase C (169) and cRaf1 protein kinase (recruitment to the intracellular side of the membrane) (170). Moreover, flipping and exposure of PS to the extracellular leaflet is an important process during platelet activation for catalyzing the activation of thrombin (171), and during the early stages of apoptosis for recognition of the cell by phagocytes (172, 173).

A third level of complexity is lateral segregation of lipids and proteins into microdomains. The most well-studied membrane microdomain is the lipid raft, which is a self-assembled region of the membrane high in cholesterol, glycosphingolipids, sphingomyelin, and GPI-anchored proteins that likely plays a role in membrane trafficking and signaling (174). Lipid rafts can also be clustered in the apical side of polarized cells due to restricted diffusion by tight junctions (175, 176). There is some evidence that phospholipids such as PIP_2 can form local gradients and even “rafts” due to restricted diffusion by cytoskeletal structures, membrane bending or clustering with proteins; however, these remain poorly tested hypotheses (177). Given the roles that anionic phospholipids such as PIPs and PS have in cell signaling, it is likely that these lipids are more laterally segregated in the cell membrane than currently appreciated. The regulation of phospholipid synthesis and metabolism is also poorly understood, and with

continued advances in lipidomics, we should anticipate finding that lipids do exhibit significant temporal as well as spatial heterogeneity, which would have important implications for how these lipids modulate membrane proteins such as ion channels (178, 179).

Lipid	Human erythrocyte-plasma membrane (154)	CHO cells-plasma membrane (155)	Inner mitochondrial membrane (160)	*E. coli* (157)
Cholesterol	25	N.A.	-	-
PE	18	21	24	75
PC	19	51	38	-
Sphingomyelin	18	9	N.A.	-
PS	9	7	4	<1
PG	0	1	-	20
CL	0	2.3	16	5
PI	1	8	16	-
Glycosphingolipid	10	N.A.	N.A.	-
PA	N.A.	1	2	<2

Table 1: Lipid composition of cellular membranes. Data reported as mole% of total lipid. N.A. indicates not analyzed and blank indicates not detected. CHO stands for Chinese hamster cells, inner mitochondrial membrane is from *S. cerevisiae*, and *E. coli* reports inner and outer membrane excluding Lipid A. Adapted from Dowhan et al (153).

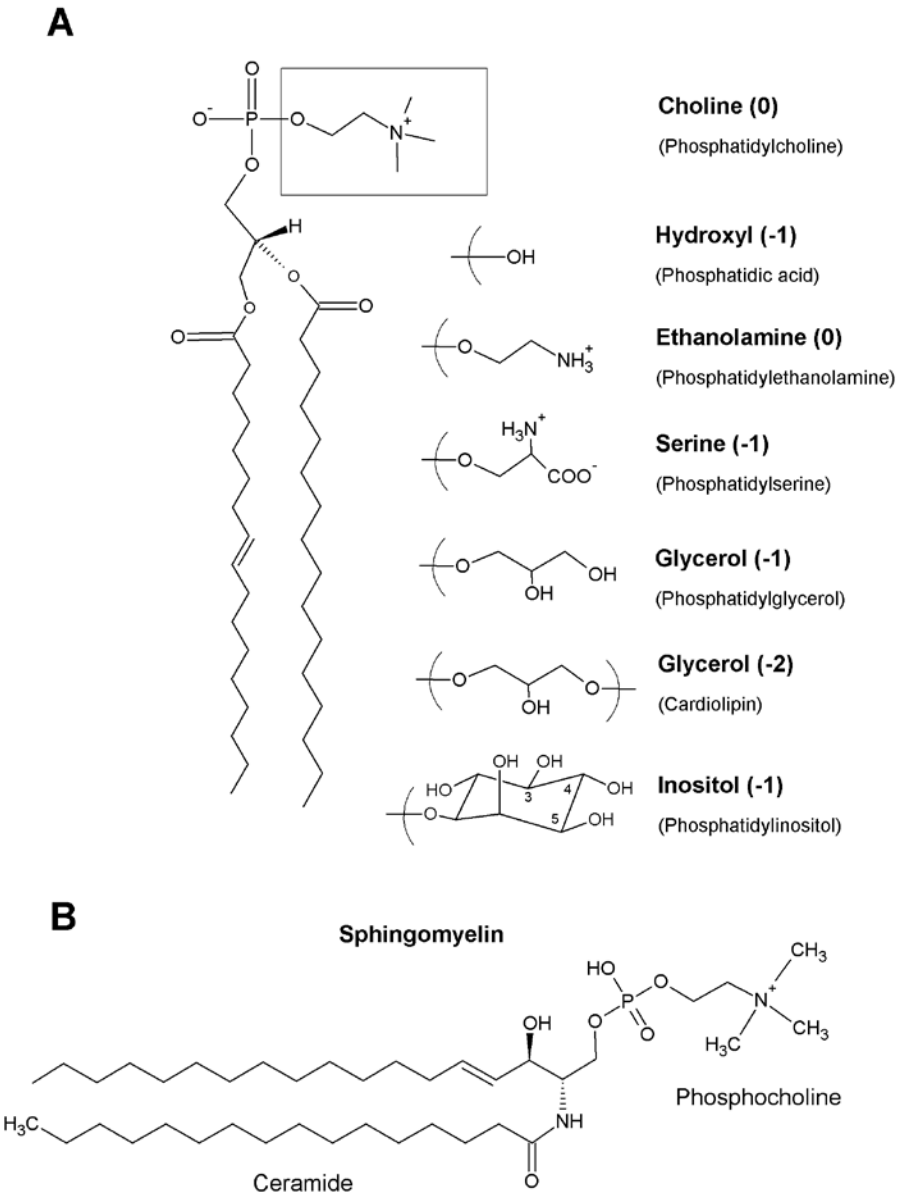

Figure 1.5: Chemical structures of phospholipids and sphingomyelin. (A) Basic chemical structure of a 1,2-diacyl glycerophospholipid showing choline and other headgroups below. The 3, 4, or 5 positions of inositol can be phosphorylated to generate phosphatidylinositol phosphates (PIPs). (B) Chemical structure of sphingomyelin, which is a sphingolipid with the lipid backbone, ceramide (N-palmitoyl-sphingosine, d18:1/16:0), and headgroup, phosphocholine.

IVB. REGULATION OF KIR CHANNELS BY PIP_2 AND OTHER ANIONIC PHOSPHOLIPIDS

Kir channels are activated by PIPs, primarily $PI(4,5)P_2$ or PIP_2 (180), as well as other anionic phospholipids such as long chain acyl CoAs (181). Activation of Kir channels by PIP_2 increases channel open probability without affecting unitary conductance (182); however, PIP_2 also suppresses the appearance of subconductances in several inward rectifiers including Kir1.1 and Kir2.1 (183, 184). Activation is highly dependent on the lipid tail, as IP_3 and di-C4-$PI(4,5)P_2$ have no effect on channel activity (185). Furthermore, Kir3.1/3.4 is more effectively activated by natural arachidonyl stearoyl PIP_2 compared to synthetic dipalmitoyl PIP_2, whereas Kir2.1 is equally activated by both (185). Di-C8-$PI(4,5)P_2$ activates Kir channels reversibly, presumably because the short-chain lipid rapidly partitions between the membrane and aqueous solution (185). Long chain PIP_2 (>16 carbons), by contrast, irreversibly activates Kir channels unless hydrolysis of PIP_2 causes slow channel "rundown" (185, 186). Channel activity can be recovered by the application of ATP, which presumably drives PIP kinases to regenerate membrane PIP_2 (186).

The effect of different lipids on channel activity can be studied by perfusing a micellar solution of lipid onto a membrane patch and observing the response in channel current (187). To generate dose-response curves, channel activity has been allowed to rundown completely, after which varying concentrations of di-C8-PIPs were applied (187). This approach only permits comparison of efficacy between lipids and is not a measure of affinity, since the actual amount of lipid in the membrane that the channel senses is unknown. For example, higher concentrations of di-C8-PIP_2 are needed to

activate Kir channels compared to long chain PIP_2, but this is likely due to lower partitioning of di-C8-PIP_2 into the membrane rather than a difference in the apparent affinity of activation.

In terms of the lipid headgroup, different Kir channels exhibit different specificities and each channel falls somewhere along the spectrum of being specific for $PI(4,5)P_2$, or non-specific and modulated by other anionic phospholipids (188). At one extreme of this spectrum is Kir6.2, which is non-specifically activated by nearly all anionic phospholipids including $PI(4,5)P_2$, $PI(3,5)P_2$, $PI(3,4)P_2$, $PI(3,4,5)P_3$, long chain acyl CoAs, PI(4)P, PI, and PS, although the latter three lipids are less effective (180, 181). The more negatively charged the PIP headgroup, the stronger the activating effect (180). At the other extreme is Kir2.1, which is activated by $PI(4,5)P_2$, but not by $PI(3,4)P_2$ or long chain acyl CoAs and only weakly by $PI(3,5)P_2$ and $PI(3,4,5)P_2$ (185, 188). Interestingly, $PI(3,4)P_2$ and long chain acyl CoAs suppress Kir2.1 activity by competitively inhibiting PIP_2 activation (189).

The activation of Kir6.2 by PIPs and acyl CoAs is thought to be through similar interactions because 1) acyl CoAs do not further activate Kir6.2 when already maximally activated by PIP_2 (188), 2) mutations that disrupt PIP_2 activation in Kir6.2 also disrupt activation by acyl CoAs (190, 191), and 3) mutations in Kir2.1 that mimic the Kir6.2 sequence make Kir2.1 sensitive to activation by acyl CoAs (188). Still, the reason for why acyl CoAs inhibit Kir2.1 activity but activate Kir6.2 remains unknown. Acyl CoAs are an intermediate of metabolism and regulation of Kir channels by acyl CoAs is thought to play an important role in insulin secretion (192) and possibly the pathophysiology of

type II diabetes. An increase in circulating free fatty acids in the diabetic state results in an increase in intracellular long chain acyl CoAs which could impair insulin secretion (181, 193).

Unlike eukaryotic Kir channels, KirBac1.1 is inhibited by PIPs (53). The efficacy of inhibition is correlated with the number of phosphates on the inositol group (PIP_3>PIP_2) and PIP, IP_3 and DAG have no effect on channel activity, suggesting that modulation is occurring by a similar mechanism as in eukaryotic channels (53). Why PIP_2 has the opposite effect on KirBac1.1 remains unknown, but it raises the interesting possibility that lipids can influence the evolution of channel structure and function (194). PIP_2 is not found in bacteria, nor in intracellular membranes, and the presence of PIP_2 in eukaryotic plasma membranes may have driven the evolution of PIP_2 activation of Kir channels (194). Studies of KirBac1.1, using purified channel protein reconstituted in liposomes, have provided definitive evidence that modulation by PIPs occurs through direct interactions, and not through an intermediary protein (53, 195). Identifying the structural determinants by which PIP_2 interacts with Kir channels has been the subject of extensive research and KirBac1.1 has provided a unique structural model for this endeavor.

IVC. PIP_2 BINDING SITE IN KIR CHANNELS

Initial characterization of PIP_2 activation of Kir channels suggested that modulation occurs through direct binding. Fusion proteins of GST with the C-terminal domains of various Kirs bind liposomes containing ^{3}H-PIP_2, and these protein-liposome

complexes can be co-immunoprecipitated with PIP_2 antibodies (186). Single point mutations of highly conserved basic residues, such as R188 for Kir1.1, abolish co-immunoprecipitation of the Kir C-terminus with PIP_2 liposomes (186), suggesting that PIP_2 directly binds to the C-terminus of Kir channels and that binding is mediated by charge interactions. These findings are corroborated by functional studies showing that polyvalent cations such as neomycin, polylysine or spermine can inhibit PIP_2 activation (180, 182), presumably by screening the negative charges of PIP_2. Similarly, PIP_2 antibodies can also inhibit activation, and the R188Q mutation in Kir1.1 speeds up antibody inhibition (186). While these mutations may be weakening channel-PIP_2 interactions, they may also be lowering open state stability of the channel and indirectly reducing PIP_2 sensitivity.

Subsequent studies have utilized either binding assays with soluble protein fragments or functional measurements (i.e. PIP_2 dose response, rate of PIP_2 antibody inhibition, or dose response of neomycin inhibition) to test the effect of various mutations and identify potential PIP_2 binding residues. A mutation that reduces PIP_2 sensitivity will result in lower channel activity in a native cell environment, and a larger increase in activity with PIP_2 application (182, 196). These approaches have their limitations (i.e. binding assays use only soluble fragments of the channel and functional readouts are indirect measures of binding), and they have identified a substantial list of candidate binding residues in the intracellular interfacial region of many Kirs, most of which are positively charged (197-202) (Figure 1.6A). Many of these residues have also been found in channelopathies such as Andersen syndrome with Kir2.1 mutations (10, 12) and

insulin secretory disorders (hyperinsulinism, DEND syndrome, and permanent neonatal diabetes mellitus) with Kir6.2 mutations (203). In particular, two basic residues that are highly conserved in all eukaryotic Kirs (R176 and R177 in Kir6.2, K188 and K189 in Kir2.1) are invariably sensitive to mutagenesis, often abolishing channel activity completely (197, 199). These residues are located in the linker between TM2 and the C-terminal cytoplasmic domain and are likely candidates for binding PIP_2. This linker is shortened by three residues in all KirBac proteins including KirBac1.1, and may account for the qualitatively opposite effects of PIP_2 on KirBac1.1 and eukaryotic Kir channels (53) (section IIC).

With twelve basic residues diffusely located on the intracellular side of Kir2.1 (Figure 1.6A) that alter PIP_2 sensitivity when mutated (199), it seems unlikely that all of these residues are involved in forming a specific binding site for PIP_2. Rather, many of these mutations may be altering the open state stability (i.e. intrinsic gating) of the channel and thus altering apparent PIP_2 sensitivity (197, 204). Potential insight into distinguishing between binding and "gating" residues has been gained from docking, course-grain and molecular dynamics simulations using the structures of KirBac1.1 (16), KirBac3.1-Kir1.3 chimera (54), and a homology model of Kir6.2 (43). The results of these studies suggest that only a subset of residues is actually likely to form a PIP_2 binding pocket (44, 45) (Figure 1.6B). The models predict that each Kir tetramer has four PIP_2 binding sites[1], which lie at the interface between subunits and are formed by

[1] Electrophysiological studies of Kir2.1 tandem tetramers with different combinations of WT and mutant K118A/R189A subunits suggest that only one bound PIP_2 is necessary to activate the channel. Binding of additional PIP_2 ligands exhibits positive cooperativity in its effect on open probability 184. Xie, L.

residues (for Kir6.2) from the N- (K67) and C-terminus (R176, E179, R206) of one subunit and the N-terminus of the neighboring subunit (R50, R54) (45). Since the general location and overall pattern of basic residues involved in forming this PIP_2 binding site are similar between Kir6.2 and KirBac1.1, the authors propose that the opposite effect of PIP_2 on eukaryotic Kir channels and KirBac1.1 is due to differences in transduction of the regulatory signal (45). Future steps in elucidating PIP_2 interactions with Kir channels will require either simulations with the full-length crystal structure of a eukaryotic Kir channel (e.g. Kir2.2 (56)), or biochemical/structural studies with full-length purified Kir channels and PIPs (205). In the present work, I have succeeded in purifying functional human Kir2.1 and Kir2.2 channels (Chapter 5), such that it is now feasible to directly assay binding of lipids to these channel proteins (Chapter 6 IIIA).

IVD. INTERACTIONS OF PIP_2 AND SOLUBLE LIGANDS IN KIR CHANNELS

The K_{ATP} channel, Kir6.2, which is inhibited by ATP, and the G-protein coupled Kir channels, Kir3.x, which are activated by Gβγ and Na^+ (206, 207), were among the first cloned Kir channels found to be activated by PIP_2 (180, 186, 208). With this discovery, it rapidly became apparent that PIP_2 could tune the sensitivity of these channels to their respective regulatory ligands and vice versa. Gβγ and Na^+ sensitize Kir3.1/Kir3.4 to PIP_2 activation (186, 209) and PIP_2 desensitizes Kir6.2 to ATP inhibition (182). Similarly, acyl CoAs also desensitize Kir6.2 to ATP inhibition (190). The $K_{1/2}$ of ATP inhibition of Kir6.2/SUR1 heterologously expressed in COS cells is ~

H., S. A. John, B. Ribalet, and J. N. Weiss. 2008. Phosphatidylinositol-4,5-bisphosphate (PIP2) regulation of strong inward rectifier Kir2.1 channels: multilevel positive cooperativity. J.Physiol 586:1833-1848.

10 μM but can shift by more than two orders of magnitude after exposure to micellar PIP_2 (182, 196). One consequence of this is significant cell-to-cell variability in the ATP sensitivity of Kir6.2 due to variations in the composition of PIPs in the membrane (210). This may explain why Kir6.2 is open in tissues such as the pancreas, where the intracellular ATP concentration is in the low mM range, and thus regulate excitability of the beta cell in response to the metabolic state of the cell (8, 203). Interestingly, metabolic inhibition of COS cells causes a biphasic effect on Kir6.2 activity: initially, channel activity increases due to the decrease in inhibitory ATP; later, channel activity decreases due to loss of PIPs in the membrane that are not being regenerated by ATP-dependent lipid kinases (210). A similar biphasic response of K_{ATP} activity has been observed in ventricular myocytes (211) and such dynamic regulation may ensure that the level of PIPs in the membrane are matched with the level of intracellular ATP such that K_{ATP} channels are always tuned to respond to changes in ATP.

The effects of PIP_2 and soluble regulatory ligands such as Gβγ or ATP suggest a mechanism whereby binding of one ligand strengthens or weakens binding of another. Gβγ slows inhibition of Kir3.1/3.4 channel activity by PIP_2 antibodies, leading some to suggest that Gβγ binding strengthens PIP_2 interactions with the channel, although Gβγ could simply affect PIP_2 sensitivity allosterically (186). Similarly, Na^+ slows PIP_2 antibody inhibition of Kir3.1/3.2 or Kir3.1/3.4 activity. Neutralization of D226 in Kir3.2 or the equivalent residue, D223, in Kir3.4 also slows PIP_2 antibody inhibition suggesting that activation by Na^+ occurs by neutralizing these negatively-charged aspartate residues (212, 213). Mutation of the equivalent residue in Kir3.1, N217, to an aspartate speeds up

PIP_2 antibody inhibition and increases the Hill coefficient for the dose-response of Na^+ activation of Kir3.1/3.2 (212, 213). This aspartate residue is nearly adjacent to a highly conserved arginine, R225 in Kir3.4, which is critical for mediating PIP_2 activation (198). Logothetis and colleagues have hypothesized that Na^+ neutralizes this aspartate in Kir3.2 or Kir3.4 and thereby strengthens PIP_2 interactions with nearby positively charged residues in the channel (214). In a recent study using the cytoplasmic domain of Kir3.1 as a structural model, molecular dynamics simulations suggest that the Na^+ binding site is formed by a cluster of residues, including D223 in Kir3.4. D223 interacts with R225 in the absence of Na^+; Na^+ coordination induces a conformational "switch" that frees R225 to bind PIP_2 (213).

In Kir6.2, activation by PIP_2 reduces sensitivity to ATP inhibition (182, 196). The fact that both PIPs and ATP contain polyphosphate moieties suggest a "negative heterotropic" effect where these ligands compete for binding of overlapping sites in Kir6.2 (182). Mutagenesis and modeling studies suggest that the PIP_2 and ATP binding sites are made up of adjacent, distinct sets of residues with possibly some overlap (44, 197, 215, 216) such that electrostatic repulsion between the two is likely. Indeed, biochemical studies support this hypothesis. PIPs and ATP show mutual competition for binding to MBP fusion constructs of the C-terminus of Kir6.1 or Kir6.2 and competition has the same dependence on headgroup charge and lipid tail as functional activation by PIPs (217). In a similar study, binding of biotinylated ATP photoaffinity analogs to purified Kir6.2 protein from *S. cerevisiae* is reduced by PIPs (205).

Broader insight into the issue of how PIP_2 alters the sensitivity of Kir6.2 to ATP has been gained from kinetic models of gating (204, 215, 218). Two key observations in response to the addition of PIP_2 must be considered to model regulation of Kir6.2 gating by PIP_2 and ATP. First, increased open probability is related to increased $K_{1/2}$ for ATP inhibition by a characteristic non-linear relationship, and mutations that alter the intrinsic open probability of Kir6.2 also follow this relationship in terms of their effect on ATP sensitivity (72, 215, 219-221). Second, Kir6.2 gating, as in other Kir channels, consists of one open time, one fast "flicker" closed time, and multiple long closed times—it is the long closed events that PIP_2 and ATP shorten and lengthen, respectively, to activate and inhibit Kir6.2 (204, 222). Although more complex models (e.g. tetrameric, fully allosteric) have been proposed to reproduce other observations, the above two observations can be replicated by a simple linear kinetic scheme ($C_1 \leftrightarrow C_0 \leftrightarrow O \leftrightarrow C_f$) where PIP_2 governs the gating transition from the long closed (C_0) to open (O) state, and ATP only binds and stabilizes the long closed state transition (C_0 to C_1) (204). C_f accounts for the fast "flicker" closed events. Thus, the competing effects of PIP_2 and ATP are replicated by a model where PIP_2 shifts the equilibrium between the C_0 and O states to the open state (as do mutations that increase open probability) making the closed state less accessible to ATP and resulting in an apparent decrease in ATP sensitivity. The model is useful for identifying putative ATP-binding residues since mutation of those residues will reduce ATP sensitivity more than predicted from the intrinsic open probability of the mutant (13, 202). Such a kinetic model is consistent with structural models that PIP_2 and ATP compete for binding at nearby sites in Kir6.2, as binding of

PIP_2 renders the channel less sensitive to ATP (215). Similar kinetic models are likely to be applicable to other Kir channels, which also show multiple modes of regulation in addition to PIP_2 (e.g. Gβγ, protons (223, 224), cholesterol (225), etc).

In summary, all Kir channels are activated by PIP_2 but are variably sensitive to other phosphatidylinositol phosphates (PIPs) as well as other anionic phospholipids (e.g. acyl CoAs). Functional, biochemical and computational studies suggest that activation by these lipids occurs through direct interactions, particularly with positively-charged residues on the cytoplasmic side of the channel. PIP_2 also affects the sensitivity of different Kir channels to other regulatory ligands such as ATP, and the mechanism for these effects is thought to occur through 1) allosteric effects of one ligand on channel structure that alter the binding of another ligand, or 2) electrostatic/steric effects of one ligand on another. Given the challenges of identifying and controlling the lipids in a cell membrane, it is likely that many classes of lipids, other than PIPs, also regulate Kir channel activity (e.g. in chapter 5, I determine that Kir2.1 and Kir2.2 exhibit two modes of regulation by lipids), and that these ligands mutually interact to ultimately determine channel function.

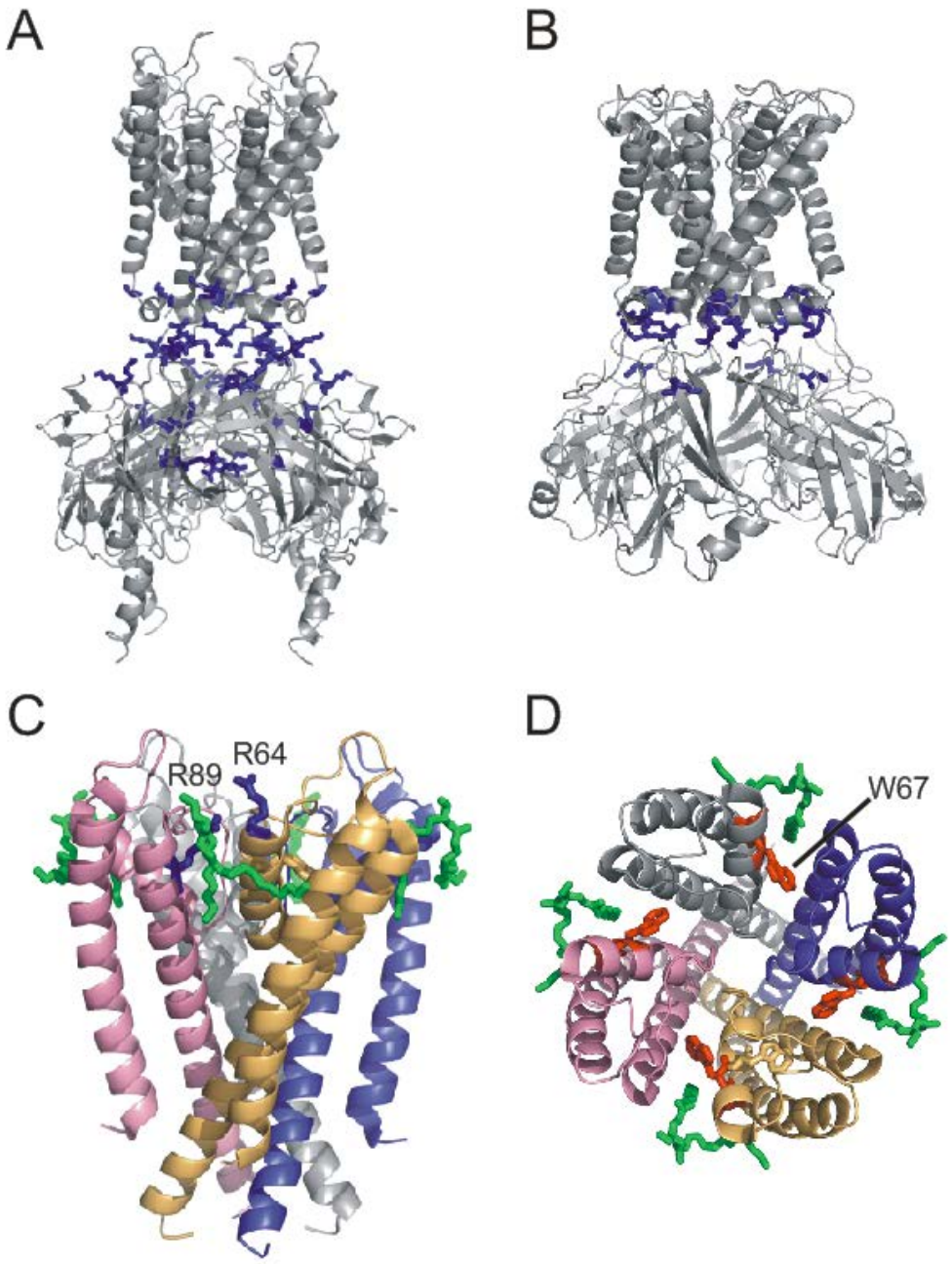

Figure 1.6: Structural basis of phospholipid interaction with K^+ channels. (A) Crystal structure of Kir2.2 (3JYC) highlighting in blue sticks twelve equivalent lysine or arginine residues determined by Lopes et al (199) in Kir2.1 to reduce PIP_2 sensitivity by putatively disrupting PIP_2-channel interactions. (B) Crystal structure of KirBac1.1

(1P7B) highlighting in blue sticks just five lysine or arginine residues determined by MD simulations to interact with the headgroup of PIP_2 (45). (C) Crystal structure of KcsA (1K4C) showing an extracellular lipid density modeled as a diacylglycerol, and highlighting R64 and R89 in blue sticks. Each subunit is a different color. (D) Same as (C) viewing from outside of channel and highlighting W67 and W68 in red sticks—W67 is nearest to the diacylglycerol lipid.

IVE. PHOSHOPHOLIPID REGULATION OF KCSA

KcsA has been a convenient and robust structural model to study the interactions of a purified K^+ channel with lipids. Initial characterization of KcsA by a $^{86}Rb^+$ flux assay determined that the channel requires negatively charged phospholipids, such as PG, PS or CL to be active (226). A more recent study of KcsA currents in lipid bilayers showed that PG increases both open probability and single channel conductance (227). The structure of KcsA solved at 2.0 Å resolution revealed a hairpin-like density bound to the extracellular side of the channel that could not be accounted for by detergent or any other components in the crystallization conditions and was thus attributed to a bound lipid molecule (23). The purified protein used for crystallography contained 0.7 mole of phosphate per mole of KcsA monomer as determined by a phosphate assay, and thin layer chromatography indicated that the source of this phosphate was bound PG (228). Since the lipid density was not completely resolved in the KcsA structure (especially the phospholipid headgroup), the density was modeled as a diacylglycerol, with a 9 carbon chain at the *sn-1* position and a 14 carbon chain at the *sn-2* position (228) (Figure 1.6C). The lipid is positioned between subunits with the *sn-1* hydrocarbon tail positioned in a groove between the TM2 helix and pore helix of adjacent subunits, illustrating the potential importance of lipid tail contacts with the channel (228, 229) (Figure 1.6C and 1.6D). The unresolved phospholipid headgroup is ideally positioned, especially if negatively-charged, to interact with the positively-charged residues R64 at the top of the pore helix and R89 on TM2 (230) (Figure 1.6C). Molecular dynamics simulations indicate that anionic phospholipids indeed favor binding to this site and form

significantly more H-bond interactions with R64 and R89 than neutral phospholipids (231). Mass spectrometric analysis of KcsA shows that the channel preferentially associates with certain phospholipids in the following sequence from greatest to least: PG~PA>>PE>PC (232). Furthermore, refolding experiments suggest that anionic phospholipids are not required to form the KcsA tetramer (228). Thus, the combination of these functional, biochemical, computational and structural data suggest that anionic phospholipids bind to a site on the extracellular side of KcsA, and that this interaction is important for gating and ion conduction of the channel rather than for stabilization of the tetramer.

A series of studies from Lee and colleagues using a fluorescence quenching technique have provided substantial insight into the nature of anionic phospholipid interactions with KcsA (227, 233, 234). KcsA contains five tryptophans: three are facing out towards the membrane (W26 and W113 on the intracellular side and W87 on the extracellular side) and two are highly conserved among K^+ channels, being packed behind the selectivity filter on the pore helix (W67 and W68) (Figure 1.6D). Brominated phospholipids quench tryptophan fluorescence depending on the affinity with which they bind and the distance of the bromine from the tryptophans (235). In WT KcsA, fluorescence quenching is much greater in mixtures of a small amount of brominated anionic phospholipid and PC compared to a mixture of any proportion of brominated PC and anionic phospholipid, suggesting that anionic phospholipids are forming unique, stronger interactions with the channel (233). The authors of this paper proposed that KcsA has two “classes” of lipid binding sites: 1) annular binding sites which contain the

boundary lipids surrounding the protein and are non-selective for neutral or anionic phospholipids and 2) non-annular binding sites which selectively bind anionic phospholipids with higher affinity (233). Anionic phospholipids bound to the non-annular site primarily quench fluorescence from W67, consistent with the proximity of this residue to the lipid density in the KcsA crystal structure (227, 234) (Figure 1.6D). Quenching is significantly reduced in 500 mM KCl, suggesting that selective binding of anionic phospholipids at the non-annular site is mediated by charge interactions, likely with R64 and R89 (233). However, not all anionic phospholipids bind equivalently, and estimated binding constants indicate that CL and PS bind more strongly than PG and PA (234). Lee and colleagues also report positive cooperativity in the PG dependence of the open probability of KcsA. Since the brominated-PG dependence of quenching is consistent with a simple non-cooperative binding event, the authors estimate that at least three or four PG lipids are needed to bind KcsA for the channel to open (227).

The regulation of integral membrane proteins by anionic phospholipids is commonly observed in nature (229, 236). Although the effects of membrane phospholipid composition on the function of K^+ channels remain poorly understood, it is likely that the principles learned from KcsA are applicable to other channels such as inward rectifiers (Chapter 5). Indeed similarities between anionic phospholipid activation of KcsA and Kir channels include: charge-based headgroup interactions, selectivity among different anionic phospholipids, hydrocarbon tail interactions, lipid binding between channel subunits, and positive cooperativity on open probability as multiple lipids bind the channel.

V. INTRODUCTION TO THESIS

The overarching theme of this thesis is the characterization of the bacterial channel, KirBac1.1, and particularly, its pore blocking properties, selectivity, and lipid dependence of activity (Chapter 3). In order to study these function properties, I have made use of a liposomal $^{86}Rb^{+}$ flux assay, and developed the methods to reconstitute purified channels in giant liposomes for patch-clamping (Chapter 2 IIC). Utilizing these techniques for studying the function of reconstituted channels in liposomes, these biophysical studies were then extended to KcsA (Chapter 4) and human Kir2.1 and Kir2.2 (Chapter 5). Comparing results from bacterial and human channels provides insights and hypotheses about the structural basis of their functional properties and when and how these properties may have evolved (Chapter 6).

CHAPTER 2

MATERIALS AND METHODS

I. MOLECULAR BIOLOGY AND PROTEIN PURIFICATION

IA. EXPRESSION AND PURIFICATION OF KIRBAC1.1 AND KCSA

KirBac1.1 and KcsA were subcloned into the pQE60 vector (QIAGEN) with a C-terminal 6-His tag. Mutations were made with the Quikchange Site-directed Mutagenesis Kit (Stratagene), and confirmed by DNA sequencing. For protein purification, BL21* (DE3) *E. coli* cells were transformed with KirBac1.1 or KcsA in pQE60, grown in 1 L cultures of LB media overnight at 37 ^{o}C to A_{600}~1.0, and induced with 1mM isopropyl β-d-thiogalactopyranoside for 3 hrs. The cultures were pelleted and each L culture was resuspended with 15 mL of 50 mM Tri-HCl, 150 mM KCl, pH 8 and half a tablet of EDTA-free protease inhibitor mixture (Roche Diagnostics). The bacteria were lysed by freeze-thaw, solubilized for 2 h in 30 mM decylmaltoside (Anatrace), and centrifuged at 30,000 x g for 30 min. The supernatant was incubated for 1 h with cobalt beads (~0.2 ml/L bacteria), washed with 40 bed volumes of wash buffer in a column (50 mM Tris-HCl, pH 8.0, 150 mM KCl, 10 mM imidazole, and 5 mM decylmaltoside), and eluted with 1-2 bed volumes of wash buffer with 500 mM imidazole. High concentrations of protein were achieved by incubating the column with small fractions of elution buffer prior to elution.

IB. EXPRESSION AND PURIFICATION OF KIR2.1 AND KIR2.2

Human Kir2.1 (KCNJ2) and Kir2.2 (KCNJ12) were sub-cloned into the pND-CTFH vector and expressed in the FGY217 strain of *S. cerevisiae*. 15 mL starter cultures were grown in 50 mL Falcon tubes overnight at 250 rpm and 30 °C in SC – Ura media supplemented with 2% Glucose then scaled up in 600 mL aliquots of SC – Ura + 2% Glucose in Ultrayield shaker flasks and shaken for an additional 24 hrs (OD_{600} ~ 1.5). SC – Ura supplemented with 2% Galactose were then inoculated with 150 mL of these cultures for induction (OD_{600} ~ 0.2) and grown for ~48 or 72 hrs respectively. Cells were harvested by centrifugation for 10 mins at 4000 x g, washed once in TBS buffer, resuspended in Lysis Buffer, and stored at -80 °C directly, or used fresh. Cells were ruptured by 10 passes at high pressure (25 -35 kPSI) using a Microfluidics Cell Disrupter. KCl was added to cell lysate to a final concentration of 500 mM. Cell debris was removed by a 5 min centrifugation at 500 x g, followed by a 25 mins centrifugation at 4000 x g. The supernatant was collected and centrifugated for 1 hr at 120,000 x g to collect crude membranes. Membranes were homogenized in resuspension buffer (50 mM Tris 7.5, 10 mM EDTA, 500 mM KCl, 2 mM DTT, 10% Glycerol, Complete-EDTA free protease inhibitor) to ~3.5 mg / mL total protein and solubilized by the addition of 1% Fos-choline 14 (Anatrace) for 3 hrs at 4 °C. Solubilized membranes were clarified by centrifugation at 56,500 x g. M2 anti-Flag resin (Sigma-Aldrich) was added to the supernatant and spun slowly on a blood-wheel for 3 hrs at 4 °C. The resin was washed in batch in the presence of 0.5% Fos-choline 14, packed into a drip-column, washed with 25 CV of wash buffer, and then eluted with the addition of 0.2 mg/mL 3xFLAG peptide (Sigma-Aldrich, UK) to the wash buffer. Elution fractions were combined and

concentrated to 1 mL using a 100,000 MWCO concentrator (Vivaspin) and separated by size exclusion chromatography using a Superdex 200 10/300 GL column (GE Healthcare, UK). Peak fractions were combined, concentrated to ~ 3 -6 mg/mL and used for functional studies.

II. FUNCTIONAL ASSAYS

IIA. LIPID REAGENTS

All lipids were purchased from Avanti Polar Lipids and experiments from Chapters 3-4 utilize a 3:1 mass ratio of synthetic POPE (1-palmitoyl 2-oleoyl phosphatidylethanolamine) and POPG (1-palmitoyl 2-oleoyl phosphatidylglycerol). For experiments in Chapter 5, additional lipids included synthetic POPS (1-palmitoyl 2-oleoyl phosphatidylserine), POPA (1-palmitoyl 2-oleoyl phosphatidic acid), POPC (-palmitoyl-2-oleoyl-phosphatidylcholine), EPC (1-palmitoyl-2-oleoyl-ethylphosphatidylcholine), CL (18:1 cardiolipin), and DGS-NTA (1,2-dioleoyl-glycero-3-[(N-(5-amino-1-carboxypentyl) iminodiacetic acid) succinyl]), and natural PI (phosphatidylinositol from bovine liver), PI(4)P (phosphatidylinositol 4-phosphate from porcine brain), and PIP_2 (phosphatidylinositol 4,5-bisphosphate from porcine brain).

IIB. RADIOTRACER FLUX ASSAY

The desired mixture of lipids was solubilized in buffer A (450 mM KCl, 10 mM HEPES, 4 mM NMG, pH 7) with 35 mM CHAPS, mixed at a 3:1 ratio, and incubated at room temperature for 2 h. Polystyrene columns (Pierce Chemical Co.) were packed with

Sephadex G-50 beads, presoaked overnight in buffer A, and spun to 1,500 x g on a Beckman TJ6 centrifuge (3,000 rpm). For KcsA fluxes, 3 μg of WT or E71A protein was added to 100 μl of lipid (1 mg) for each sample; for KirBac1.1, 10 μg of protein; and for Kir2.1 and Kir2.2, 5 μg. Protein was incubated in detergent-solubilized lipids for 20 min. Liposomes were formed by adding the protein/lipid sample to the partially-dehydrated buffer A columns and spinning to 1,000 x g. The extraliposomal solution was exchanged by spinning the sample to 1,000 x g in partially-dehydrated columns, now containing beads soaked in buffer B (450 mM sorbitol, 10 mM HEPES, 4 mM NMG, pH 7). Uptake was initiated by adding 400 μl of buffer B with 1-5 μl of $^{86}Rb^{+}$ (yielding a $[^{86}Rb^{+}] \sim 0.1$ nM). $^{22}Na^{+}$ flux measurements were performed identically to $^{86}Rb^{+}$ flux using an equivalent volume of $^{22}Na^{+}$, and yielding a concentration about 10x more than $^{86}Rb^{+}$ ($[^{22}Na^{+}] \sim 1$ nM). At various time points, aliquots were flowed through 0.5 ml Dowex cation exchange columns in the $NMGH^{+}$ form to remove extraliposomal $^{86}Rb^{+}$. These aliquots were then mixed with scintillation fluid and counted in a liquid scintillation counter. Whenever K^{+} was used as the intra-liposomal cation, valinomycin-mediated uptake was measured by adding 1 μl of 0.1 mg/ml valinomycin in buffer B to the sample and collecting a time point at 30 min. Although the rate of valinomycin-mediated uptake varies with membrane lipid composition, 30 min. was sufficient to reach maximum levels in all lipid conditions tested. Counts were normalized to valinomycin-mediated uptake to account for experimental variations in maximum liposome capacity. Spermine inhibition of KirBac1.1 [I131C/I138D] was tested by adding varying concentrations of spermine to

the extra-liposomal buffer C solution. The intra-liposomal cation was varied by replacing K^+ in buffer A with other cations.

IIC. PATCH-CLAMP OF GIANT LIPOSOMES

2 mg of the desired lipids were solubilized in K-MOPS buffer (158 mM KCl, 10 mM MOPS, pH 7.4) with 35 mM CHAPS, and KirBac1.1, KcsA or Kir2.1 protein was added to the lipids at lipid to protein mass ratios ranging from 500:1 (single channel recordings) to 10:1 (macroscopic recordings) and incubated at room temperature for 30 min. Liposomes were formed by gel filtration as described for radiotracer flux assay and centrifuged at 100,000 x g for 1 h at 4^{o}C (Beckman TL-100). The liposome pellet was resuspended in 3 μl of K-MOPS buffer and dried in a dessicator as 1-2 μl spots on a clean microscope slide for ~30 min or until completely dried. These spots were then rehydrated with 15 μl of K-MOPS buffer overnight at 4^{o}C. Rehydration at room temperature for ~2 h the next day was sufficient to form giant liposomes.

For patch-clamping, a glass coverslip was coated overnight with 1 mg/ml polylysine. The giant proteo-liposomes were pipetted onto the polylysine-coated coverslip in an oil-gate chamber and allowed to settle for ~5 min before starting the solution exchange to wash away debris. Unless indicated, patch-clamp recordings were done in symmetrical K^+ conditions of K-MOPS buffer. Membrane patches were voltage-clamped using a CV-4 headstage, an Axopatch 1-D amplifier, and a Digidata 1322A digitizer board (Axon Instruments). Patch pipettes were pulled from soda lime glass microhematocrit tubes (Kimble) to a resistance of ~2-3 MΩ. The voltage-step protocol

for blocking measurements stepped from -100 mV to +100 mV at 10 mV increments holding at -50 mV briefly before each step. Single channel data was digitized at a sampling rate of 3 kHz and a low-pass analog filter was set to 1 kHz. Idealization of single channel data and generation of amplitude histograms were performed using the pClamp 9.2 software suite (Axon Instruments). The remaining data analysis was performed using Microsoft Excel (Microsoft, Inc.).

IID. SINGLE CHANNEL LIPID BILAYER RECORDING AND DATA ANALYSIS

A horizontal planar bilayer system was used to incorporate channels and record currents (237, 238). The system contained two chambers separated by a partition containing a 100 μm diameter hole upon which a lipid bilayer (3:1 mass ratio of POPE and POPG solubilized in n-decane) was formed. The *cis* chamber was filled with 90 mM KCl, 10 mM KOH, and 10 mM HEPES, pH 7. Under control conditions the *trans* chamber was filled with 90 mM KCl, 10 mM KOH, and 10 mM succinic acid, pH 4.0. To observe the effect of Na^+, 10 mM NaCl was added to the internal solution. An Axopatch 200 amplifier was used to record currents sampled at 20 kHz with low-pass filtering at 2 kHz. Na^+-modified current voltage (IV) curves were fitted with eq. 1 at intermediate voltages (+25 to +150 mV), which describes the equilibrium block process for Na^+ binding in the low-affinity cavity binding site (239).

$$I(V) = \frac{I_0(V)}{1 + \frac{[Na^+]}{K_B(0)e^{-\frac{zFV}{RT}}}} \qquad \text{Eq. 1}$$

$I_0(V)$, was obtained by fitting the control IV curve with an empirical function. The apparent affinity at 0 mV, $K_B(0)$, and voltage dependence, z of the block were the fitted block parameters. All data fits were performed with Origin (Microcal).

In order to incorporate the subsequent rise in current at higher voltages into the model we assume the cavity-bound Na^+ can move either forward through the selectivity filter or back to the intracellular milieu and that the Na^+ contribution to the current (when moving forward through the filter) is insignificant relative to K^+, as verified by replacing K^+ with Na^+ on the intracellular side (data not shown). The entire Na^+ block IV curve can then be fit by assuming a model (Scheme 1) where the vestibule (V) can be occupied by either a Na^+ or a K^+ and that both ions can dissociate either back toward the intracellular solution (b_{-1} for Na^+, negligible for K^+ at high voltages where punchthrough becomes visible), or forward through the selectivity filter (b_2 for Na^+, k_2 for K^+). Consequently, current through the channel will be described by Eq.2, derivation of which is detailed in Nimigean and Miller, 2002(240):

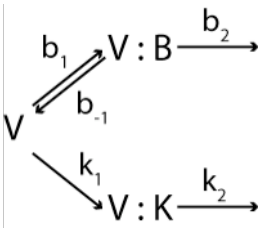

Scheme 1

$$I(V) = I_0(V)\left(1 + \frac{[Na^+]}{(1 + \frac{[K^+]}{k_2/k_1})(b_{-1}/b_1 + b_2/b_1)}\right)^{-1} \qquad \text{Eq.2}$$

where k_1 and b_1 are the on-rates for K^+ and Na^+ binding to the cavity, k_2 and b_2 are the rates of K^+ and Na^+ expulsion through the selectivity filter, and b_{-1} is the off-rate of

dissociating back to the intracellular milieu. Fits of Eq.2 will yield values for the "punchthrough" constant, b_2/b_1, the Michaelis-type constant for K^+, k_2/k_1, and the equilibrium block parameter b_{-1}/b_1. Under conditions of high voltage such that the expulsion of Na^+ toward the outside is much faster than its dissociation towards the intracellular milieu, eq. 2 can be modified to calculate a lower limit on k_2/b_2, a measure of the number of K^+ ions exiting the channel per Na^+ ion (240).

$$k_2/b_2 \geq \left(\frac{I_{Na}}{I} - 1\right)\left(\frac{[K^+]}{[Na^+]}\right)\left(\frac{k_1}{b_1}\right)\left(1 + \frac{k_2/k_1}{[K^+]}\right) \qquad \text{Eq.3}$$

where k_2/k_1 is set to 0 in order to obtain a lower limit and k_1/b_1 to 2.5, same value as for WT (240). The justification for using the same value of k_1/b_1 as in WT is our finding (see text) that the equilibrium Na^+ block in E71A displays similar parameters ($K_B(0)$, z) as the WT channel. An extended description of this analysis can be found in (240).

III. CRYSTALLIZATION AND STRUCTURE DETERMINATION

KcsA protein for crystallization was purified as described in IA. Following affinity chromatography, the protein was chymotrypsinized for 1 hour and then run over a superdex 200 gel filtration column. The protein was then incubated with F_{AB} (monoclonal antibody fragment) (23) in a 2:1 F_{AB}:KcsA ratio for 30 minutes and rerun over another superdex 200 column in 5 mM decylmaltoside, 150 mM KCl, and 10 mM Tris pH 7.5. Protein giving rise to the chromatographic peak corresponding to F_{AB} bound E71A KcsA was collected, concentrated to 10 mg/ml, and dialyzed for 2 days in buffer containing 5 mM decylmaltoside, 150 mM NaCl, and 10 mM Tris pH 7.5 at 4^{o}C. Dialysis buffer was

exchanged at least four times during the two-day period. Crystals were grown from KcsA E71A complexed with F_{AB} (23) by the hanging drop vapor-diffusion method. The reservoir solution contained 20–23% (w/v) polyethylene glycol 400, 25-50 mM MgSO4, and 100 mM MES pH 6.5. The hanging drop consisted of 2 μL of protein solution (E71A KcsA/F_{AB} at a final concentration of 10 mg/ml) mixed with 2 μL of reservoir solution. Crystallization trays were stored at 20°C. Crystals took approximately one month to reach full size. Cryoprotection was accomplished by increasing the polyethylene glycol 400 concentration in the reservoir to 40% (m/v) for a period of 24 hours and then freezing the crystal in liquid N_2.

Crystals were screened and diffraction data collected at the Brookhaven National Laboratory on beamlines X25 and X6A. The data was collected at a wavelength of 1.10 Å and a temperature of 93 K. Reflections were indexed, integrated, and scaled using the HKL2000 package (241). The structure was solved by molecular replacement via molrep from the CCP4 suite of programs using the previously deposited E71A KcsA structure, 2ATK as the initial model (242). The structure was completed through multiple rounds of model building with Coot and refinement with REFMAC (243, 244). TLS groups were chosen based on the output of the TLSMD server (245).

CHAPTER 3

KIRBAC1.1: IT'S AN INWARD RECTIFYING POTASSIUM CHANNEL

Published in an altered form in *J. Gen. Physiol.* (2009) 133(3): 295-305.

Cheng WWL, Enkvetchakul D, and Nichols CG

I. INTRODUCTION

Since the discovery of KirBac, a family of prokaryotic genes homologous to eukaryotic Kirs (37), KirBac1.1, KirBac3.1, and more recently, a KirBac3.1/Kir3.1 chimera, have been crystallized, revealing transmembrane structures that resemble the prototypical potassium channel, KcsA (16, 54, 55, 246). Attempts to model ligand interactions and molecular dynamics in eukaryotic inward rectifying potassium channels have relied upon generating homology models based on the KirBac structures (43-45, 247). While the predictions of these models are largely consistent with functional data, functional studies of KirBac1.1 itself are essential to make such structural inferences by homology. We have successfully used a liposome $^{86}Rb^{+}$ uptake assay to demonstrate that KirBac1.1 generates a potassium-selective permeability that can be inhibited by Ba^{2+}, Ca^{2+}, and by acidic conditions (52). In contrast to all eukaryotic Kir channels, KirBac1.1 activity is inhibited by phosphatidylinositol phosphates such as PIP_2 (53). Until now, functional studies of KirBac1.1 have been limited to such $^{86}Rb^{+}$ flux assays of

proteoliposomes as well as bacteria or yeast complementation screens (52, 248), and no voltage-clamp analysis has been reported. In this study, we present the first electrophysiological evidence that KirBac1.1 generates functional, potassium-selective channels that exhibit the same key features of rectification found in eukaryotic inward rectifying potassium channels.

II. RESULTS

Electrical Characterization of KirBac1.1

Excised patch-clamp experiments were performed using giant liposomes reconstituted with or without KirBac1.1 in symmetrical 158 mM KCl except as indicated (Figure 3.1A). Patches from liposomes without protein yielded minimal currents. In contrast, recordings from liposomes reconstituted with KirBac1.1 show significant current with a near linear voltage-current relationship in symmetrical K^+ conditions. When bath K^+ is lowered to 28 mM, there is a +31 ± 1 mV (n = 6, SEM) shift in the reversal potential. The largest shift observed was +34 mV indicating a minimum K^+/ Na^+ permeability ratio of 10:1. Current at positive voltages is blocked by 1 mM Ba^{2+} (Figure 3.1B) with a $V_{1/2}$ of 25 mV and a $z\delta$ of 1.5 (Figure 3.1C). The data indicate that these currents are due to functional potassium-selective channels.

We have previously shown by $^{86}Rb^+$ flux experiments that, unlike eukaryotic Kir channels, KirBac1.1 activity is inhibited by PIP_2 (53). This behavior is recapitulated in voltage-clamp recordings (Figure 3.2A) with almost complete channel inhibition by 5 μM PIP_2 (94 ± 3 % inhibition, n = 5, SEM). This method of applying micellar PIP_2 to

excised membrane patches has been widely used for eukaryotic Kir channels, which are activated by incorporation of PIP_2 in the inner leaflet of the membrane (180, 197). If micellar PIP_2 incorporates into only one side of the membrane, then KirBac1.1 inhibition

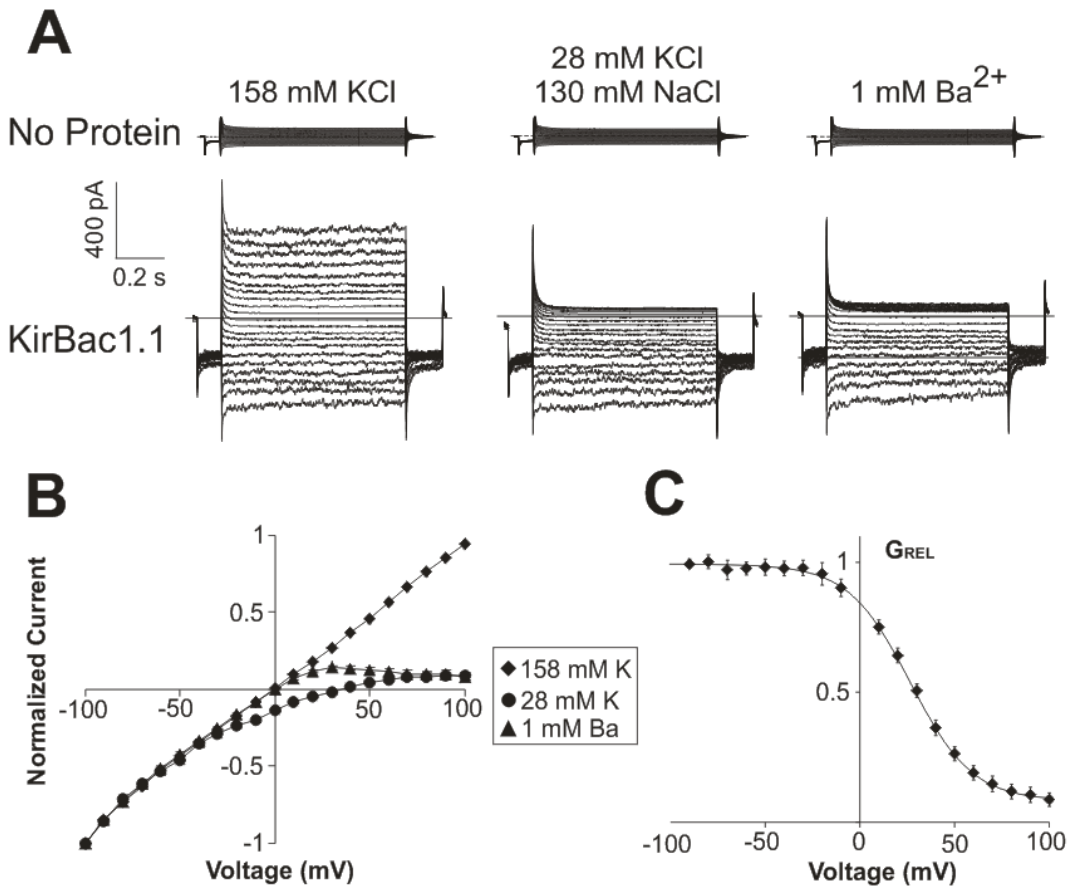

Figure 3.1 KirBac1.1 voltage-clamped currents are potassium-selective and blocked by barium. Inside-out patches were excised from giant liposomes reconstituted with no protein or WT KirBac1.1. (A) Representative currents from an inside-out patch from giant liposomes with or without KirBac1.1 protein. The pipette was filled with 158 mM K^+ and the bath with the indicated solutions. The voltage was held at -50 mV and then stepped from -100 mV to +100 mV at 10 mV increments. (B) Plot of normalized current versus voltage for WT KirBac1.1 in the solutions shown in (B) (n = 6, ± s.e.m.). (C) Relative conductance versus voltage plot of KirBac1.1 block in 1 mM Ba^{2+} (n = 6 ± s.e.m.). Fitting with a Boltzmann function gives the following parameter values: $V_{1/2}$ = 25 mV, δz = 1.5, residual G_{REL} = 0.08, scaling factor = 0.9.

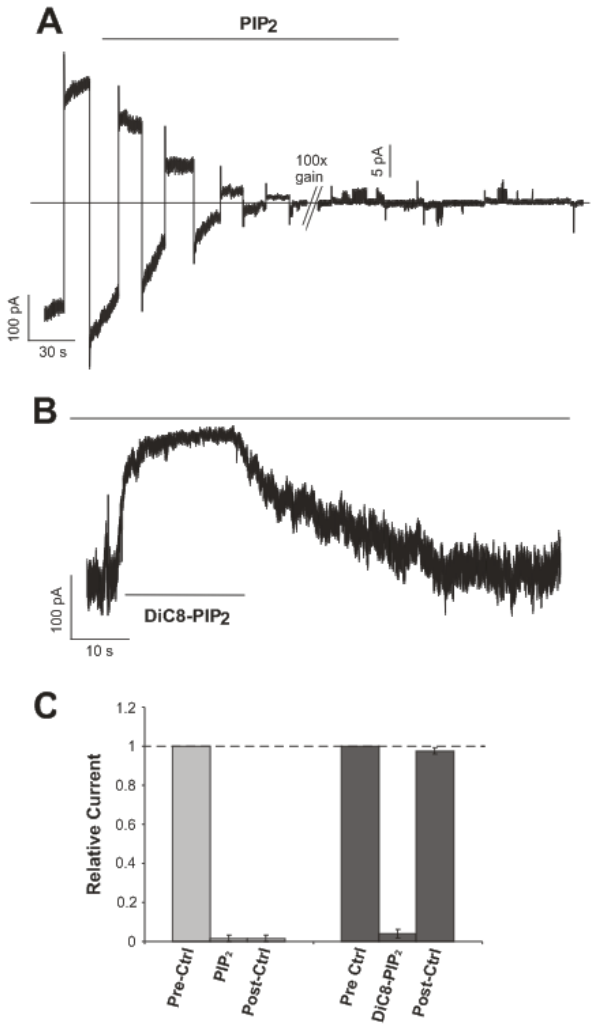

Figure 3.2 KirBac1.1 currents are inhibited by PIP_2. (A) Continuous recording of potassium-selective and barium-sensitive KirBac1.1 current alternating between +100 mV and -100 mV clamp in symmetrical K^+ conditions. The patch was moved into a 5 μM PIP2 buffer when indicated. The gain on the amplifier was increased by 100x when indicated. (B) Continuous recording of KirBac1.1 current held at -100 mV. 50 μM diC8-PIP_2 was applied when indicated. (C) Data from recordings for PIP_2 (n = 5) and diC8-PIP_2 (n = 3) inhibition. Currents in PIP_2, diC8-PIP_2, and after 2 min. of washout (post-ctrl) are normalized to the initial current (pre-ctrl).

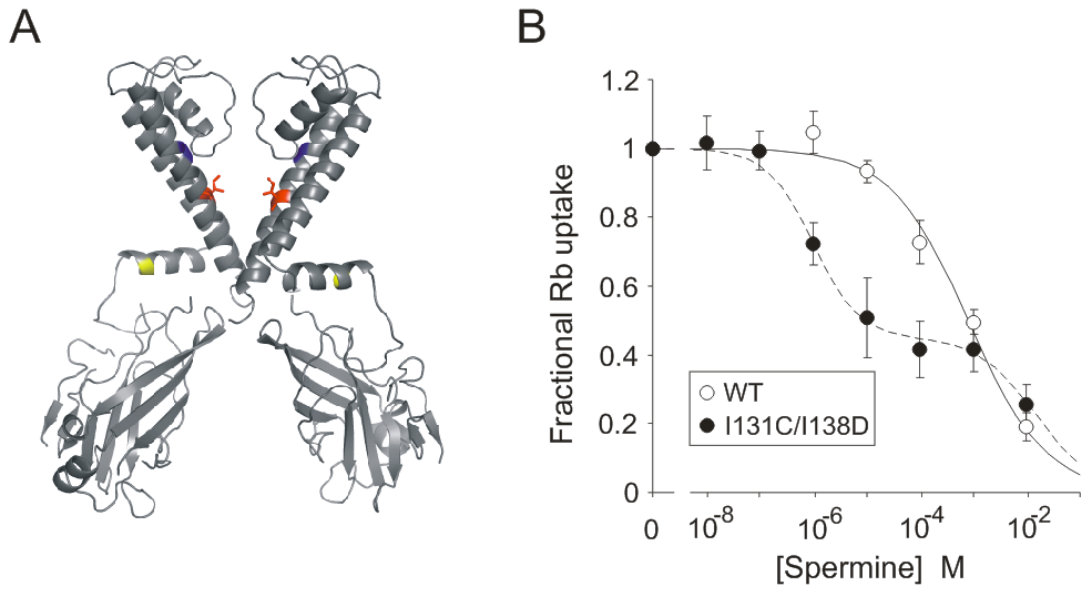

Figure 3.3 The I131C/I138D mutant is more sensitive to spermine inhibition than WT. (A) Structure of two opposing subunits of KirBac1.1 highlighting the residues I131 (blue) and I138 (red) that were mutated to cysteine and asparate, respectively. R49 is also highlighted in yellow. Mutation of this residue to a cysteine renders an inactive channel that can be rescued by MTSET modification. (B) Plot of relative $^{86}Rb^{+}$ uptake of WT and I131C/I138D in liposomes at different concentrations of externally applied spermine, normalized to uptake without spermine (n = 9 ± s.e.m.). The I131C/I138D data are fit with the sum of two Hill functions ($K_{1/2}$ = 1 μM, H = 1; $K_{1/2}$ = 15 mM, H = 0.8), and the WT data with one ($K_{1/2}$ = 0.8 mM, H = 0.6).

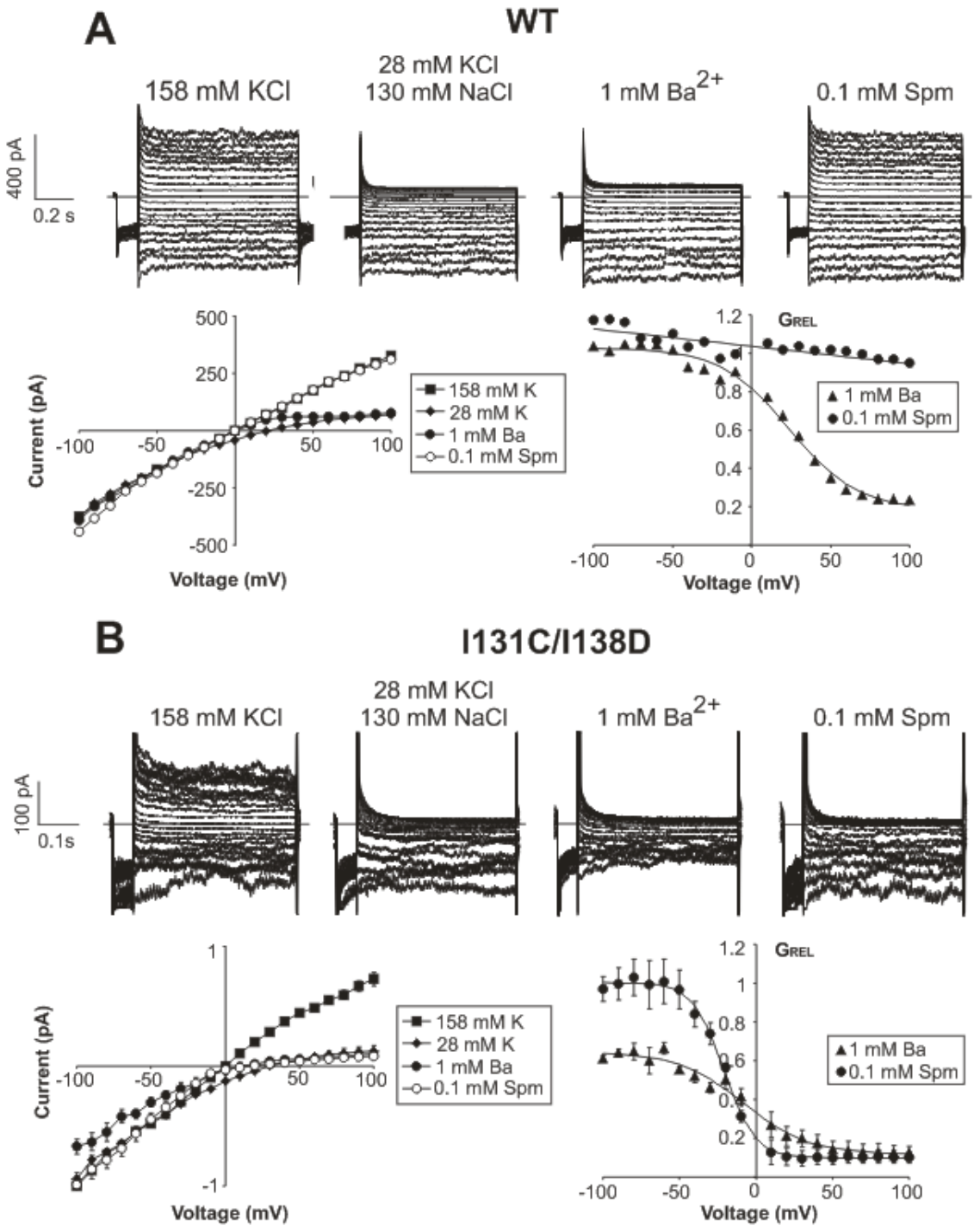

Figure 3.4 I131C/I138D is blocked by spermine with strong voltage-dependence. Voltage step recordings are presented, as in Figure 3.1, of (A) WT KirBac1.1 and (B)

I131C/I138D in the indicated solutions. (A) Representative recordings of WT KirBac1.1 and its corresponding I-V and G_{REL}-V curves. (B) Representative recordings of I131C/I138D and its corresponding I-V and G_{REL}-V curves (n = 4 ± s.e.m.). The relative conductance curves are fit with Boltzmann functions with the following parameter values: for 1 mM Ba^{2+}: $V_{1/2}$ = -8 mV, δz = 1.2, scaling factor = 0.5, and residual G_{REL} = 0.1; for 0.1 mM spermine: $V_{1/2}$ = -21 mV, δz = 2.5, scaling factor = 0.9, and residual G_{REL} = 0.1.

should be dependent on channel orientation. The fact that PIP_2 inhibits almost all the current in a patch suggests that most KirBac1.1 channels reconstituted in giant liposomes are oriented with their intracellular/cytoplasmic domain towards the inside of the liposome and exposed to bath solution in inside-out mode (see Discussion). Inhibition by long-chain micellar PIP_2 from porcine brain extract was irreversible during the time-scale of the recording (Figure 3.2C). However, DiC8-PIP_2, a synthetic water-soluble dioctanoyl form of PIP_2, causes reversible inhibition of KirBac1.1 (Figure 3.2, B and C), washing out in ~30 s (27±5 s, n = 3). This is consistent with previously reported reversible activation of eukaryotic Kir channels by this synthetic short acyl-chain lipid (185, 187). This suggests that the dependence of the kinetics of KirBac1.1 inhibition on the hydrocarbon chains of phosphotidylinositol phosphates is similar to that of activation in eukaryotic Kirs, and argues that inhibition and activation occur by a similar mechanism involving partitioning into the membrane and direct interaction with the channel.

Strong rectification in KirBac1.1 [I131C/I138D]

WT KirBac1.1 behaves as a weak inward rectifier, and is insensitive to block by spermine in both patch-clamp and $^{86}Rb^+$ flux assays (Figures 4.3 and 4.4A). We hypothesized that mutation of I138, which is equivalent to the “rectification controller” residue in eukaryotic Kir channels, to an aspartate would confer sensitivity to polyamines just as in Kir1.1 (N171D) and Kir6.2 (N160D) (Figure 3.3A, red). Initially, multiple preparations of I138D mutant KirBac1.1 were inactive when tested by the $^{86}Rb^+$ flux

assay (data not shown). We found, instead, that mutation of residue 131 (located in the upper region of TM2, adjacent to the base of the pore helix and near the selectivity filter, Figure 3.3A, blue) from isoleucine to cysteine stabilizes the channel tetramer in SDS-PAGE (144). On the I131C background, the I138D mutant generated functional channels assessed by $^{86}Rb^{+}$ flux (Figure 3.3B). $^{86}Rb^{+}$ flux assays of WT and I131C/I138D in different concentrations of spermine illustrate that the double mutant, I131C/I138D, is strongly inhibited by spermine, and the concentration dependence of inhibition shows two distinct components. The I131C/I138D data can be fit with the sum of two Hill equations ($K_{1/2}$ = 1 μM and 15 mM), and the WT data with a single Hill equation ($K_{1/2}$ = 0.8 mM). The fact that only 50% of $^{86}Rb^{+}$ uptake is inhibited with high affinity is consistent with generation of high affinity block only to internal/cytoplasmic spermine in I131C/I138D, and with channels being bi-directionally oriented (see Discussion).

I131C/I138D also produces K^{+}-selective and Ba^{2+}-sensitive currents by patch-clamp (Figure 3.4). WT currents, as well as I131C currents (data not shown), are blocked by 1 mM Ba^{2+} but are essentially insensitive to spermine (Figure 3.4A), while I131C/I138D currents are potently blocked by spermine (Figure 3.4B), with steep voltage-dependence (for Ba^{2+}, a $V_{1/2}$ of -8 mV and a zδ of 1.2; for spermine, a $V_{1/2}$ of -20 mV and a zδ of 2.5). It is notable that, in contrast to the ~50% high affinity spermine block in the liposome flux assay, 80-90% of WT and I131C/I138D current are consistently blocked with a single voltage-dependent component by Ba^{2+} (WT and I131C/I138D) and spermine (I131C/I138D), which suggests that the channels are not bi-directionally oriented (50:50) in the excised patches from giant liposomes as they are in

the smaller liposomes used for the Rb^+ flux assay (see Discussion). I131C/I138D also shows stronger block by 1 mM Ba^{2+} ($V_{1/2}$ = -8 mV) compared to WT ($V_{1/2}$ = 25 mV) or I131C ($V_{1/2}$ = 21 mV) with a partial block of current that appears voltage-independent, at least up to -100 mV. In summary, introduction of I138D, the "rectification controller" position in KirBac1.1, on the I131C background produces functional channels that exhibit steep voltage-dependent block by spermine[2].

Complex single channel properties: multiple conductances and gating heterogeneity

Patch-clamp recordings that resolve single channel openings are readily obtained by reconstituting liposomes with smaller amounts of protein. Figure 3.5 shows recordings of WT, I131C/I138D and I131C with variable numbers of channels in a patch held at +100 mV. At single channel resolution, WT and I131C activity are blocked by 1 mM Ba^{2+} but insensitive to 0.1 mM spermine, while I131C/I138D is potently blocked by spermine, consistent with the macroscopic data.

Single channel currents of KirBac1.1 also show complex properties, most obviously multiple conductance states. Figure 3.6A shows representative channel openings from two individual patches of WT and I131C/I138D. Both exhibit at least five conductance states. All-points-histograms of all channel openings in these two recordings show that smaller conductance states predominate (Figure 3.6B). During bursts of smaller amplitude openings short transitions to larger conductance states are typically present.

[2] We have since found that the I131C mutation is unnecessary and that the I138D mutant is active and sensitive to spermine (Figure 7.2). The reason for why earlier attempts to obtain functional I138D channels failed is unknown.

The largest single channel amplitude observed for WT had a conductance of ~46 pS (chord conductance at -100 mV), and for I131C/I138D, ~56 pS. However, all single channel recordings primarily showed two smaller conductance states: the most prevalent at ~15 pS, and a larger opening at ~32 pS, measured at -100 mV (Figure 3.6C). These histograms only include channel openings; the area of the baseline peak (Figure 3.6C shows only one in gray) gives no indication of open probability. Figure 3.7A shows all-points-histograms of all single channel openings at +100 mV and -100 mV from a WT patch, with representative traces from the recording shown above. The red dotted lines in the traces indicate the current levels that correspond with the peaks in the histograms. The two predominant conductance peaks shift to a lower amplitude at +100 mV compared to -100 mV, and stepping from -100 mV to +100 mV during a single channel burst shows that the ~32 pS conductance state at -100 mV corresponds to a conductance of ~21 pS at +100 mV (Figure 3.7B). All-points-histograms were used to determine the major single channel amplitudes over a range of voltages. Plots of single channel amplitude versus voltage show that the two major conductance states exhibit a mild intrinsic inward rectification in WT and I131C/I138D (Figure 3.7C, n = 4).

Single channel gating kinetics of KirBac1.1 are also complex. Open probability varies significantly from patch to patch. Figure 3.8A shows two WT recordings with contrasting open probabilities. Open probability also tends to be higher at positive voltages than negative voltages as seen in Figure 3.8B. This may explain why, although WT macroscopic currents show a near linear current-voltage relationship (Figure 3.1), single channel amplitudes exhibit inward rectification (Figure 3.7B). At positive voltages,

openings are usually more frequent and short-lived (Figure 3.7A). By contrast, openings at negative voltages typically show infrequent, distinct bursts. Detailed inspection of these recordings reveals variations in intraburst gating kinetics at negative voltages (Figure 3.8C). Single channel bursts at -100 mV were idealized using a "50% threshold" criterion based on the current amplitude, and this was used to calculate intraburst open probability. A plot of the intraburst open probability for all bursts in patches of WT and I131C/I138D show at least two gating modes at -100 mV. Generally, most openings have a high P (o) of ~0.9, but occasionally, openings will switch to a flicker mode where P (o) is ~0.65. Such gating heterogeneities are uncommon among eukaryotic potassium channels in cellular membranes but similar behaviors have been reported for KcsA reconstituted in liposomes (249).

One-sided activation of R49C

In a prior study, using the $^{86}Rb^{+}$ flux assay, we showed that cysteine mutants of KirBac1.1 in the slide helix can be activated by modification with MTS reagents. In particular, the mutations R49C or K57C render the channel inactive, but can be rescued by MTSEA or MTSET modification (195). KirBac1.1 channels reconstituted in giant liposomes are not necessarily oriented in the same direction as eukaryotic channels expressed in cell membranes. Since R49 is located in the slide helix (Figure 3.3A), application of MTSET in the bath can only activate those channels in which the "cytoplasmic" end is also facing the bath. Figure 3.9 shows a continuous recording of R49C single channel activity following activation by MTSET. The currents behave

exactly as WT: they are inhibited by 1 mM Ba^{2+} but insensitive to 0.1 mM spermine. Amplitude histograms as well as the general appearance of channel gating at +100 mV compared to -100 mV are similar to WT and I131C/I138D (Figure 3.7, 3.8, and 3.9). The fact that WT and I131C/I138D exhibit similar single channel amplitudes and gating behavior as activated R49C is consistent with most of the reconstituted channels being oriented with their “cytoplasmic” end facing the bath in an inside-out patch.

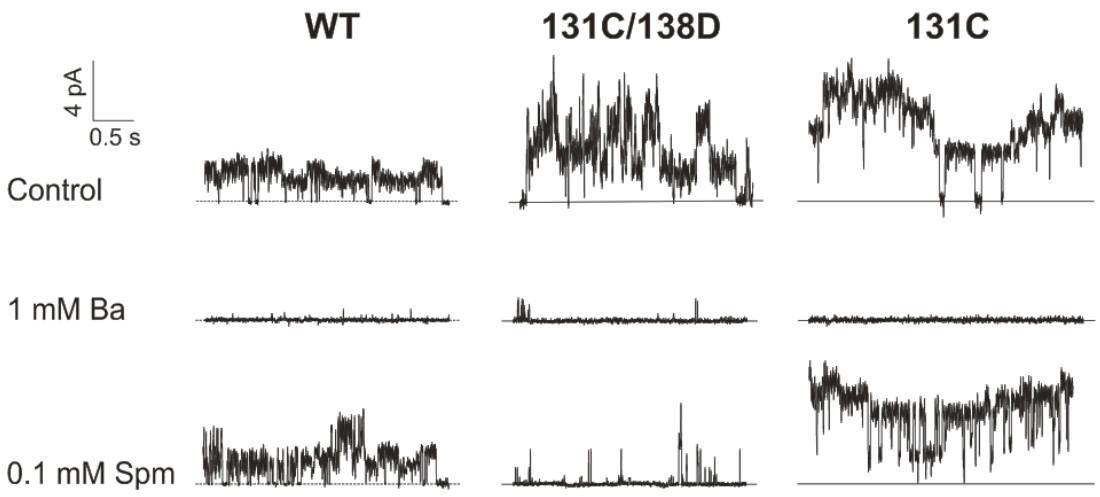

Figure 3.5 Currents from WT, I131C/I138D and I131C that resolve single channel openings are consistent with findings from macroscopic recordings. Shown here are segments from recordings of WT, I131C/I138D and I131C at +100 mV with the indicated solutions in the bath.

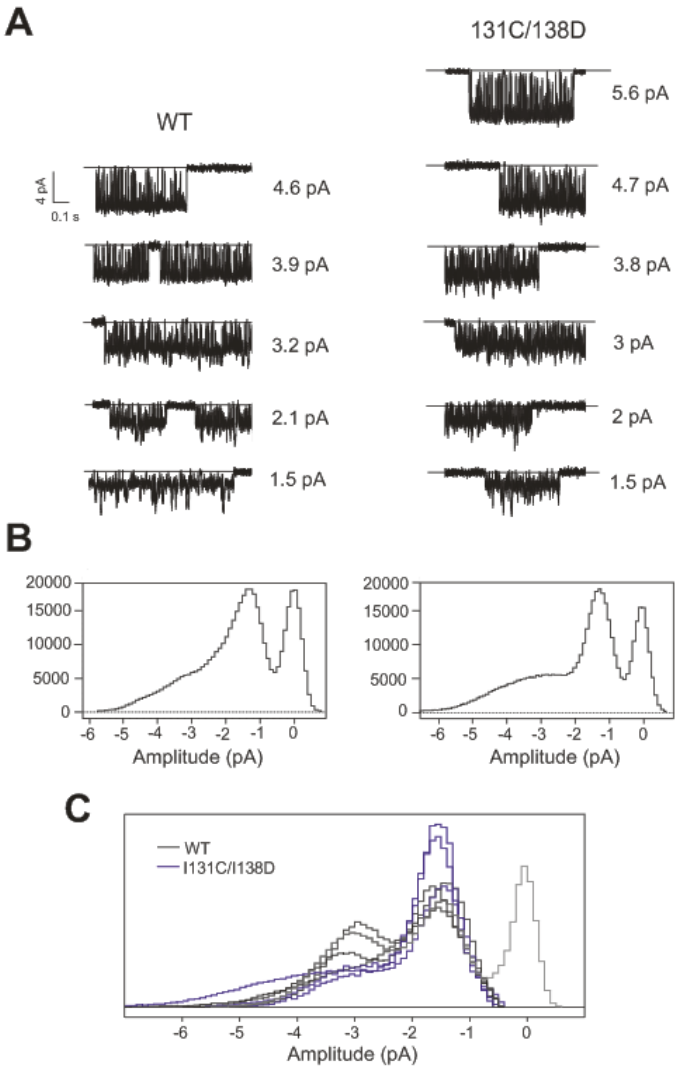

Figure 3.6 Single channel openings of KirBac1.1 show multiple conductance levels. (A) The currents shown are representative single channel openings at -100 mV at all amplitude levels from a patch of WT and I131C/I138D. (B) All-points-histograms of all channel openings from each recording. (C) A compilation of all-points-histograms of channel openings from WT (n = 4, black) and I131C/I138D (n = 3, blue) recordings. The baseline (zero channel current) peak is included for one histogram only (gray), and each histogram is scaled, for the sake of comparison, by dividing the bin values by the total number of points in each respective histogram.

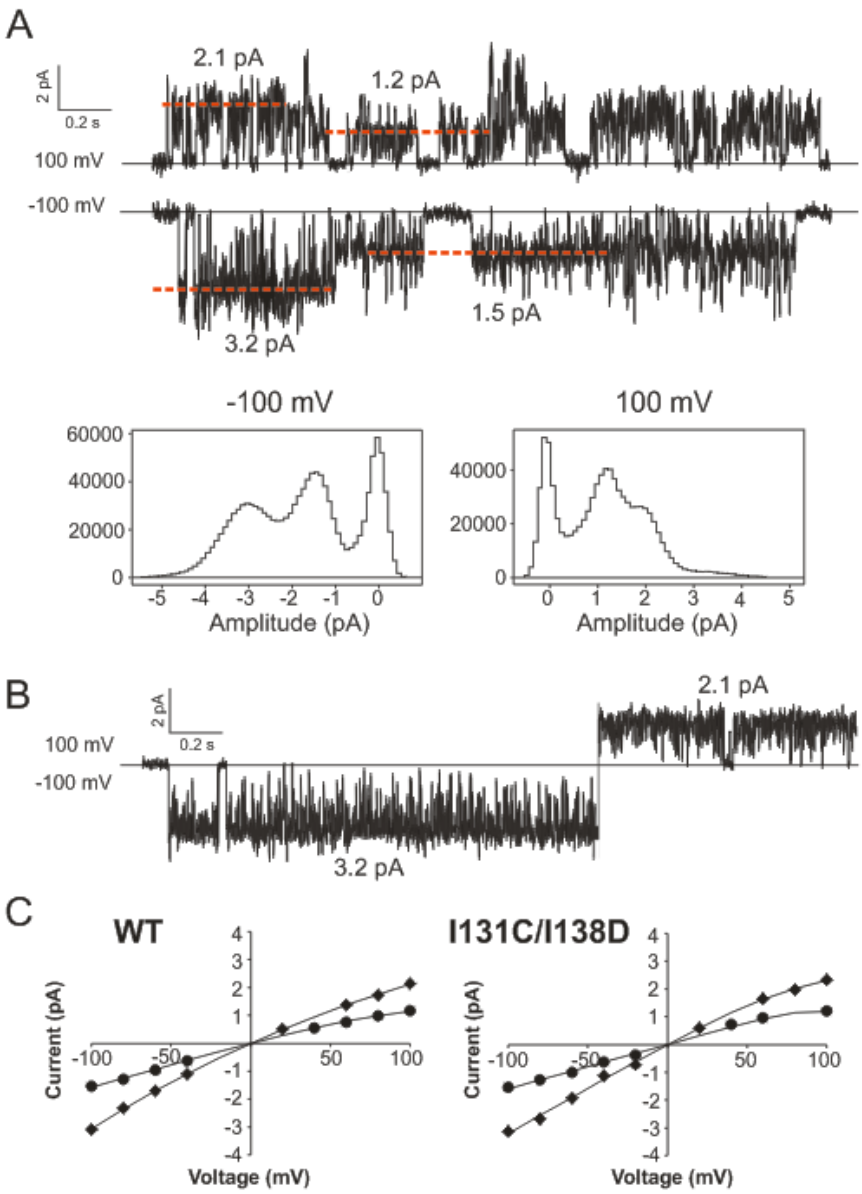

Figure 3.7 Single channel amplitudes of KirBac1.1 show two predominant conductance levels and inward rectification. (A) Representative traces from a WT single channel recording at +100 mV and -100 mV. The red dashed lines indicate the current amplitudes of the single channel openings and correspond with the peaks in the histograms. Below are all-points-histograms of all channel openings from the entire recording. (B) Single channel opening from the same recording as in (A) showing the

current amplitude of a single opening/conductance state at -100 mV and +100 mV. (C) Averaged I-V plots of single channel amplitudes for WT and I131C/I138D (n= 4 ± s.e.m., the error bars are too small to be seen). The data points show only the two most prevalent conductance states (for WT, 15 pS and 32 pS at -100 mV, 12 pS and 22 pS at +100 mV). The solid lines have no theoretical meaning.

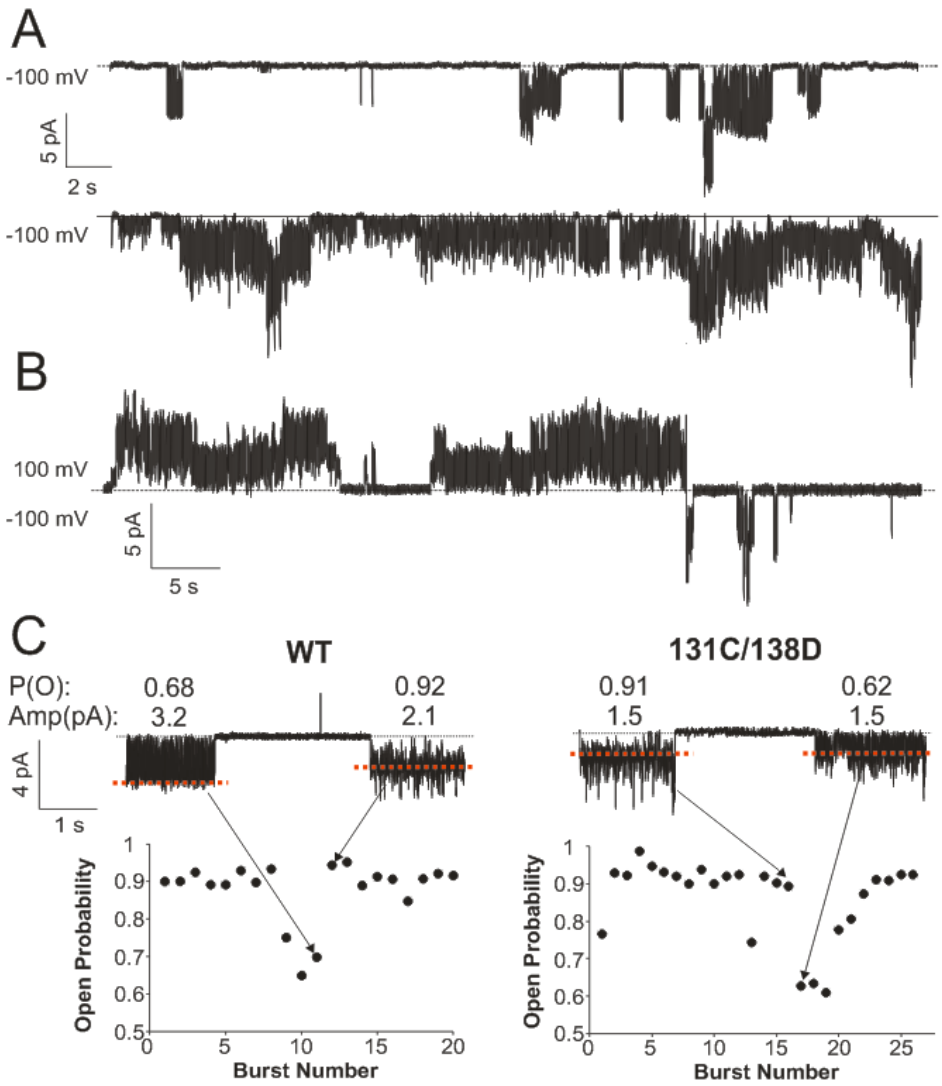

Figure 3.8 Single channel recordings show significant gating heterogeneity. (A) Two continuous recordings of WT single channels at -100 mV showing low open probability (top) and high open probability (bottom) currents. (B) A continuous recording of WT single channels at the indicated voltages. (C) Plots of intraburst open probability for every channel burst in a patch of WT and I131C/I138D. The currents above show two bursts at -100 mV with open probabilities that correspond to the data points indicated by the arrows. Open probability and current amplitude are shown above each burst.

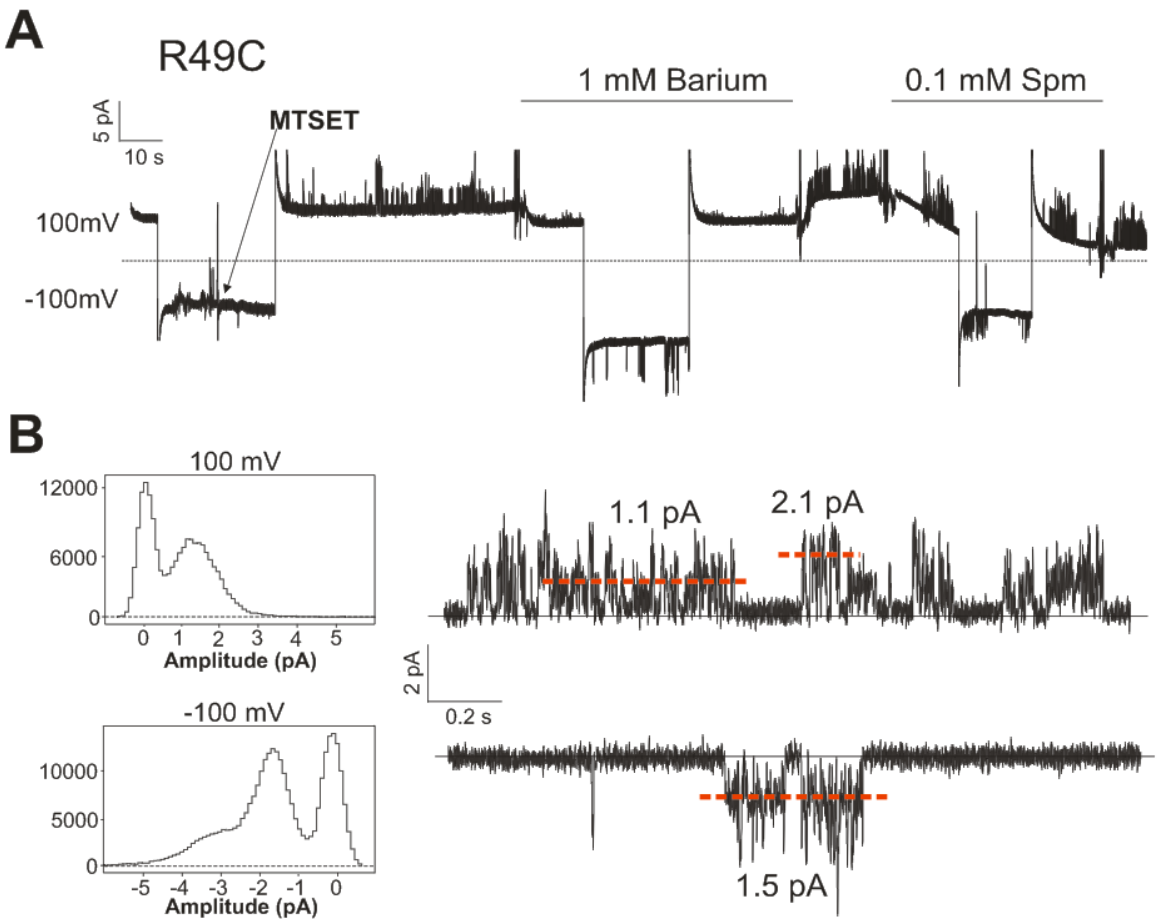

Figure 3.9 Activation of KirBac1.1[R49C] by MTSET. (A) Continuous recording of R49C held at +100 mV and -100 mV. The recording shows significant leak current and discrete channel currents above leak. 0.1 mM MTSET solution was applied as shown by the arrow, and solution changes were made at the indicated bars. (B) All-points-histograms of the recording above with representative traces at +100 mV and -100 mV. The red dashed lines indicate current amplitudes that correspond with peaks in the histograms.

III. DISCUSSION

Validation of KirBac1.1 as a Kir channel

The prokaryotic potassium channel, KcsA, has been widely used as a model channel to investigate mechanisms of ion permeation, selectivity and gating. Other prokaryotic potassium channels, such as MthK and KvAP have followed suit in becoming the subject of numerous structural and electrophysiological studies. Since the structure was solved, however, functional studies of KirBac1.1 have been limited to $^{86}Rb^{+}$ flux assays and bacteria or yeast complementation screens (52, 53, 195, 248). In this report, we confirm by patch-clamping giant liposomes that KirBac1.1 is a functional potassium channel and that voltage-clamped currents exhibit behavior that is consistent with the findings of $^{86}Rb^{+}$ flux assays. Here, we show that the mutation I138D, equivalent to the "rectification controller" residue in eukaryotic Kir channels, confers the signature strong inward rectification as in Kir1.1 and Kir6.2. The I131C/I138D mutant exhibits strong block by spermine with steep voltage-dependence confirming that KirBac1.1 is a bona fide inward rectifying potassium channel, and strengthening the validity of structural homology models of eukaryotic Kirs generated using the KirBac1.1 structure. Such homology models will be useful in understanding interactions of polyamines and other blockers within the pore of Kirs.

Multiple single channel conductances in KirBac1.1

Single channel analyses of KcsA have revealed unusual features such as prominent subconductance states and variable gating kinetics that are rarely seen among eukaryotic

channels. For instance, multiple subconductance states have been reported for KcsA reconstituted in liposome-protoplast vesicles (17), lipid bilayers (18, 250, 251), and giant liposomes (249). In excised patch-clamping of giant liposomes, the open probability of KcsA is highly variable from patch to patch (20, 252). Intraburst kinetics also show multiple, distinct gating modes (249). Interestingly, we show in this study that KirBac1.1 exhibits many of these same features in terms of multiple single channel levels and kinetic heterogeneity. The unusual single channel conductance and gating properties of the prokaryotic channels, KcsA and KirBac1.1, lead us to speculate whether there are key differences between the protein and lipid environment of these channels reconstituted in liposomes and that of eukaryotic channels expressed in cell membranes. However, the fact that single channel currents of purified, reconstituted human Kir2.1 channels in giant liposomes behave similarly to previous reports in cellular systems and do not show multiple conductance states argues against such a hypothesis (Chapter 5).

Several studies have reported multi-conductance behavior in steady-state single channel recordings of other K^+ channels. For example, Kir2.1 single channel currents can show multiple levels due to block by micromolar concentrations of cations like Ca^{2+} and Mg^{2+} (253, 254). Such behavior is unlikely to underlie multiple conductances in the present case, since the addition of 1 mM EDTA to the recording solutions does not alter the multi-conductance behavior of KirBac1.1 (data not shown). In KcsA, multiple current levels have been attributed to coupled gating from clusters of channels (252). However, this too is unlikely since the levels observed in KirBac1.1 are not obvious multiples of a unit conductance.

One interesting possibility arises from a series of studies where protonatable residues such as lysine, arginine and histidine were systematically engineered along the M1 and M2 transmembrane helices of the nicotinic acetylcholine receptor, resulting in two fluctuating conductance levels that correspond to the protonated and deprotonated states (255, 256). A similar mechanism, where positively-charged moieties in the pore cause subconductances, has been reported in the Kir channel, Kir6.2 (257). Modification of the pore cysteine mutant, Kir6.2[L164C], with MTSEA leads to subconductances when less than all four subunits are hit. It is possible that the multi-conductance behavior of KirBac1.1 is due, in part, to protonatable residues such as H117, H124, H210 and H219 that produce reversible positive charges near the channel pore. That these multiple conductances are likely to be a consequence of permeant ion interactions with the pore is strengthened by studies of single channel properties of Kir2.1 with mutations in the selectivity filter or in the presence of permeant ions other than K^+ (146, 258). These studies also reveal complex subconductance behaviors, including bursts of a subconductance level with brief transitions to larger openings.

Orientation of KirBac1.1 reconstiuted in giant liposomes

The first electrophysiological studies of KcsA were performed using planar lipid bilayers and it was quickly recognized that channels could conceivably insert in either orientation (19, 250, 259). The problem of channel orientation was addressed by exploiting known asymmetries in channel block (CTX or TEA) and structure (modification of substituted cysteines). These studies demonstrated that KcsA is oriented predominantly in one

direction in a reconstituted lipid bilayer, which corresponds to the C-terminus of the channel facing the bath in an excised patch (249). A number of observations from the present study suggest that KirBac1.1 reconstituted in giant liposomes has a similar preference for this orientation. First, Ba^{2+} and spermine block consistently show a single component, leaving ~10% residual current, some of which could be accounted for by leak (Figure 3.4). If channel orientation is 50:50, one would expect to see only half of the current blocked by a single component. This, in fact, is what is seen with spermine inhibition in small proteoliposomes using the Rb^{+} flux assay (Figure 3.3B). The strong and near-complete block by spermine, however, in I131C/I138D observed by patch-clamp is consistent with most of the channels oriented with their C- and N-terminal ends facing the bath. Intuitively, it seems possible that KirBac1.1 channels reconstituted in liposomes for $^{86}Rb^{+}$ flux may have a 50:50 channel orientation, while giant liposomes for patch-clamp show a preferential one-sided orientation since the formation of giant liposomes involves an extra dehydration/rehydration step that could alter orientation (see Methods). During the dehydration step, a thin layer of lipid and channel protein is presumably formed on the glass slide, and the channels may have a preferential orientation in terms of how they interact with the glass surface.

A second observation is that PIP_2 applied in the bath inhibits most KirBac1.1 currents (Figure 3.2). Overwhelming evidence from eukaryotic Kir channels indicate that PIP_2 activation occurs by interaction with the cytoplasmic end of the channel at the inner leaflet of the membrane (45, 180, 197). PIP_2 inhibition of KirBac1.1 also has a similar dependence on the number of phosphate groups (greater inhibition with more negative

charges in the head group) and the length of the lipid tail (short-chain PIP_2 inhibition is reversible) as eukaryotic Kirs (53). Assuming a similar interaction of PIP_2 with KirBac1.1 as with eukaryotic Kirs, and assuming that PIP_2 partitions into only one side of the membrane leaflet, most of the channels, again, must be oriented with their "cytoplasmic" end facing the bath. Similar to the spermine block results, extraliposomal application of PIP_2 in the $^{86}Rb^+$ flux assay causes only ~50% block suggesting a 50:50 orientation in these smaller liposomes (53).

Lastly, all single channel recordings consistently show the same amplitude-voltage relationship (inward rectification) and gating pattern, suggesting a preferential channel orientation. Indeed, single channel currents of MTSET-activated R49C, which requires that the channels be oriented with their "cytoplasmic" end facing the bath, resemble those of WT and I131C/I138D (Figure 3.9). Future electrophysiological studies of KirBac1.1 should focus on resolving this uncertainty about channel sidedness. Cysteine mutants such as R49C and K57C that require MTSET modification for activity should provide a useful tool for isolating channels of a single orientation.

Conclusion

The KirBac1.1 and KirBac3.1 crystal structures have been used extensively in a number of molecular modeling studies (47, 50). In particular, a structural model of KirBac1.1 in the open conformation has been generated from 2D crystals of KirBac3.1 captured in two distinct conformations (246, 260). Simulations using the open and closed structures of KirBac1.1 have led to unique insights on how channel conformation affects ion

permeation, membrane-channel interactions and drug-channel interactions (48, 261, 262). Until now, no electrophysiological data has been available to supplement these computational studies. We report voltage-clamp recordings of KirBac1.1 currents and confirm that this prokaryotic protein behaves functionally as an inward rectifying potassium channel. Recent studies of KcsA have been a testament to the power of combining structural and biochemical information with electrophysiology in understanding channel function (20, 263). It is now possible to take a similar approach in a model Kir channel and to develop more detailed molecular models of permeation, gating and strong inward rectification.

CHAPTER 4

MECHANISM FOR CATION SELECTIVITY-INACTIVATION COUPLING IN POTASSIUM CHANNELS

Published in an altered form in PNAS. 108(13): 5272-5277.

Cheng WWL, McCoy JG, Thompson AN, Nichols CG, and Nimigean CM

I. INTRODUCTION

In inward rectifying potassium (Kir) channels, a key structural feature of this network is a salt bridge that forms a molecular "bowstring" (118) bridging the top and bottom of the selectivity filter loop (56, 118, 119) (Figure 4.1). Alterations in this salt bridge interaction are known to disrupt selectivity (118-120); several mutations have dramatic effects on permeation, rendering the channel essentially non-selective and highly permeable to Na^+. It has also been proposed that members of one subgroup of this family, the HCN channels, are less K^+-selective because they lack this network of molecular restraints (264), but the relevance of this structural network for selectivity in channels other than inward rectifiers as well as the mechanism responsible for variable selectivity remains to be seen. Furthermore, disruption of this salt bridge in Kir1.1, which alters K^+ selectivity (120), also leads to the induction of an inactivation phenomenon similar to C-type inactivation in voltage-gated K^+ channels (265). There is also a correlation between C-type inactivation and ion selectivity in eukaryotic voltage-gated K^+

channels: *Shaker* channels and other Kv channels such as Kv2.1 show decreased K^+ and increased Na^+ permeability when progressing to a C-type inactivated state (114, 115). By contrast, Na^+ and even the large glucose-like molecule, NMG, are permeable through open Kv3 channels or a Kv1.5 mutant (R487V) where C-type inactivation is reduced (117, 266). The mechanism by which changes in selectivity are brought about by C-type inactivation is as of yet unknown.

High resolution structures of KcsA (23, 100) reveal that E71 and D80 form a hydrogen bond interaction (267) at a similar location to the salt bridge in Kir channels (119) (Figure 4.1). The E71A mutant that disrupts this bridge has been extensively studied to elucidate the mechanism of inactivation in KcsA, which is attributed to gating at the selectivity filter and likened to C-type inactivation in Kv channels (268-270). The E71A mutation abolishes pH-dependent inactivation, and the consequent high steady state open probability makes E71A a convenient model for electrophysiological studies (271-273). Given the similarity between the E71-D80 interaction in KcsA and the salt bridge in Kir channels and the non-inactivating phenotype of E71A, we questioned whether this mutation also alters selectivity of the channel. Molecular simulations show that the mutation changes the conformational dynamics and energy landscape of the selectivity filter (267, 269), and crystal structures of E71A in high concentrations of K^+ reveal two selectivity filter conformations: one which resembles the WT "conductive" structure (23) and a "flipped" structure showing outward movement of the D80 side chain along with distortion of carbonyls and changes in the location and occupancy of the ion binding sites (268) (Figure 4.1). E71A channels also show reduced extracellular affinity

of TEA block and a pH-dependent increase in inward conductance compared to WT channels that may be related to the conformational changes in the "flipped" structure (274, 275). However, reversal potential shifts in bi-ionic conditions suggest no change, or even increased, selectivity for K^+ over Na^+ between E71A and WT KcsA (268, 276). In the present study, we demonstrate that disruption of the E71-D80 interaction in E71A KcsA does reduce cation selectivity and we correlate these findings with crystal structures of E71A in the presence of high Na^+ and no K^+, which show that this mutation prevents collapse of the selectivity filter.

II. RESULTS

E71A KcsA displays altered K^+ selectivity in $^{86}Rb^+$ flux assays

We examined selective permeation of E71A by assaying liposomal $^{86}Rb^+$ accumulation driven by different cations. Uptake of $^{86}Rb^+$ into proteo-liposomes loaded with a high concentration of a test cation is dependent on the trans-liposomal permeability of this cation. At pH 7, K^+ drives $^{86}Rb^+$ uptake in both WT and E71A (Figure 4.2A). However, while WT shows no detectable Na^+-driven $^{86}Rb^+$ uptake, E71A is clearly permeable to Na^+, which drives ~20% of the uptake driven by K^+ (Figure 4.2A). The time course of K^+-driven uptake for E71A is much faster (>10x) than for WT KcsA, and it is conceivable that the apparent increase in Na^+ permeation is simply a result of the kinetics of uptake. However, KcsA is pH-sensitive, and pH can be varied to make the rates of WT and E71A uptake comparable. At pH 8 for E71A and pH 4 for WT, the rate of K^+-driven uptake is nearly equivalent, and still only E71A shows measurable

Na^+-driven $^{86}Rb^+$ uptake (Figure 4.2B). $^{86}Rb^+$ flux through WT KcsA is undetectable when Na^+, Li^+, and NMG^+ are used to drive uptake, while Cs^+ and NH_4^+ show moderate uptake, consistent with previously published results (226) (Figure 4.2C). By contrast, E71A shows significant $^{86}Rb^+$ uptake, driven by Na^+, Li^+, Cs^+ and NH_4^+ (Figure 4.2C), indicating a reduction of K^+-selectivity in E71A.

E71A KcsA displays altered K^+ selectivity in $^{22}Na^+$ flux assays

To test the role of K^+ in determining Na^+ permeation, we extended the flux experiment to assay $^{22}Na^+$ accumulation. When K^+ is the intra-liposomal cation, both WT and E71A show robust $^{22}Na^+$ uptake that is significantly slower than $^{86}Rb^+$ uptake, as would be expected for a cation of lower permeability (Figure 4.3A and 4.3B). However, when Na^+ is the intra-liposomal cation, WT shows nearly immeasurable $^{22}Na^+$ uptake in stark contrast to E71A, which remains highly permeable to $^{22}Na^+$ (Figure 4.3A and 4.3B). These data indicate that WT KcsA becomes non-conductive in the absence of K^+, while E71A remains conductive and permeable to Na^+.

Intuitively, it seems appropriate to compare differences in permeability between WT and E71A of different cations by measuring rates of radiotracer uptake (226). However, rate of uptake is not the only indicator of permeability or channel activity in the flux assay. A decrease in channel activity also typically results in a decrease in the amount of uptake and the reason for this remains unclear (277). E71A shows more $^{22}Na^+$ uptake than WT when K^+ is the intra-liposomal cation (Figure 4.3A and 4.3B), suggesting that the mutant is more permeable to Na^+ even in the presence of K^+.

Furthermore, E71A shows more $^{22}Na^+$ uptake driven by Na^+ than driven by K^+ (Figure 4.3B), suggesting that Na^+ is less permeable through E71A when K^+ is present, consistent with previous findings that a multi-K^+ ion configuration in the selectivity filter is an important determinant of selectivity in KcsA (238).

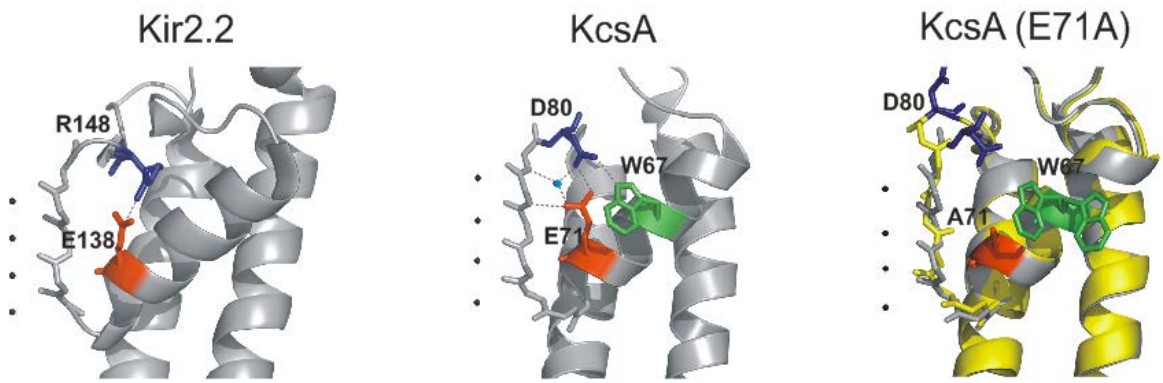

Figure 4.1 The E71-D80 interaction is structurally analogous to the molecular "bowstring" in Kir channels and is disrupted in the E71A KcsA mutant. Images are taken from crystal structures of Kir2.2 (3JYC), KcsA (1K4C), and the "flipped" (yellow) and "non-flipped" (grey) structures of the E71A mutant of KcsA (1ZWI, 2ATK), showing the selectivity filter region from one subunit and highlighting the residues involved in a salt bridge interaction in Kir2.2, and the hydrogen bond interactions in KcsA. Black spheres represent potassium ions and the blue sphere represents water.

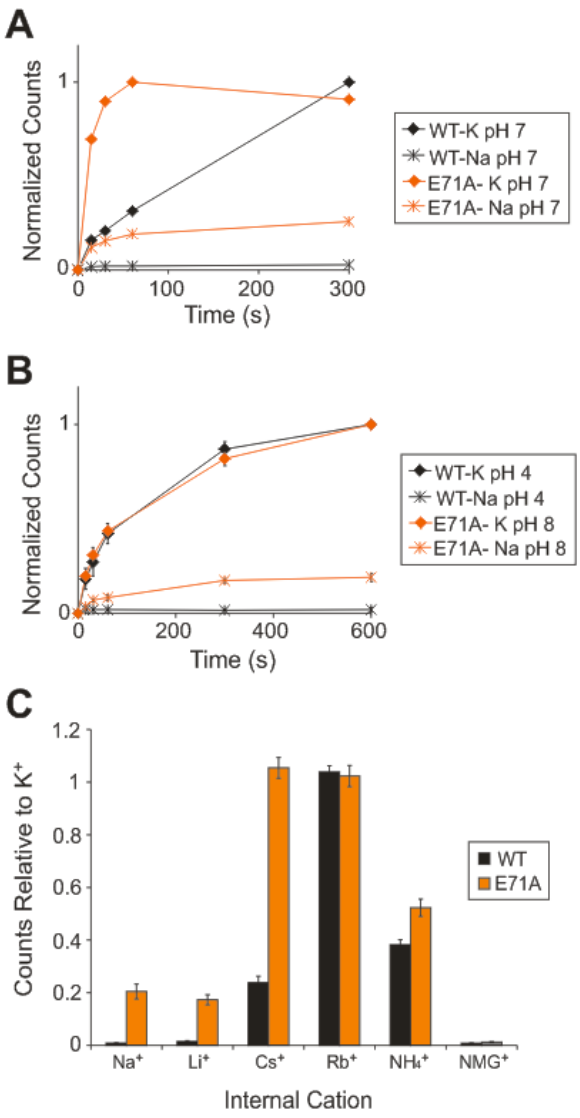

Figure 4.2 The E71A KcsA mutant is more permeable to Na^+, Li^+, Cs^+ and NH_4^+. (A) Representative time courses of a liposomal $^{86}Rb^+$ flux assay of WT and E71A at pH 7 driven by intra-liposomal K^+ or Na^+. Each time course is normalized to its own maximum level of uptake. (B) Same as (A) except assay performed at pH 4 for WT and pH 8 for E71A (n = 4, mean ± s.e.m.). (C) Maximum $^{86}Rb^+$ uptake for WT and E71A at pH 7 driven by different intra-liposomal cations and normalized to uptake driven by K^+ (n = 5, mean ± s.e.m.).

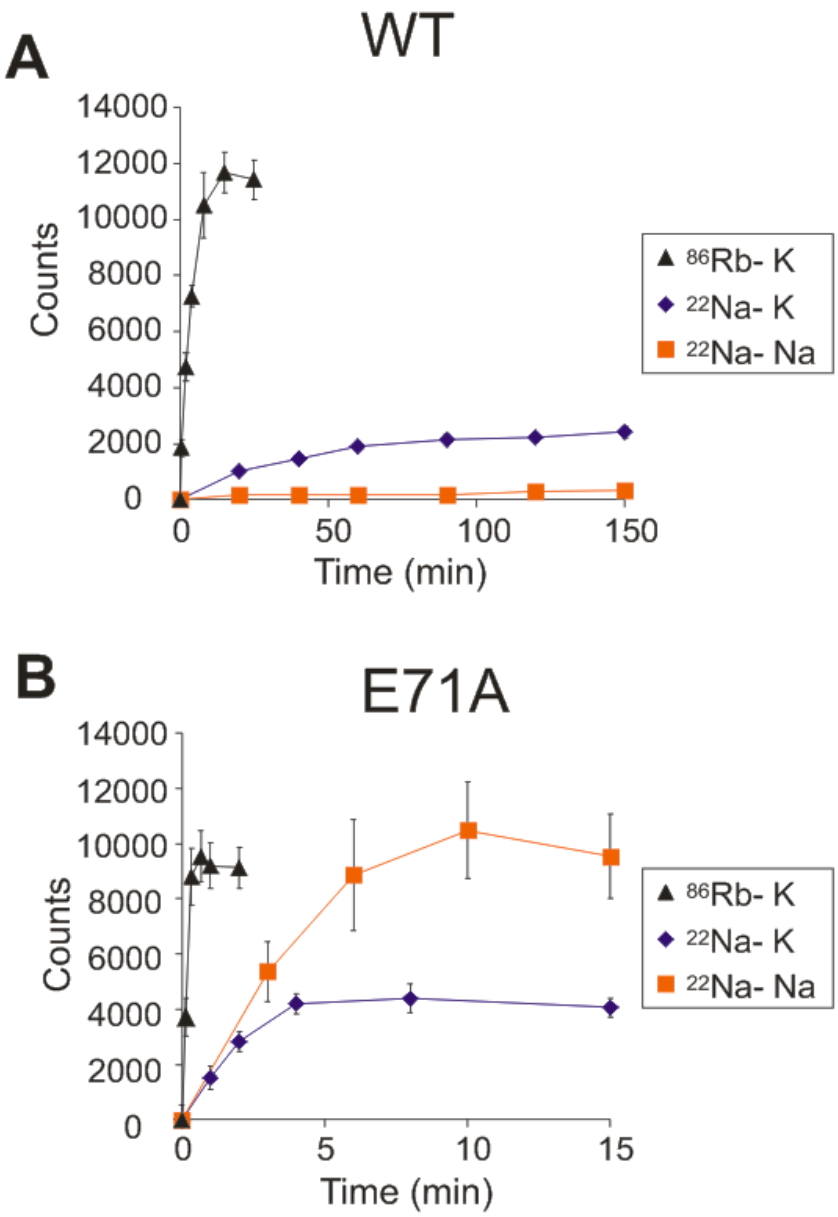

Figure 4.3 WT KcsA, but not E71A, becomes non-conductive in the absence of K^+ and presence of Na^+. (A) Time courses of WT fluxes at pH 7, showing K^+-driven $^{86}Rb^+$ uptake (black), K^+-driven $^{22}Na^+$ uptake (blue), and Na^+-driven $^{22}Na^+$ uptake (orange) (n = 3, mean ± s.e.m.). (B) Same as (A) except for E71A (n = 3, mean ± s.e.m.).

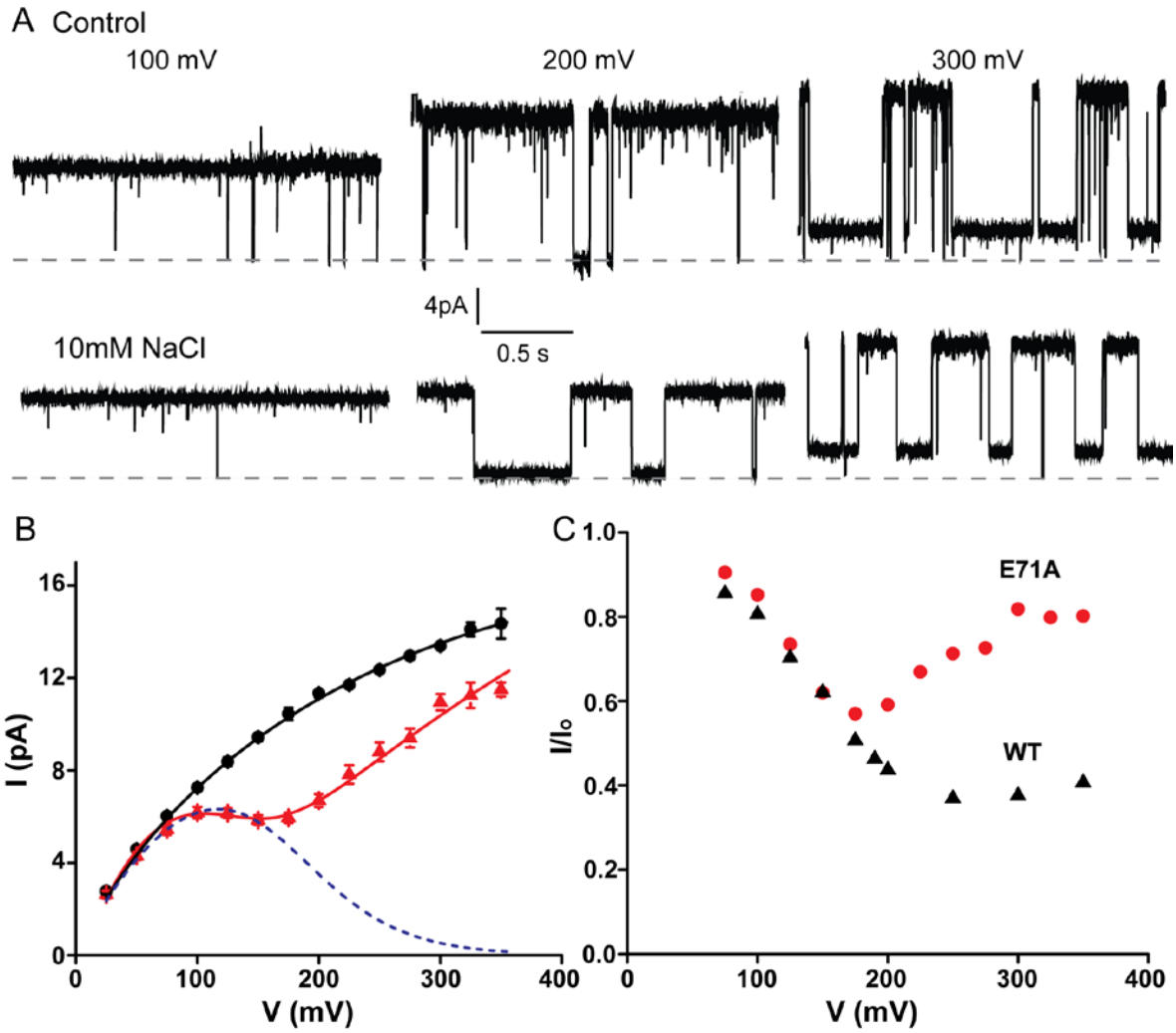

Figure 4.4 Na^+ blocks E71A KcsA current in a voltage-dependent manner. (A) Representative traces from single channel recordings of E71A KcsA currents with or without the presence of 10 mM NaCl at 100, 200, and 300 mV. There is a highly reproducible voltage-dependent subconductance level in the E71A KcsA channel that becomes prevalent at voltages higher than 200 mV in both the control and the Na^+-modified currents that we did not investigate in detail. (B) Open channel IV curves calculated from control (black circles, n=8, mean ± s.e.m.) and Na^+-blocked (red triangles, n=4, mean ± s.e.m.) single-channel currents. The curve through the control

points is a hyperbolic fit with no theoretical significance. The dotted blue curve is a fit with eq.1 with the fitted block parameters: $K_B(0)$= 573 mM and Z= 0.64 (compared with 500 mM and 0.55 for WT) and the smooth red line is a fit with the equation: $I(V)=I_0(V)(1+B/((1+K/Q_K)(K_B+Q_B)))^{-1}$, where $K_B=K_B^{ap}(0)\exp(-zFV/RT)$ and Q_K and Q_B are Michaelis-type constants for K^+ and Na^+ (see (240)). Fitted parameters are: Q_K is $6.1\exp(z_1FV/RT)$ where z_1 is 0.34, Q_B was set to $0.5\exp(-z_1FV/RT)$, and K_B is $283\exp(-z_2FV/RT)$ where z_2 is 0.9. (C) Plot of the ratio of Na^+-blocked and control currents (I/I_0) for E71A KcsA (red) and WT (black) showing the much larger increase in current from Na^+-modified E71A currents in the punchthrough region.

Pronounced relief of Na^+ block at high voltages in E71A KcsA

If Na^+ shows increased permeability through E71A KcsA, one would expect to see differences between intracellular Na^+ block in the pores of the E71A and WT channels. Similar to its effects in WT KcsA (240), intracellular Na^+ modifies K^+ current through E71A KcsA by binding with very fast, unresolved kinetics in the pore thus reducing the apparent single-channel amplitude of the current in a voltage-dependent manner (Figure 4.4). While the current-voltage (IV) curve in the absence of Na^+ displays the expected monotonic increase with voltage, the Na^+-modified E71A IV curve is distinctly biphasic (Figure 4.4B). In the first region, from 0 to 150-175 mV, intracellular Na^+ causes weak voltage-dependent block in the inner cavity, leading to a region of negative conductance. A similar, but more pronounced, negative conductance region is also present in the WT KcsA channel (240). This first part of the curve can be approximated with a Woodhull equilibrium model for block ((239), dashed blue line, eq. 1) with similar parameters to those obtained from the WT channel (Figure 4.4, legend)), suggesting that the inner cavity binding site for Na^+ is the same in WT and E71A. At the most positive voltages the Na^+-modified current increases after a slight dip, almost linearly and parallel to the control curve (Figure 4.4B). This "punchthrough" region was previously interpreted as relief of block by Na^+ ions dissociating forward through the selectivity filter rather than backwards towards the intracellular solution. Na^+ begins to punch through the selectivity filter of E71A at a lower voltage than in the WT channel (~175 mV compared to ~225 mV, Figure 4.4C) and the current following relief of block by Na^+ is significantly larger in E71A suggesting that Na^+ escapes through the selectivity

filter with greater ease than in WT (Figure 4.4C). As detailed in Methods, we calculated a lower limit for the selectivity of punchthrough, which we term the escape ratio (Eq.3). This escape ratio, calculated at a voltage where punchthrough dominates but the control current is not yet diffusion limited (275-300 mV), is between 6-10 ($k_2/b_2<10$); i.e. for each Na^+ ion escaping through the selectivity filter at high voltages there are at least 6 K^+ ions accompanying it. In contrast, the escape ratio previously obtained for WT KcsA channel was at least 30 K^+ ions permeating through the pore for each Na^+ ion ($k_2/b_2>30$) (240).

Summarizing our functional data, the E71A mutation in KcsA reduces cation selectivity. E71A is more permeable to Na^+, Li^+, Cs^+, and NH_4^+ than the WT channel as determined by radiotracer flux assays. The reduced cation selectivity of E71A is most apparent in the absence of K^+, where WT KcsA becomes non-conductive but E71A remains conductive and permeable to Na^+. E71A also shows reduced selectivity (i.e. increased permeability to Na^+) in the presence of K^+, as determined by $^{22}Na^+$ flux, and this finding is substantiated by an increased probability, in E71A, for blocking Na^+ ions to escape through the selectivity filter at high voltages compared to WT.

Reversal potential measurements lack sensitivity to detect altered selectivity in this case

The suggestion of Cordero-Morales et al (20) that K^+ selectivity is increased in the E71A channel was based on extrapolated reversal potentials in bi-ionic conditions (200 mM Na^+ inside and 200 mM K^+ outside). Given the lack of any measurable Na^+ currents, and the fact that KcsA channels are predominantly blocked by high concentrations of

intracellular Na^+ (20),(237), conclusions about permeability ratios extracted from these measurements must be taken tentatively. We repeated these experiments by measuring reversal potential shifts with intracellular K^+ and varying concentrations of extracellular (pipette) K^+ and Na^+ chosen to maintain equal ionic strength across the membrane (Figure 4.5A). Under these conditions, E71A reversal potentials are statistically not different from WT (Figure 4.5B). E71A reversal potential shifts with varying extracellular K^+ and no Na^+ (Figure 4.5B, black diamonds) are significantly different from pure K^+-selectivity (black line) and surprisingly close to the values obtained with Na^+, indicating that such measurements with Na^+ are approaching the limit of the analysis. Indeed, a more sensitive strategy using comparative analysis with the highly selective ionophore, valinomycin, was needed to achieve a more accurate estimate of selectivity in KcsA (237). The fact that slightly higher reversal potential shifts were obtained for E71A (Figure 4.5B) (20), may be due to higher open probability, making the measurements more accurate than for WT. We propose that, in the presence of K^+, E71A exhibits a small reduction in selectivity that is detectable in more sensitive flux assays (Figure 4.3) and a Na^+ blocker punchthrough experiment (Figure 4.4), but not reversal potential measurements.

E71A selectivity filter does not collapse in the absence of K^+

To gain insight to the structural features leading to these selectivity differences between WT and E71A KcsA, we crystallized E71A KcsA in the absence of K^+ but in the presence of 150 mM NaCl (relevant statistics are listed in Table 2). The resulting model,

shown in Figure 4.6A, has a selectivity filter that looks very similar to that of a previously published E71A KcsA "flipped" structure solved in the presence of high K^+ (PDBID 2ATK (20)) (Figure 4.6C). Specifically D80, which was shown to coordinate E71 and W67 in the high-resolution WT KcsA structure (PDBID 1K4C (23)) (Figure 4.6B), is flipped such that the backbone atoms of residues 79, 80, and 81 are displaced from their previous positions by as much as 5 Å (Figure 4.6D). In addition, the carbonyls in the selectivity filter, which form the K^+ binding sites, are noticeably shifted from their positions in the WT structure, particularly that of V76, which is rotated almost 180° away from the pore. Importantly, our E71A KcsA structure in 150 mM Na^+ bears no resemblance to the collapsed, "non-conductive" low K^+ WT KcsA structure (PDBID 1K4D (23)) (compare Figure 4.6A and 4.6B).

In contrast with the "flipped" high K^+ structure, where four K^+ ions were modeled in the S1 through S4 positions, in our "flipped" high Na^+ structure we only observed electron density in two locations within the filter, directly between the carbonyls of G77 and between the carbonyls of T75 (Figure 4.6A and 4.6C). As the centers of the densities are relatively planar with the carbonyls, and the structures were obtained in high Na^+, they likely correspond to either Na^+ or water molecules. The distances between the atoms modeled into these densities and the carbonyl atoms range from 2.5 to 2.6 Å, which is intermediate between what would be expected for coordination of Na^+ or K^+. The available resolution, coupled with uncertainties due to the selectivity filter being aligned along a symmetry axis, does not permit us to identify the atoms/molecules bound within the selectivity filter with any certainty, and we tentatively modeled them as Na^+ ions

based on our functional measurements suggesting there is Na^+ flux through the E71A KcsA channel (Figure 4.2, 4.3, and 4.4). However, and regardless of the nature of these densities, the fact that we did not obtain the collapsed, putatively non-conductive filter structure (23) with E71A in the absence of K^+ is consistent with the notion that the collapsed structure represents the inactivated state (278) and, unlike the highly selective WT KcsA, E71A remains conductive and permeable to Na^+ in the absence of K^+ (Figure 4.3).

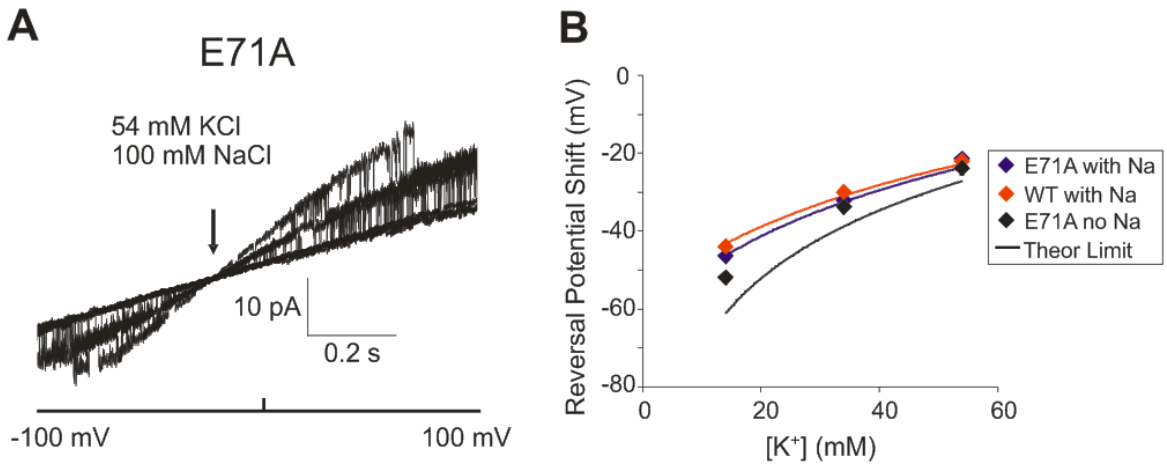

Figure 4.5 Reversal potential shifts indicate minimal effect of E71A on selectivity. (A) Representative voltage ramp (-100 mV to 100 mV over 1 s) currents of E71A from excised patch-clamp of giant liposomes with 154 mM KCl in the bath and 54 mM KCl and 100 mM NaCl in the pipette. Arrow indicates reversal potential. (B) Reversal potential shifts vs. varying concentrations of K^+ and Na^+ (i.e. in mM, 54 K and 100 Na, 34 K and 120 Na, 14 K and 140 Na) in the pipette for WT (red) and E71A (blue). Fitting these data with the GHK equation yields a P_{Na}/P_K of 0.10 and 0.08, respectively. Also shown are reversal potential shifts for E71A with no Na^+, varying pipette K^+ concentration (black diamonds), and the prediction for an ideal K^+ selective channel based on the Nernst equation (black line).

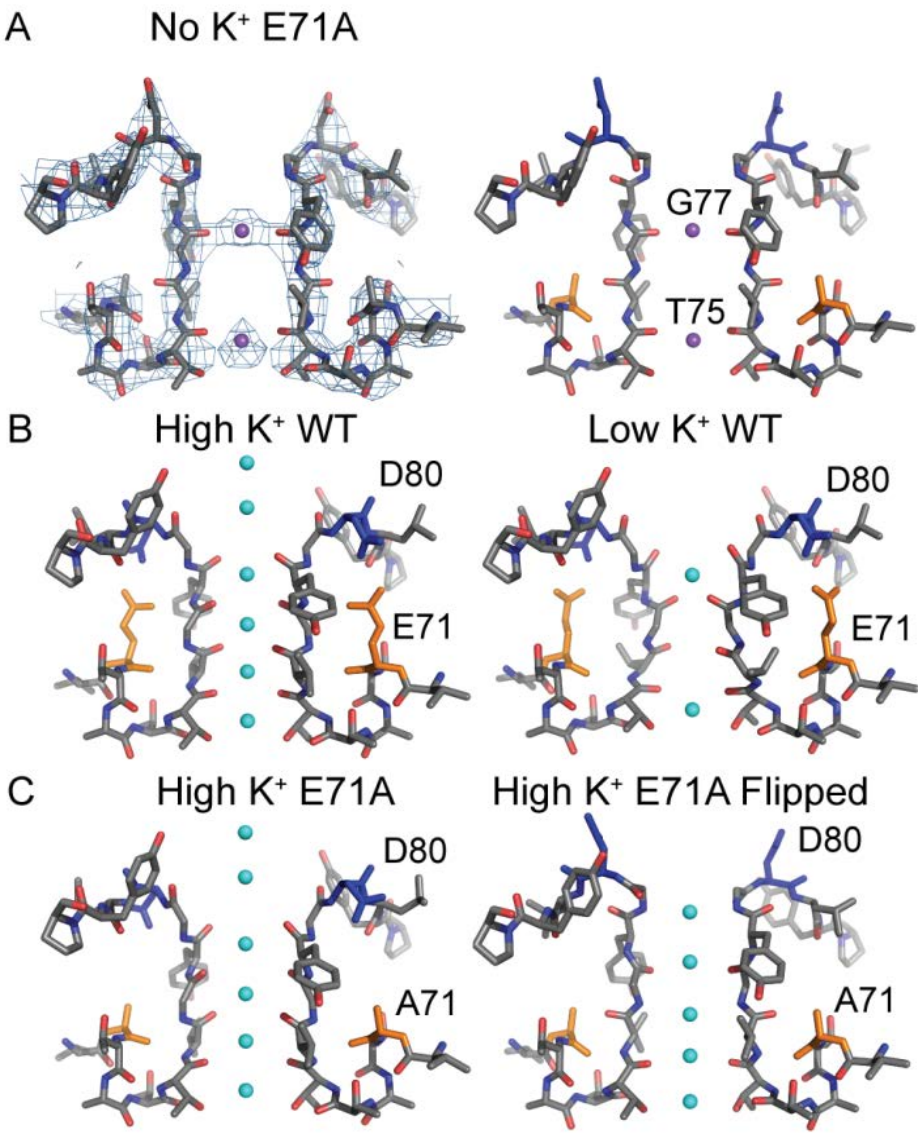

Figure 4.6 Crystal structure of E71A KcsA features a non-collapsed selectivity filter. (A) Stick model of selectivity filter from E71A KcsA in the presence of 150 mM NaCl and accompanying electron density (2Fo-Fc) contoured at 1.0 sigma. Residues G77 and T75 are labeled. For comparison, (B) Stick models of filters of the conductive and collapsed states of WT KcsA (1K4C and 1K4D (23)). (C) Stick models of filters of the non-flipped and flipped structures of E71A KcsA (2ATK and 1ZWI (20)). Bound ions are purple (Na^+) or cyan (K^+) spheres.

Table 2 Data collection and refinement statistics (molecular replacement)

	High Na^+
Data collection	
Space group	I4
Cell dimensions	
a, *b*, *c* (Å)	154.90,154.90,75.49
α, β, γ (°)	90.0,90.0,90.0
Resolution (Å)	50.0-3.8(3.89-3.80) *
R_{sym} or R_{merge}	10.7(44.5)
$I / \sigma I$	11.9(2.7)
Completeness (%)	99.8(100.0)
Redundancy	3.6(3.6)
Refinement	
Resolution (Å)	3.80
No. reflections	8449
R_{work} / R_{free}	24.9 / 28.4
No. atoms	
Protein	4070
Ligand/ion	2
Water	0
B-factors	
Protein	79.5
Ligand/ion	19.6
Water	N/A
R.m.s. deviations	
Bond lengths (Å)	0.005
Bond angles (°)	0.791

*Number of xtals for each structure should be noted in footnote. *Values in parentheses are for highest-resolution shell.

III. DISCUSSION

Role of the E71-D80 interaction in determining K^+-dependent cation selectivity

The H-bond interaction between E71 and D80 in KcsA is equivalent to the R-E salt-bridge in inward rectifiers that is an important molecular determinant of K^+-selectivity in these channels (118-120) (Figure 4.1). The E71A mutation exhibits a non-inactivating phenotype, and has been used as a structural model of C-type inactivation (20, 269). There is a well-established connection between C-type inactivation and ion selectivity in Kv channels (114, 115, 117, 266). However, despite marked structural changes in the E71A selectivity filter (20) (Figure 4.1), the E71A mutation is not reported to significantly alter K^+ selectivity against Na^+ (20) (Figure 4.5). Using flux assays, we find that E71A markedly alters selectivity in KcsA by increasing permeability to Na^+, Li^+, Cs^+, and NH_4^+ in the absence of K^+ (Figure 4.2C and Figure 4.3). Furthermore, even in the presence of K^+, E71A shows reduced cation selectivity as detected by an increase in $^{22}Na^+$ flux (Figure 4.3) and punchthrough of blocking Na^+ ions (Figure 4.4).

In the presence of Na^+ but no K^+, KcsA exhibits what has been called a 'second layer' of selectivity where the filter adopts a collapsed, non-conductive structure and becomes impermeable to Na^+ (23, 107, 279). Our data provide a functional correlate to this structural observation by demonstrating that, in the absence of K^+, KcsA becomes non-conductive and impermeable to Na^+ (Figure 4.3A). E71A, on the other hand, abolishes this second layer of selectivity (Figure 4.3B), similar to a KcsA mutant, in which residue G77 is replaced by D-Ala. In the absence of K^+, $KcsA^{D\text{-}Ala77}$ is permeable

to Na^+ and does not show a collapsed filter (280). This suggests that E71A must maintain a conductive filter in the absence of K^+, and is exactly what we observe in our K^+-deficient E71A structures, which show selectivity filters in a conformation identical to the "flipped" E71A high K^+ structure (Figure 4.6). Maintained pore conformation in zero K^+ has also recently been observed in the K^+ channel MthK, and was attributed to differences in the H-bond network behind the filter between MthK and KcsA (138).

The functional difference between E71A and WT in the presence of ions other than K^+ is not just whether the WT channel is conductive or non-conductive. When $^{86}Rb^+$ uptake is driven by Cs^+ or NH_4^+, conductive WT channels show low, non-zero permeability to these ions but less so than E71A, especially in the case of Cs^+ (Fig. 4.3C). Taken together, our functional and structural data suggest that, in the absence of K^+, the E71A selectivity filter interacts with and responds differently to various cations compared to the WT channel such that the mutant becomes more permeable to Cs^+, NH_4^+, Na^+ and Li^+. The low K^+ or no K^+ E71A structures indicate that, in the case of Na^+, this altered response is to maintain a conductive filter presence of Na^+ and no K^+.

Relationship between the defunct and the inactivated state

Potassium or other permeant cations are cofactors for potassium channels, essential for maintaining their structure and function (141, 144). In *Shaker* channels, removal of all cations drives the channel into a dilated state with loss of selectivity, and ultimately into a long-lasting defunct state that is non-conductive (132, 135). Interestingly, *Shaker* mutants that disrupt C-type inactivation are more resistant to becoming defunct (133). The

relationship between permeant ions and C-type inactivation is also apparent from the fact that increased permeant ion concentrations slow C-type inactivation- an observation that is attributed to a "foot-in-the-door" mechanism (281, 282). It has been hypothesized that the collapsed low-K^+ structure of KcsA is representative of a closed and potentially inactivated state (147, 283), and two recent, putative "open-inactivated" structures of KcsA (3F5W and 3F7V) (278) show selectivity filters that resemble the collapsed conformation of the low K^+ structure (23). Our results demonstrate that KcsA also enters a "defunct" state in the absence of K^+, in which it becomes very impermeable to Na^+ or Li^+ (Figure 4.3A). E71A, a non-inactivating mutant, is immune to this state: it remains permeable to Na^+ in the absence of K^+ (Figure 4.3B), and the zero K^+ structure of E71A reveals a presumably conductive selectivity filter (Figure 4.6A). This suggests that the "defunct" state in KcsA is the inactivated state and supports the conclusion that the low-K^+/high-Na^+ collapsed structure of KcsA is representative of the inactivated filter structure (278). Conversely, our findings also suggest that the same structural forces, dependent on the E71-D80 interaction, which induce inactivation in KcsA (269) are important for maintaining exquisite selectivity against Na^+ or Li^+ permeation in the absence of K^+.

Reduced cation selectivity of E71A in the presence of K^+ and the significance of the "flipped" state in the E71A structures

In addition to the marked differences between WT and E71A in zero K^+, E71A shows a reduced selectivity for K^+ over Na^+ in the presence of K^+, evident in our $^{22}Na^+$ flux and

Na^+ blocking punchthrough experiments. E71A crystals obtained in high K^+ display both "flipped" and "non-flipped" conformations in relatively equal proportions (20) (data not shown). While the "non-flipped" structure resembles the WT high K^+ structures, there are notable differences in the position of the carbonyls and K^+ ion densities in the "flipped" E71A structure (20). It is conceivable that the "flipped" selectivity filter conformation is yet another conductive filter state encountered with equal frequency during the normal E71A KcsA gating cycle. This state displays non-subtly different cation binding sites, perhaps an indication that it may have different cation selectivity and be more permeable to Na^+ than the WT "non-flipped" filter structure. In support of this hypothesis, the only filter conformation encountered in our crystallization efforts of E71A in high Na^+ no K^+ was the flipped one (Figure 4.6A).

We propose a model where E71A switches back and forth between the non-flipped (high K^+ selectivity) and the flipped (low K^+ selectivity) filter conformations during normal conduction, thus making the channel overall less K^+-selective than if the main filter conformation during conduction were the "non-flipped" state. This model also predicts, in agreement with our $^{22}Na^+$ flux data (Figure 4.3B), that in the presence of Na^+ and no K^+, the "flipped", less K^+-selective filter conformation will be favored, making the channel even less selective than in the presence of K^+. What change in the structure and energetic landscape of the E71A pore facilitates increased permeation or "punchthrough" of Na^+ through its pore? It is possible that the "flipped" state seen in E71A and not in WT KcsA allows greater Na^+ permeation by either having lower energy

barriers to Na entry/exit or by having a shallower binding site(s) for Na^+ in the filter (238).

Conclusions

The E71A mutation in KcsA not only reduces pH-dependent inactivation, but also cation selectivity both in the absence and presence of K^+. In the absence of K^+, while WT KcsA becomes non-conductive and "defunct", E71A remains conductive and permeable to Na^+. In the presence of K^+, E71A shows an increase in Na^+ permeability by $^{22}Na^+$ flux and Na^+ blocking punchthrough experiments. The combination of our functional and structural results suggests two mechanisms whereby E71A reduces cation selectivity: in the absence of K^+, E71A prevents the selectivity filter from collapsing and favors a conductive, "flipped" filter conformation; in the presence of K^+, sampling of the "flipped" conformation facilitates Na^+ movement through the filter. Our findings suggest that the non-conductive selectivity filter associated with removal of permeant ions in KcsA is functionally and structurally similar to the inactivated state. More generally, our results stress the importance of the scaffolding amino acid network behind the selectivity filter for modulating cation selectivity in channels with the same canonical GYG signature sequence.

CHAPTER 5

DUAL-MODE PHOSPHOLIPID REGULATION OF HUMAN INWARD RECTIFYING POTASSIUM CHANNELS

Cheng WWL, D'Avanzo N, Doyle DA, and Nichols CG

Combination of one article published in *J. Biol. Chem.* 285(48): 37129-37132 and another published in *Biophys. J.* 100(3): 620-628.

I. INTRODUCTION

Ion channels are embedded in the membrane bilayer and the lipid environment is an important determinant of channel activity (180, 186, 226, 284-286). Recent advances in mass spectrometry reveal cell membranes to be composed of a diverse host of lipid species that are heterogeneously organized and constantly remodeling (179). But how does the lipid bilayer modulate the function of ion channels? Perhaps the best characterized lipid modulator of ion channel activity is phosphatidylinositol 4,5-bisphosphate (PIP_2) (148). Inward rectifying potassium channels (Kir) are just one of a host of ion channels that are regulated by PIP_2 (148), and a number of genetic diseases, including Anderson-Tawil syndrome (10, 12, 199), Bartter's syndrome (199) and neonatal diabetes (203) result from Kir channel mutations that alter PIP_2-sensitivity. Structure-function studies and molecular simulations suggest a PIP_2 binding site at the

top of the cytoplasmic domain, just below the surface of the inner membrane leaflet (45, 197-201). These studies, however, have provided limited and largely qualitative information on how such lipids influence Kir channel function because they all utilize cell-based systems where the membrane composition is unknown and cannot be precisely controlled. Alternative approaches using in vitro systems are needed to expand our current knowledge (148).

Over the past decade, efforts to achieve recombinant expression of ion channels have not only led to the first high resolution crystal structures, but have made functional studies of reconstituted proteins more feasible. Recently, high resolution structures of four different potassium channels co-crystallized with lipid or detergent molecules have provided images of channel-lipid interactions (23, 54, 55, 287). These structures affirm that ion channels are intimately surrounded by lipids, some of which make apparently tight interactions. One crystal structure of the prokaryotic channel KcsA revealed two partial bound lipids one of which was modeled as a diacylglycerol, consistent with the observation that KcsA requires anionic phospholipids for channel activity in lipid bilayers (23, 226). Of the other three channels for which a crystal structure shows bound detergent or lipid molecules (Kir3.1-KirBac1.3, KirBac3.1 and Kv1.2-Kv2.1 chimeras, respectively), no functional description of their regulation by lipids is available.

Until recently, high-yield recombinant expression and purification of functional ion channels has been technically prohibitive and restricted to prokaryotic channels (53, 226). To quantitatively examine the lipid dependence of eukaryotic Kir channel activity, we have purified human Kir2.1 (KCNJ2) and Kir2.2 (KCNJ12) recombinantly expressed

in *S. cerevisiae* and performed functional studies using both liposomal $^{86}Rb^{+}$ flux assays and patch-clamp assays of giant liposomes. We determine the PIP_2 dependence of Kir channel activity, and definitively confirm that PIP_2 directly activates Kir channels without need of intermediary proteins. Moreover, we identify a novel non-specific requirement of Kir2.1 and Kir2.2 for anionic phospholipids.

II. RESULTS

PIP_2 Activation of Kir2.1 and Kir2.2

Human Kir2.1 and Kir2.2 proteins were expressed in *S. cerevisiae*, purified in milligram quantities as mono-disperse tetrameric complexes, reconstituted in liposomes and assayed for activity by $^{86}Rb^{+}$ flux assay (288). All experiments were performed on liposomes composed of the neutral phospholipid POPE with replacement by varying amounts of other lipids, reported as a mass:mass ratio. On a 25% POPG background, no activity was detected in liposomes without PIP_2, but both Kir2.1 and Kir2.2 channels show robust time courses of $^{86}Rb^{+}$ flux with increasing PIP_2 (Figure 5.1A and 5.1B). Kir2.1 and Kir2.2 activity is detectable in as little as 0.01% PIP_2, and appears to plateau ~1-3% (Figure 5.1B). The prokaryotic Kir channel, KirBac1.1, is also directly modulated by PIP_2 in reconstituted liposomes, except that PIP_2 has the opposite effect and inhibits the channel (Figure 5.1B) (53, 289). Interestingly, the dynamic ranges of PIP_2 modulation of Kir2.1, Kir2.2 and KirBac1.1 activity are approximately similar (Figure 6.1B), although Kir2.1 and Kir2.2 appear to be more sensitive. Indeed, Kir2 channels may be more sensitive to PIP_2 than other Kir channels such as Kir3.1 (186).

Kir2.1 was reconstituted in giant liposomes, to permit voltage-clamp recordings of channel currents (289). Measured single channel currents have a unitary conductance (~35 pS slope conductance) and gating behavior similar to Kir2.1 currents measured from heterologous or native expression systems (Figure 5.2A) (184, 290). On a 25% POPG background, increasing PIP_2 within the range of concentrations observed in cells, increases open probability (Figure 5.2B), but not unitary conductance (Figure 5.2C), consistent with previous reports of the effect of PIP_2 on single channel currents (182, 184). The PIP_2-activity relationship plateaus at ~1-3% PIP_2 as was also observed in $^{86}Rb^+$ flux assays (Figure 5.1C and 5.2B). Measured open probability reaches a maximum of ~0.4 at 1% PIP_2 (Figure 5.2B) over the range of -80 to -120 mV (data not shown), much lower than the high open probabilities (>0.9) previously reported in heterologous expression systems (184). This discrepancy might suggest that other lipid/protein modulators may be involved in activating Kir2.1 in cellular membranes.

We tested the effect of all PIPs on Kir2.1 activity and show that Kir2.1 is selectively activated by PIP_2 compared to other PIPs (Figure 5.3). On a 25% POPG background and at concentrations of 1%, $PI(3,4,5)P_3$ activated Kir2.1 to 11.3 ± 0.7 % of activity induced by $PI(4,5)P_2$. $PI(3,5)P_2$, $PI(3,4)P_2$ and PI(3)P very weakly activated Kir2.1 channels in the range of 1 – 4 % of $PI(4,5)P_2$ activation. PI, PI(4)P, and PI(5)P, did not activate the channel above background (Figure 5.3). These results are consistent with previous studies that suggest some of these PIP variants can activate Kir2.1 channels only at high concentrations, while others were unable to activate Kir2.1 channels (188).

Kir2.1 and Kir2.2 have a non-specific secondary requirement for anionic phospholipids

While PIP_2 is present at ≤1% in eukaryotic membranes (177), a significant fraction (10-20%) of eukaryotic cell membranes are composed of other anionic phospholipids (153-156). In the absence of POPG, the PIP_2 dependence of activity for

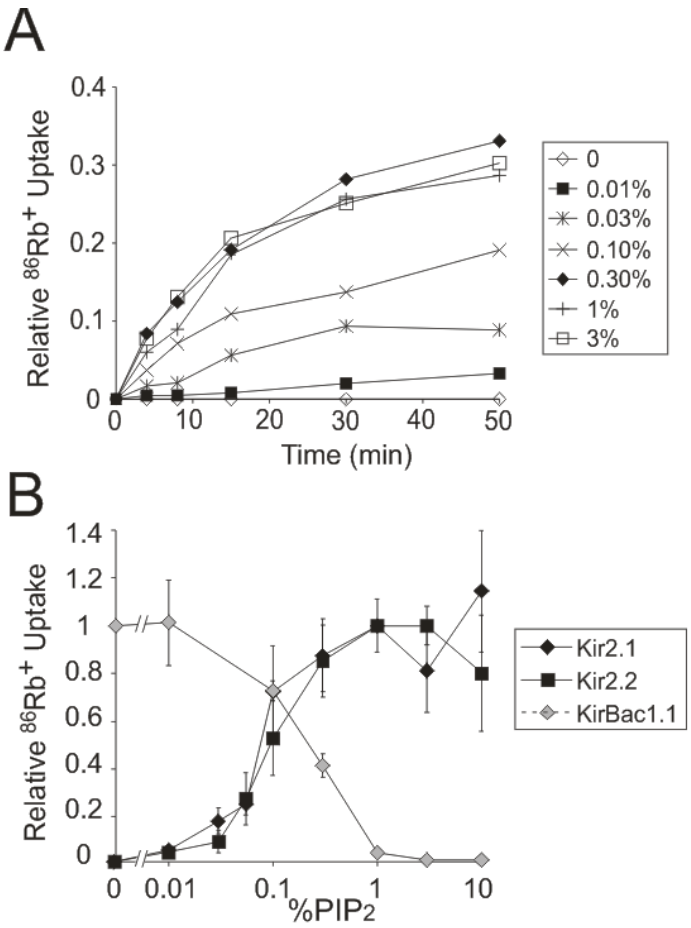

Figure 5.1 Reconstituted human Kir2.1 and Kir2.2 require PIP_2 for activity. (A) Representative $^{86}Rb^+$ uptake time courses of Kir2.1 in liposomes composed of 25% POPG and increasing % PIP_2 on a POPE background. (B) Activity-% PIP_2 relationship for Kir2.1 (black diamonds, n = 4, +/- s.e.m.), Kir2.2 (black squares, n = 3, +/- s.e.m.), and KirBac1.1 (grey diamonds, n = 2, +/- s.e.m.) in liposomes composed of 25% POPG and increasing % PIP_2 on a POPE background. $^{86}Rb^+$ uptake counts were taken at 15 min in the time course for Kir2.1, 20 min. for Kir2.2, and 4 min. for KirBac1.1. Counts were normalized to % PIP_2 of highest uptake for Kir2.1 and Kir2.2, and to uptake in no PIP_2 for KirBac1.1.

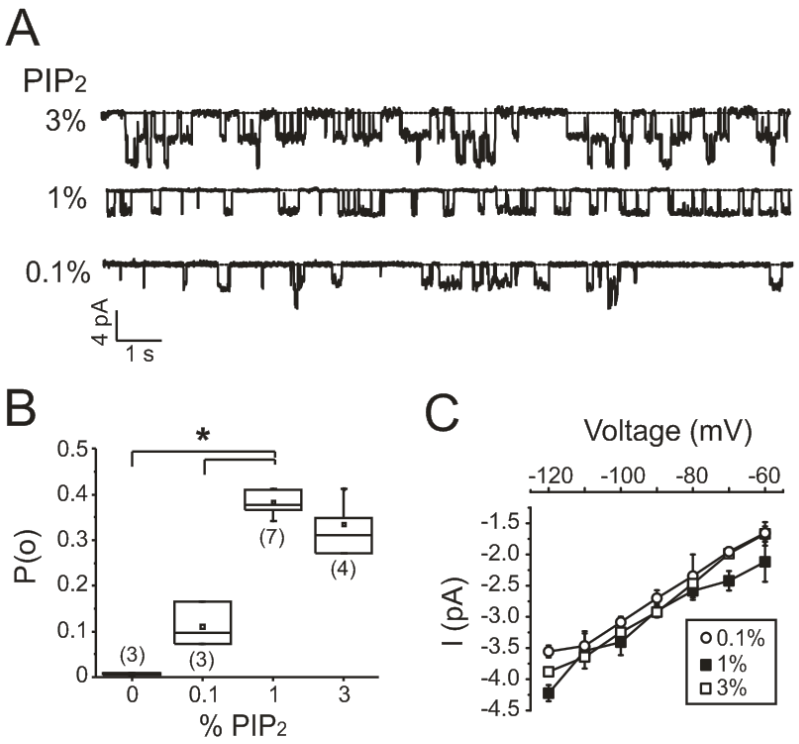

Figure 5.2 Relationship between PIP_2 and Kir2.1 open probability. (A) Representative continuous recordings of Kir2.1 currents at -100 mV from giant liposome inside-out excised patches composed of the indicated % PIP_2 and 25% POPG on a POPE background. (B) Box-and-whisker plot of measured Kir2.1 open probabilities in liposomes with the same compositions as in A. The mean open probabilities, represented by the square box, are 0.11 +/- 0.03 for 0.1% PIP_2, 0.38 +/- 0.01 for 1% PIP_2, and 0.34 +/- 0.03 for 3% PIP_2 (+/- s.e.m.). The number of recordings for each condition is indicated in brackets, the whiskers indicate data range, the box shows the upper and lower quartile values and median, and the asterisk indicates statistical significance ($p<0.05$). (C) Current-voltage plot of Kir2.1 analyzed from the same recordings as in A. The derived slope conductances are 35.0 +/- 0.8 pS for 0.1% PIP_2, 34.5 +/- 1.5 pS for 1% PIP_2, and 36.8 +/- 1.5 pS for 3% PIP_2 (+/- s.e.m.).

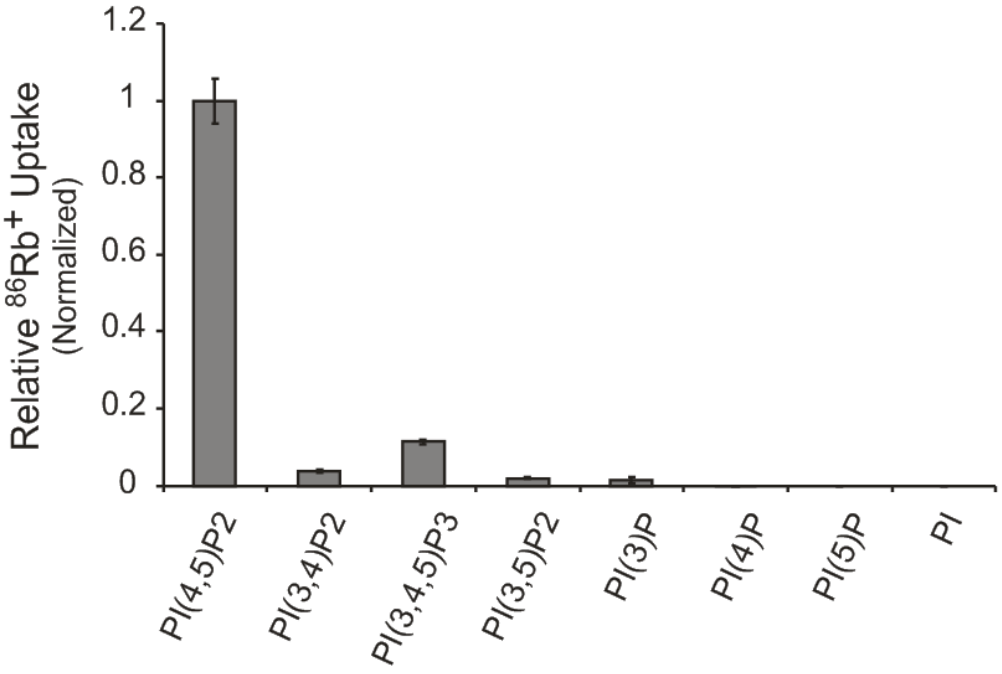

Figure 5.3 Reconstituted human Kir2.1 is highly selective of PI(4,5)P_2 over other PIPs. $^{86}Rb^+$ uptake of Kir2.1 in liposomes composed of 25% POPG, 74% POPE and 1% of the indicated PI species. All counts were taken at 30 min. in the time course and normalized to PI(4,5)P_2 (n = 3, +/- s.e.m.).

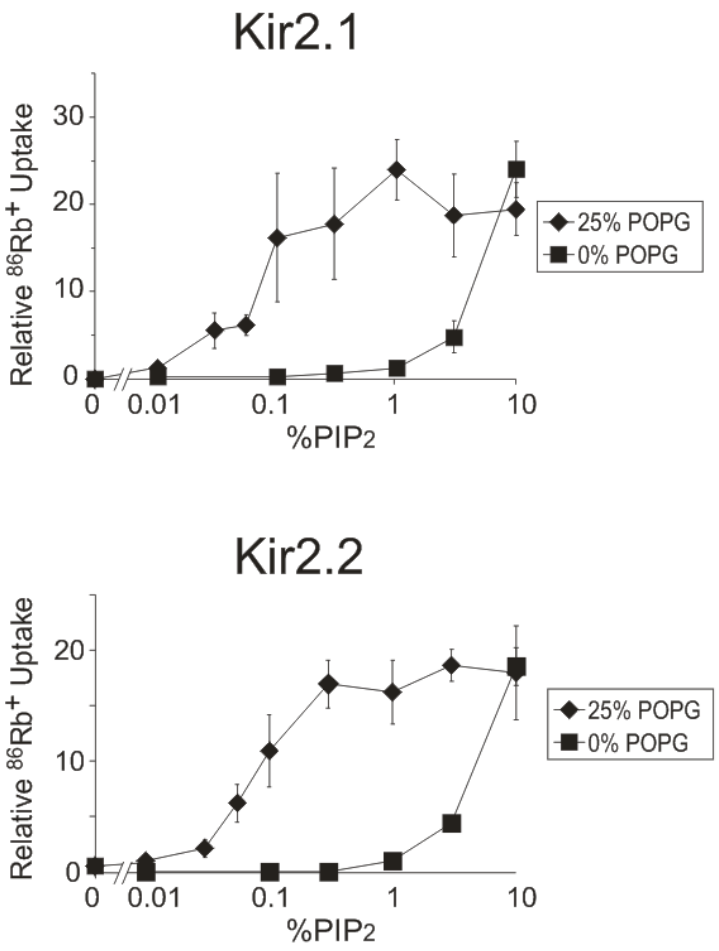

Figure 5.4 Reconstituted human Kir2.1 and Kir2.2 activity is regulated by POPG. (A) Kir2.1 activity-% PIP_2 relationship obtained from $^{86}Rb^+$ uptake counts at 15 min (all counts are reported from this time point), in 25% POPG (n=3 +/- s.e.m.) or POPE-only liposomes (n=3 +/- s.e.m.). The data are normalized to uptake at 0.01% PIP_2 and 25% POPG. (B) Same as in (A) except for Kir2.2, and $^{86}Rb^+$ uptake counts taken at 20 min (for 25% POPG, n=2 +/- s.e.m.; for POPE-only liposomes, n=3 +/- s.e.m.).

Kir2.1 and Kir2.2 is significantly right-shifted ~100x such that at least 1% PIP_2 is needed to detect $^{86}Rb^+$ flux (Figure 5.4). These data suggest that Kir2.1 and Kir2.2 have both a primary PIP_2 requirement and a novel secondary POPG requirement for activity. This second lipid requirement is quite non-specific as multiple lipids with negatively-charged headgroups activate these channels, including POPS, POPA, PI, CL, and the PIP_2 analogue, DGS-NTA (Figure 5.5A and 5.5B). Furthermore, ~100x more anionic lipid (~10%) than PIP_2 is required to substantially activate Kir2.1 and Kir2.2. By contrast, neither the neutral POPC nor the cationic EPC activate either channel (Figure 5.5A and 5.5B). Conceivably, these anionic lipids could be acting as weak PIP_2 surrogates and do not represent a secondary mode of regulation. However, in the absence of PIP_2 on a POPE-only background, none of these anionic phospholipids activate Kir2.1 up to 30% (Figure 5.5C) suggesting that they cannot substitute for PIP_2, and that PIP_2 activation of Kir2.1 is specific (185).

Activation by POPG increases Kir2.1 open probability and unitary conductance

Surprisingly, and in contrast to the singular effect of PIP_2 on P(o) (Figure 5.2), increasing POPG from 15% to 25% on a 1% PIP_2 background not only increases open probability but also increases unitary conductance (Figure 5.6). This result is reminiscent of the effect of anionic phospholipids on the prokaryotic K^+ channel, KcsA, for which there is evidence that binding of anionic phospholipids to positively-charged residues on the extracellular side of the KcsA activates the channel by increasing both open probability and unitary conductance (227, 228, 231). An effect on unitary conductance

may indicate a direct electrostatic effect on local permeant ion concentration, or an effect through changes in protein conformation. Importantly, this differential action on conductance is consistent with the conclusion that POPG is not acting simply as a PIP_2 surrogate.

Inhibition of Kir2.1 by oleoyl CoA and EPC

Long chain acyl CoAs such as oleoyl CoA have been shown to antagonize PIP_2 activation of Kir2.1 in cellular membranes (189). On a 1% PIP_2/10% POPG background, 1-3% oleoyl CoA effectively inhibits Kir2.1 activity, whereas on a 10% PIP_2 background, ~10% oleoyl CoA is needed for inhibition (Figure 5.7A), consistent with oleoyl CoA competitively inhibiting PIP_2 activation. By contrast, on a 1% PIP_2/10% POPG background, 10% EPC is required to inhibit Kir2.1, and there is no inhibitory effect on a 10% PIP_2 background (Fig. 5.7B). We were unable to form liposomes in which the amount of EPC exceeded total anionic phospholipid content, but these data suggest that EPC, a positively-charged phospholipid, can counteract the negative charge conferred by POPG and thus antagonize the secondary anionic lipid requirement.

PIPs can have dual regulatory roles on Kir2.1 activity

Collectively, the above data demonstrate two distinct modes of anionic phospholipid regulation in Kir2.1: a primary specific requirement for PIP_2, and a secondary non-specific requirement for anionic phospholipids. Since the secondary requirement for anionic phospholipids is non-specific, this raises the question of whether

PIP_2 activates Kir2.1 on a POPE-only background (Figure 5.4) by meeting both lipid requirements. In liposomes composed of 5% PIP_2, Kir2.1 is partially activated, and the effect of POPG is diminished (Figure 5.8A) consistent with PIP_2 at high levels meeting both lipid requirements and thus having dual regulatory roles in Kir2.1.

Dual regulatory roles of PIP_2 are also implied by the finding that other phosphatidylinositol phosphates (PIPs) can have competing effects on Kir2.1 activity. On a 1% PIP_2 background, all PIPs at 10% can activate Kir2.1, but with variable efficacy—PI is the most effective, followed by PI(3)P, PI(4)P and PI(5)P, with the least effective being multi-phosphorylated PIPs ($PI(3,4)P_2$, $PI(3,5)P_2$ and $PI(3,4,5)P_4$) (Figure 5.8B). By contrast, on a 1% PIP_2/25% POPG background, all PIPs but not PI inhibit Kir2.1 activity, with multi-phosphorylated PIPs being most effective (Figure 5.8C). As with oleoyl CoA, PIPs are most likely inhibiting Kir2.1 activity by antagonizing the primary PIP_2 requirement as opposed to the secondary requirement (i.e. POPG), since the secondary requirement is non-specific for anionic lipids (Figure 5.5A).

These results suggest that PIPs are acting on both modes of lipid regulation. PIPs activate Kir2.1 on a 1% PIP_2 background by meeting the secondary requirement (Figure 5.8B); however, this activation is less effective compared to PI because PIPs also antagonize the primary PIP_2 requirement (Figure 5.8C). Consistent with this mechanism, multi-phosphorylated PIPs (e.g. $PI(3,4)P_2$), which are the most effective inhibitors of PIP_2 (Figure 5.8C), are the least effective in activating Kir2.1 on a 1% PIP_2 background (Figure 5.8B). Thus, PIPs can have dual regulatory roles on Kir2.1 activity. The overall effect of a PIP on Kir2.1 depends on the background lipid composition.

Intracellular Residues Mediate Anionic Phospholipid Regulation

In KcsA, there is evidence that anionic phospholipids act in the 'outer' leaflet by headgroup interaction with two arginine residues (R64 and R89) on the 'extracellular' side of the channel (228, 231, 291). While there are multiple positively-charged residues in the intracellular side of Kir2.1, there are only two positive charges (K117 and K120) in the extracellular region that could conceivably be involved in charge-dependent anionic phospholipid activation of Kir2.1 (Figure 5.9A). To test the effect of these residues on the lipid dependence of reconstituted Kir2.1 activity, we expressed and purified three mutants: K117A, K120A and the double mutant K117A/K120A (Figure 5.10). None of these mutants affect the PIP_2 or POPG dependence of activity (Figure 5.9B and 5.9C), indicating that the secondary requirement for anionic phospholipids in Kir2.1 is not mediated by charge interactions on the extracellular side of the channel, and suggesting instead that the secondary requirement may involve residues on the cytoplasmic domain.

In eukaryotic Kir channels, many residues that reduce PIP_2 sensitivity have been identified (197, 199, 200), and some of these may form a specific binding site in the cytoplasmic domain near the surface of the membrane (45). Of the thirteen positively-charged residues in Kir2.1 that were found to affect PIP_2 sensitivity (199), we tested the effects of three mutants R189Q, K182Q, and K219Q because of their disparate effects on PIP_2 sensitivity, and proximity to the membrane interface. In Kir2.1, R189 is located on the TM2-cytoplasmic domain flexible linker, and the equivalent residue is highly conserved in all eukaryotic Kir channels. K182 is on the bottom of TM2 just below the

bundle crossing, and K219 is on the CD loop on the top of the cytoplasmic domain (Figure 5.9A). R189Q Kir2.1 channels show no detectable fluxes up to 10% PIP_2, while K182Q is minimally active, and K219Q shifts the PIP_2 dependence of activation by ~10-fold (Figure 5.9D and Figure 5.10), which agrees with the relative effect of these mutations on sensitivity of Kir2.1 to PIP_2 activation in cellular membranes (199). The POPG dependence of these mutants show a similar trend, as K182Q is more weakly activated by POPG than K219Q, whose POPG dependence is unchanged from WT (Figure 5.9E). The effect of these mutations in purified and reconstituted Kir2.1 suggests that positively-charged residues on the cytoplasmic side, as opposed to the extracellular side of the channel, are important in mediating both modes of anionic phospholipid regulation in Kir2.1.

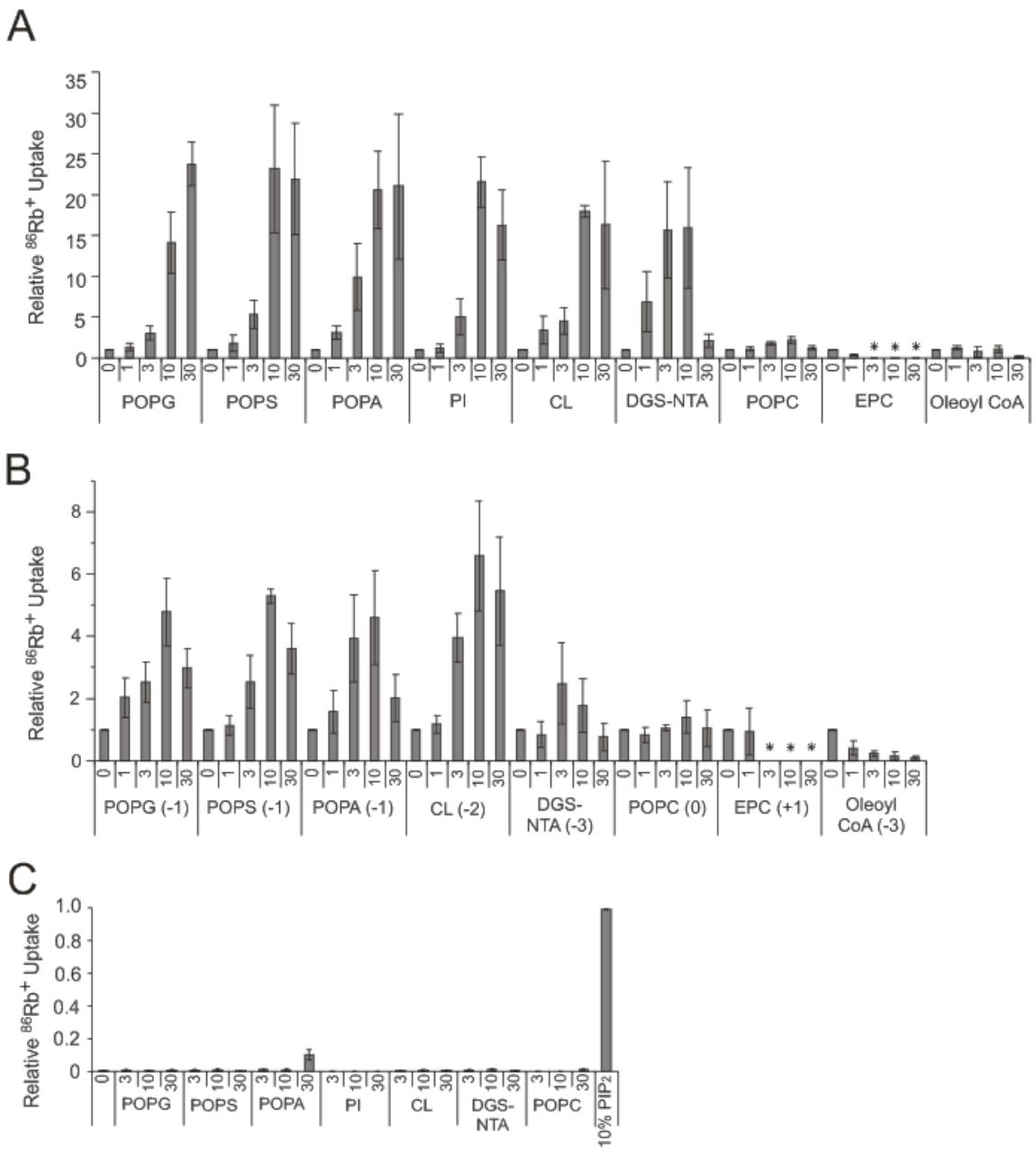

Figure 5.5 Kir2.1 and Kir2.2 has a secondary non-specific requirement for anionic phospholipids. (A) $^{86}Rb^+$ uptake counts of Kir2.1 in liposomes composed of increasing % of the indicated lipid and 1% PIP_2 (n=3, +/- s.e.m.). All data are normalized to uptake in 1% PIP_2. The asterisks indicate conditions where liposomes failed to form. (B) Same

as (A) except for Kir2.2 (n=3, +/- s.e.m.). (C) $^{86}Rb^{+}$ uptake counts of Kir2.1 in liposomes composed of POPE and increasing % of the indicated lipid. Counts are normalized to uptake in 10% PIP_2 (n=3, +/- s.e.m.).

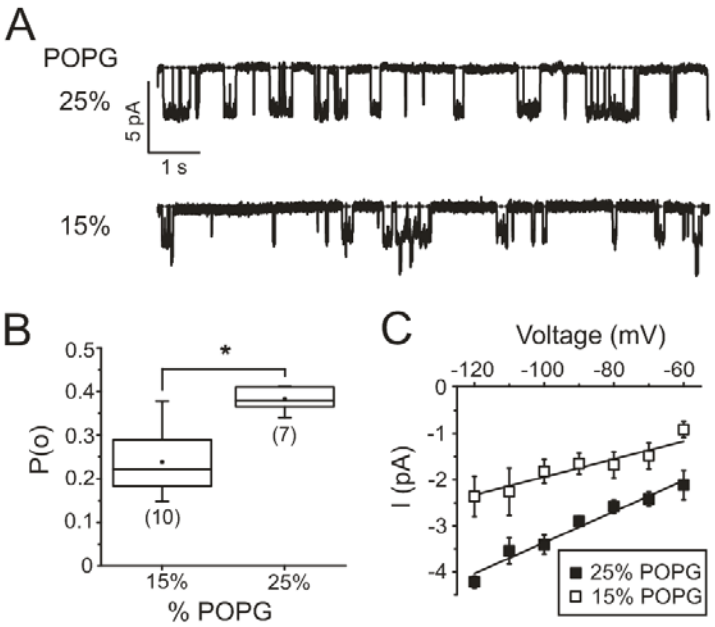

Figure 5.6 Secondary anionic phospholipid activation increases open probability and unitary conductance. (A) Representative continuous recordings of Kir2.1 currents at -100 mV from giant liposomes composed of the indicated % POPG and 1% PIP_2. (B) Box-and-whisker plot of measured Kir2.1 open probabilities of the entire recording from giant liposomes composed of 1% PIP_2 and either 15% or 25% POPG. The mean open probabilities, represented by the square box, are 0.24 +/- 0.02 for 0.15% POPG and 0.38 +/- 0.01 for 25% POPG (+/- s.e.m.). The number of recordings for each condition is indicated in brackets, the whiskers indicate data range, the box shows the upper and lower quartile values and median, and the asterisk indicates statistical significance ($p<0.05$). (C) Current-voltage plot of Kir2.1 analyzed from the same recordings as in (B). The derived slope conductances are 19.4 +/- 0.6 pS for 15% POPG and 34.5 +/- 1.5 pS for 1% PIP_2 (+/- s.e.m.).

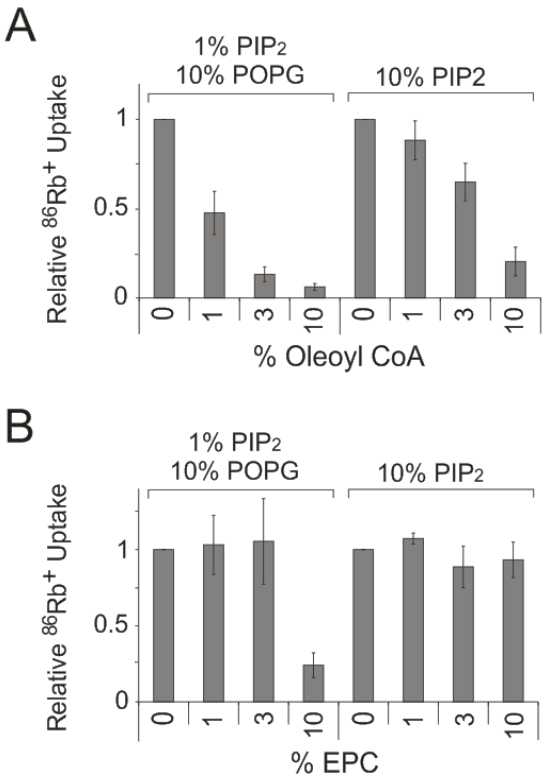

Figure 5.7 Effects of oleoyl CoA and EPC on Kir2.1 activity. (A) $^{86}Rb^{+}$ uptake counts of Kir2.1 in liposomes with increasing % oleoyl CoA and the indicated lipids shown above the graph (n=3, +/- s.e.m.). Data are normalized to uptake in 0% oleoyl CoA. (B) Same as in (A) except with increasing % EPC (n=3, +/- s.e.m.).

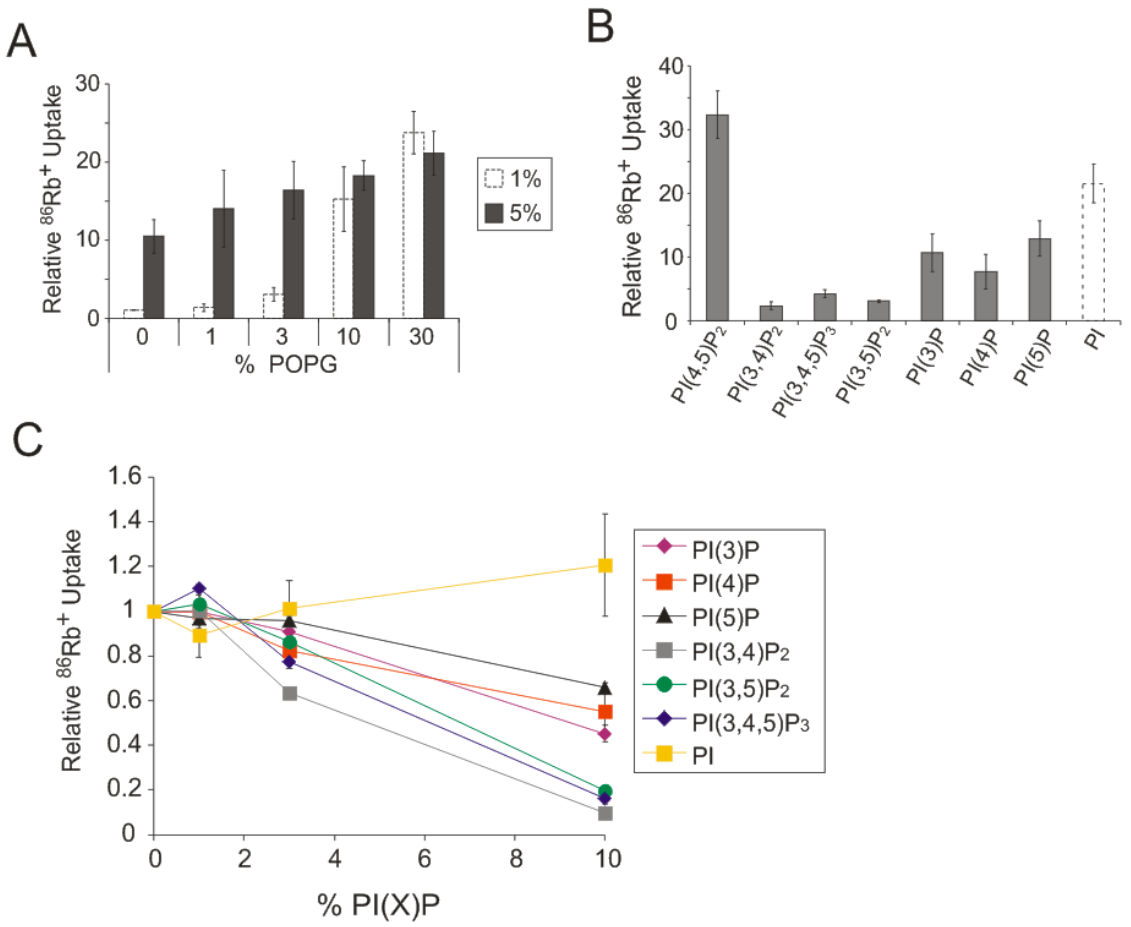

Figure 5.8 PIPs act on both modes of lipid regulation. (A) $^{86}Rb^{+}$ uptake counts of Kir2.1 in liposomes composed of increasing % POPG and 5% PIP_2 (n=3, +/- s.e.m.). POPG dependence from Figure 5.5A is shown in white with dotted lines. Counts are renormalized to uptake in 1% PIP_2. (B) $^{86}Rb^{+}$ uptake counts of Kir2.1 in liposomes composed of 1% PIP_2 and 10% of the indicated lipids (n=3, +/- s.e.m.). Data are normalized to uptake in 1% PIP_2 only, and PI data in dashed lines is from Figure 5.5A. (C) $^{86}Rb^{+}$ uptake counts of Kir2.1 in liposomes composed of 1% PIP_2, 25% POPG, and increasing % of the indicated lipids (n=3, +/- s.e.m.). Data are normalized to uptake in 1% PIP_2 and 25% POPG.

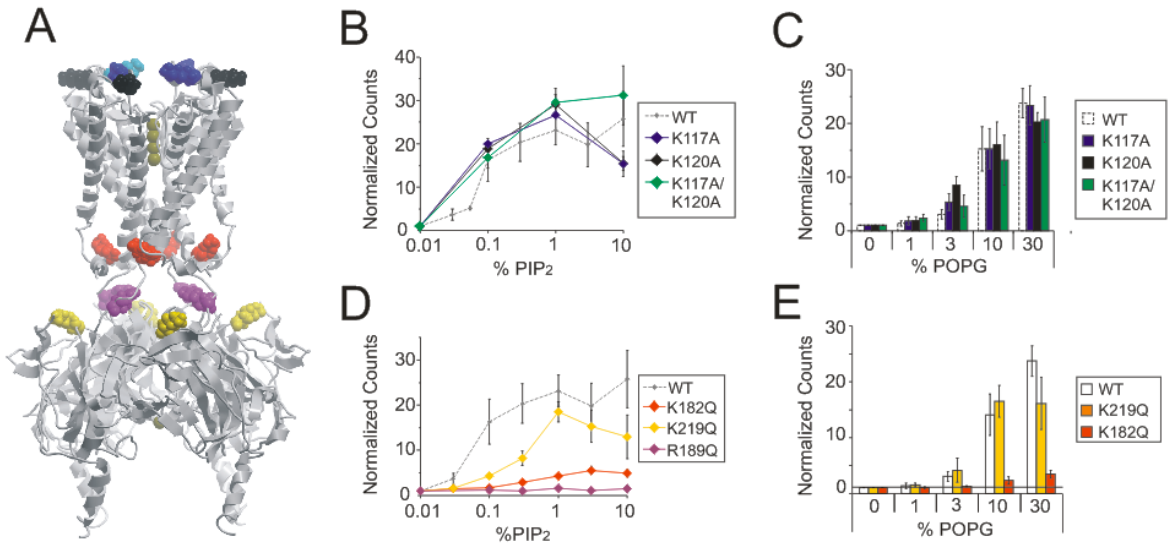

Figure 5.9 Activation by anionic phospholipids is dependent on intracellular basic residues. (A) Homology model structure of Kir2.1 derived from the Kir2.2 crystal structure (3JYC). Space-filling representations of amino acid side chains are shown for K117 (blue), K120 (black), K182 (red), R189 (pink), and K219 (yellow). (B) $^{86}Rb^{+}$ uptake counts of Kir2.1 mutants K117A, K120A, and K117A/K120A in liposomes composed of increasing % PIP_2 and 25% POPG (n=3, +/- s.e.m.). WT Kir2.1 PIP_2 dependence from Fig. 6.1B is shown in gray with dotted lines (C) Same as in (B) except in liposomes composed of 1% PIP_2 and increasing % POPG. WT Kir2.1 POPG dependence from Figure 6.5A. (D) and (E) Same as in (B) and (C) except for the Kir2.1 mutants K182Q, R189Q, and K219Q (n=3, +/- s.e.m.).

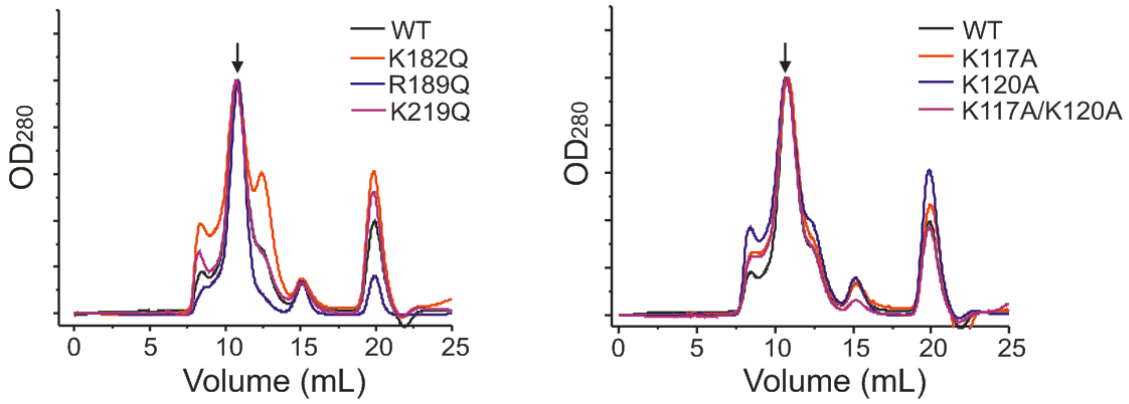

Figure 5.10 Gel Filtration profiles of WT and mutant Kir2.1 channels. Gel filtration profiles of Kir2.1 and all mutants tested were similar with the protein peak eluting at the same volume for all the mutants. Three 0.5 mL fractions were collected from 10-11.5 mL and concentrated for functional experiments.

III. DISCUSSION

Physiological regulation of Kir channels by lipids

The cell membrane, in which ion channels are embedded, is a complex and dynamic environment that is predicted to play a critical role in regulating membrane excitability (180, 186, 226, 284-286). In this study, we show that human Kir2.1 and Kir2.2 channels are directly activated by anionic phospholipids via two distinct modes of action: there is a specific requirement for PIP_2 and a secondary nonspecific requirement for anionic phospholipids. By reconstituting channel proteins in model liposomes, we have generated a quantitative description of the lipid dependence of channel activity. Kir2.1 activity is modulated over a large range of PIP_2 (from 0.01% to at least 1%) (Figure 5.1B), covering the estimated levels of PIP_2 in a cell membrane (~0.25% of total phospholipids) (148, 164, 177). Total anionic phospholipids in cell membranes are in the order of 10-20% of total lipid, which is also within the range we find for modulation by the secondary lipid requirement (Figure 5.5A and 5.6B) (153-156). If we assume that these lipids activate Kir2.1 from the intracellular side of the channel (see discussion below), we may be over-estimating the quantity of lipids needed to activate these channels, since the anionic phospholipids are presumably not located exclusively in the inner leaflet of the liposome bilayer. However, even if the values for the dose response of PIP_2 or anionic phospholipid are halved, they are still within physiologically relevant ranges.

Cell membrane anionic phospholipid content (in mammalian cells, primarily PI, its derivatives and PS) is constantly being remodeled to regulate numerous cellular

functions. PIP_2 and other PIPs play important roles in signaling, membrane trafficking and regulation of various protein effectors including ion channels and components of the actin cytoskeleton (163, 168, 292). PS is also a bio-active lipid, regulating enzymes such as protein kinase C, and tagging apoptotic cells for recognition by phagocytes (169, 173, 293). Many diseases are associated with altered metabolism of phospholipids. For example, mice with diabetic cardiomyopathy show dramatic changes in anionic phospholipid composition that are correlated with contractile dysfunction in the heart (294, 295), where Kir2.1 and other inward rectifiers are critical repolarizing forces in the action potential. Specifically, there is a major depletion of cardiolipin at the earliest stages of disease and, later, a large (40%) increase in PI species and smaller though significant increase in PG and PS species (295, 296). Such changes in PI species (including the phosphorylated derivatives) will have complex effects on Kir2.1 channel function. Significant changes in anionic phospholipid content have also been reported in myocardium of spontaneously hypertensive rats (297), hypoxemic myocardium of children with congenital heart disease (298), and human brains with Alzheimer's disease (299-301). Our results demonstrate that such alterations to lipid membrane content will significantly affect Kir channel activity, and future studies will be important in clarifying the physiological and pathophysiological consequence of these effects.

Overcoming Experimental Limitations

Prior studies of PIP_2 modulation of eukaryotic Kir channels have relied on cell-based systems, which pose a number of limitations. First, changing the lipid composition

typically requires diffusing micelles onto a membrane patch- a poorly controlled method that provides no quantification of lipid incorporation into the membrane (302). Even perfusing water soluble di-C8 PIP derivatives onto membranes permits only relative quantification of the effects of different lipids (187) since partitioning cannot be easily quantified. Second, the exact composition of the cell membrane cannot be determined, and thus, the influence of unknown protein/lipid modulators cannot be excluded (303). We have overcome these limitations by using reconstituted liposomes of defined lipid composition. To our knowledge, this result is the first reported dose response relationship for PIP_2 activation of a eukaryotic ion channel. Furthermore, this result definitively shows that Kir2.1, Kir2.2 and likely all eukaryotic Kir channels absolutely require PIP_2 for activity, and that activation occurs through direct interactions without intermediary proteins.

Complex dual-mode regulation of Kir2.1

The secondary regulatory mode or requirement adds another dimension of complexity to Kir2.1 regulation by lipids, especially since PIPs can act on both the primary PIP_2 requirement and the secondary requirement. Certain PIPs have been reported to only activate ($PI(3,5)P_2$, $PI(3,4,5)P_3$, PI(4)P) (185) or inhibit ($PI(3,4)P_2$) (189) Kir2.1. Instead, we find that all PIPs can either activate or inhibit Kir2.1 depending on the lipid background (Figure 5.8B and 5.8C). The overall effect of a certain PIP on Kir2.1 activity is the combination of: 1) its effect as an inhibitor of the PIP_2-specific requirement, and 2) its contribution to the overall anionic lipid content in the membrane.

In addition to anionic phospholipids, cholesterol has been implicated as an inhibitor of Kir channel activity (225). We anticipate that other lipid variants such as lysophospholipids, sphingolipids, or polyunsaturated fatty acids may also regulate Kir2.1 activity, so that the overall effect of a single lipid species will depend on all the regulatory modes that it acts upon and the lipids that make up the rest of the membrane.

Molecular Basis of Activation by Anionic Phospholipids

Satisfaction of the secondary requirement by POPG increases Kir2.1 open probability and unitary conductance. This is reminiscent of anionic phospholipid activation of KcsA, where crystallographic and fluorescence studies have identified an intersubunit phospholipid binding site on the extracellular side of the channel (227, 228). We tested a similar hypothesis in Kir2.1 by mutating the only two basic residues (K117 and K120) on the extracellular side of the channel but found that such mutations are without effect on lipid modulation (Figure 5.9B and 5.9C). Rather, mutations of intracellular residues, especially R189Q and K182Q, significantly affect activation of Kir2.1 by PIP_2 and POPG (Figure 5.9D and 5.9E). These data do not exclude the possibility that these mutations are simply altering channel open state stability and not channel-lipid interactions. However, they suggest that the intracellular and not extracellular side of the channel mediates anionic phospholipid activation. This is consistent with the fact that anionic phospholipids are almost exclusively localized to the inner leaflet of eukaryotic plasma membranes (165, 293), contrary to prokaryotic membranes (167). Thus, the molecular mechanism of anionic phospholipid modulation of

Kir channels differs from KcsA, despite functional similarities. There has perhaps been a similar evolutionary pressure for Kir2.1 and KcsA to adopt a requirement for anionic phospholipids (304) but different structural components are apparently utilized. We hypothesize that of the twelve basic residues previously identified to affect PIP_2 sensitivity in Kir2.1 (199), some of these may also be involved in mediating the secondary requirement for anionic phospholipids.

Conclusion

In conclusion, Kir2.1 and Kir2.2 have two distinct lipid requirements for channel activity: a specific requirement for PIP_2 and a non-specific requirement for anionic phospholipids. It seems highly likely that this mechanistic scenario will hold for other Kir channels, but the general applicability to other K^+ channels, or to other cation channel superfamily members will require further advances in expression and purification. This study represents a technical breakthrough in the use of model liposomes to study lipid regulation of ion channels, permitting quantification of lipid effects and providing the definitive evidence that PIP_2 and other anionic phospholipids directly activate human Kir channels. As knowledge of cellular lipidomes accumulate and the ability to purify novel integral membrane proteins expands, further studies utilizing such approaches will further understanding of how the membrane bilayer influences excitability in physiology and disease.

CHAPTER 6

DISCUSSION AND FUTURE DIRECTIONS

I. GENERAL IMPLICATIONS OF THE THESIS

At the onset of my thesis work, functional studies of recombinant inward rectifying potassium channels, although relatively scarce, were becoming the subject of increased investigation. The interest for these studies was motivated by a family of prokaryotic proteins, called KirBacs, which are homologous to eukaryotic Kir channels and had become exciting targets for crystal structure determination. At the time, it was thought, based on the crystal structures of KirBac1.1 (16) and KirBac3.1 (55), that these KirBac proteins are structurally similar to eukaryotic Kir channels. Also, radiotracer flux assays (52) and yeast complementation screens (248) had demonstrated that some of these prokaryotic proteins are functional K^+ channels. However, with no reports of voltage-clamp currents, it remained uncertain to what degree these channels resemble eukaryotic inward rectifiers functionally, and the finding that KirBac1.1 is inhibited by PIP_2 was both surprising and unsettling since the opposite effect is observed in eukaryotic channels (53). We now know that KirBac1.1 is a functional K^+-selective channel that resembles eukaryotic Kirs, and this is likely to be the case for all KirBac channels. In particular, based on my studies of KirBac1.1, I predict that all KirBac channels resemble weak inward rectifying K^+ channels, in that mutation of the rectification controller residue (all KirBac channels have a neutral residue at this position) would confer sensitivity to steeply voltage-dependent block by polyamines.

Thus, KirBac channels are structurally and functionally related to eukaryotic Kir channels, and insights gained about polyamine block or other properties, from structures of KirBac channels and computational studies using these structures, should be relevant to their eukaryotic counterparts (45, 87).

Before the studies in this thesis were reported, it was known that eukaryotic Kir channels are activated by PIP_2, and it was widely accepted that this regulatory effect occurs through direct channel-lipid interactions (Chapter 1, IVC). This inference has now been definitively substantiated by studies of recombinant KirBac1.1 and human Kir channels in model liposomes showing that PIP_2 directly and specifically regulates the activity of these channels. Furthermore, we now know that other lipids regulate Kir channel activity: that is, KirBac1.1 and human Kir2.1 and Kir2.2 exhibit a secondary mode of regulation for anionic phospholipids. This finding suggests that the activity of Kir channels as well as other ion channels are likely to be influenced by many components of their lipid environment, and not simply trace lipids, such as PIP_2, that have well-recognized roles in cell signaling. This finding also illustrates how a single lipid species can act on two or perhaps more modes of regulation, such that the effect of that lipid on channel activity is a complex function of all the modes that it acts upon and other relevant lipids in the membrane. Thus, the findings of these studies have broadened the field of lipid regulation of Kir channels, demonstrating that lipids other than phosphatidylinositol phosphates can influence channel activity, and pioneering the investigation of other modes of regulation.

During the course of my thesis work, experiments were performed on KirBac1.1 that were not included in the publications adapted for the above chapters. These experiments are relevant to my thesis and will be incorporated into the following sections in which I address specific implications and future directions of this work.

II. KIRBAC1.1 AS A STRUCTURAL MODEL OF EUKARYOTIC KIR CHANNELS

The purpose of the study in Chapter 3 was to test the hypothesis that KirBac1.1 behaves functionally like a eukaryotic inward rectifier. My analysis of KirBac1.1 currents recorded from giant liposomes demonstrates that the key functional characteristic of Kir channels—sensitivity to polyamine block—is present in KirBac1.1 (I131C/I138D) leading to the conclusion that this prokaryotic K^+ channel is a genuine inward rectifier. However, there are a number of notable differences between KirBac1.1 and eukaryotic Kir channels that must be considered in assessing the utility of KirBac1.1 as a structural model of eukaryotic Kir channels.

IIA. SIMILARITIES AND DIFFERENCES BETWEEN KIRBAC1.1 AND EUKARYOTIC KIR CHANNELS

The major functional similarities between KirBac1.1 and eukaryotic Kir channels, determined by $^{86}Rb^+$ flux assay or patch-clamp, include the following: both are K^+-selective channels that are blocked by Ba^{2+}, inhibited by acidic pH, and modulated by membrane PIP_2 (Chapter 3) (52, 53). KirBac1.1 resembles weak inward rectifiers (Kir1.1

and Kir6.2), which are only sensitive to Mg^{2+} and polyamine block when the rectification controller residue is mutated to an acidic residue such as aspartate (I138D in KirBac1.1). Furthermore, the voltage dependence of polyamine block ($\delta z = 2.5$) is steeper than Ba^{2+} block ($\delta z = 1.2$) in KirBac1.1 as observed in eukaryotic Kir channels (Chapter 3).

Although there is significant functional diversity among eukaryotic Kir channels (305) (Chapter 1, IA and IVD), there are certain features characteristic of all eukaryotic Kir channels that differ in KirBac1.1. Most notably, KirBac1.1 is inhibited by PIP_2, while all eukaryotic Kir channels are activated by PIP_2 (Chapter 3) (53). Also, while the single channel currents of eukaryotic Kir channels generally exhibit one primary maximum conductance state with rare subconductances, KirBac1.1 currents exhibit multiple conductance states with most of the channel openings being at the smallest conductance state (Chapter 3). In addition to these functional differences, significant structural differences are also evident. The transmembrane-cytoplasmic linkers in KirBac1.1, and all identified KirBac channels, are shortened by three residues compared to eukaryotic Kir channels (Chapter 1, IVC) (53). Comparing the crystal structures of KirBac1.1 with chicken Kir2.2 (Figure 6.1) illustrates how the longer linkers in Kir2.2 extend the pore in comparison to KirBac1.1 and potentially alter interactions between the slide helix and cytoplasmic domain. A computational study by Robertson et al examining the electrostatic energy of K^+ in the pore also demonstrated significant differences between KirBac1.1 and eukaryotic Kir channels (51). Notably, the electrostatic energy of K^+ in the cytoplasmic pore is highly favorable in all eukaryotic Kir channels due to numerous acidic residues lining the pore (51). By contrast, the cytoplasmic pore in KirBac1.1

contains relatively more basic residues resulting in an energetically unfavorable environment for K^+ (51). Whether these structural differences are related to functional differences observed between KirBac1.1 and eukaryotic Kir channels can be the subject of future investigation.

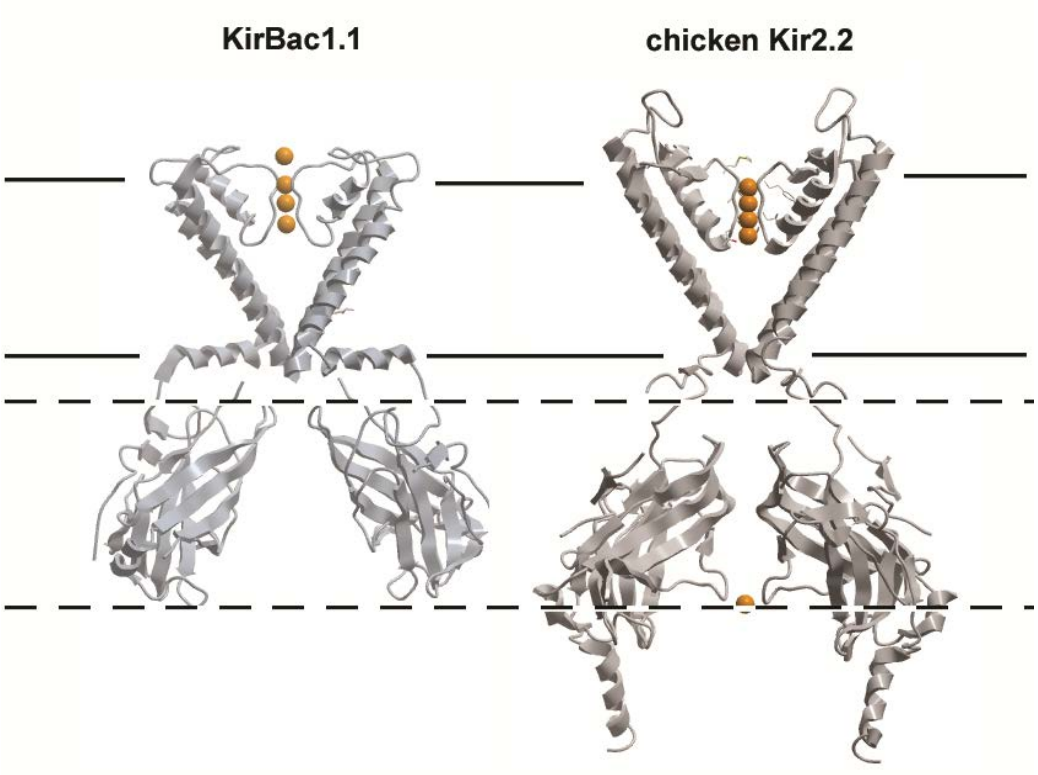

Figure 6.1: Structural comparison of KirBac1.1 and Kir2.2. Structures of KirBac1.1 (1P7B) and chicken Kir2.2 (3YJC). For clarity, chain A and C TM domains, and chain B and D cytoplasmic domains are shown. The tetrameric assembly of the chicken Kir2.2 soluble domain is rotated ~60º compared to the KirBac1.1 structure, and is displaced away from the cell membrane lengthening the pore and affecting interactions between the slide helix and the cytoplasmic domain.

IIB. KIRBAC1.1 AS A COMPARATIVE STRUCTURAL MODEL

With the crystal structures of chicken Kir2.2 (56) and KirBac3.1 (55) (Chapter 1 ID), KirBac1.1 is no longer the only available full length structure of a Kir channel. Homology models of eukaryotic Kir channels can now be made using Kir2.2 as a template. KirBac1.1 now provides an interesting tool for comparison—that is, to determine what structural differences between KirBac1.1 and Kir2.2 may account for the observed functional differences. Below, I will briefly consider the rationale for future studies of three such functional differences: PIP_2 regulation, multiple conductance states, and polyamine block.

PIP_2 Regulation

MD simulations of PIP_2 binding to KirBac1.1 compared to a homology model of Kir6.2 show only subtle differences (45), suggesting that the opposite effect of PIP_2 on KirBac1.1 compared to eukaryotic Kir channels is not predominantly due to a different binding site, but rather to altered transduction of the signal or to gating in the channel. To identify the structural features that account for this difference in PIP_2 regulation, various chimeras of KirBac1.1 and eukaryotic Kir channels can be generated that transition between the two channels at different points above and below the intracellular interface, similar to the KirBac1.3/Kir3.1 chimera for which there is a crystal structure (54) and reports that this channel is functional and activated by PIP_2 when reconstituted in lipid bilayers (communication from D. Logothetis et al, Virginia Commonwealth University). Whether these chimeras are activated or inhibited by PIP_2 may implicate specific regions

of the channel (e.g. linkers, slide helix, cytoplasmic domain) for differential transduction of the PIP_2 signal. Mutations in Kir2.1 that disrupt interactions between the slide helix and cytoplasmic domain cause a loss-of-function phenotype (42). Thus, one hypothesis is that interactions between the slide helix and cytoplasmic domain are critical for effecting channel opening and that differential lengths of the transembrane-cytoplasmic linkers determine why KirBac1.1 and eukaryotic Kir channels are open and closed, respectively, in the absence of PIP_2 (Figure 6.1). The longer transmembrane-cytoplasmic linkers in eukaryotic Kir channels may minimize these interactions, resulting in closed channels. PIP_2 stabilizes these interactions, opening the channel. Lengthening the linker in KirBac1.1 or shortening the linker in Kir2.1 may be one approach to test this hypothesis. In addition, cysteine cross-linking between residues in the slide helix and cytoplasmic domain may be a useful approach to test the role of interactions between these two domains in channel gating and PIP_2-dependent modulation.

Multiple Conductance States

In eukaryotic Kir channels, charged residues in the cytoplasmic pore play an important role in determining ion conductance (306). As mentioned above, Robertson et al determined that the interaction energy of K^+ in the cytoplasmic pore of all eukaryotic Kir channels is highly favorable, unlike KirBac1.1 which contains several lysine and arginine residues (R189, K191, K208, K213) that make the cytoplasmic pore marginally unfavorable for K^+ occupancy (51). It is possible that the unfavorable electrostatic environment in the cytoplasmic pore contributes to the predominance of low conductance

states in KirBac1.1. Chimeras, discussed in the section above, consisting of a KirBac1.1 transmembrane domain and a eukaryotic Kir channel cytoplasmic domain could test this hypothesis. There are also four histidine residues (H117, H124, H210, and H219) proximal to the pore (H210 and H219 line the cytoplasmic pore) of KirBac1.1, and protonation and deprotonation of these residues may contribute to the observed multiple conductance states, similar to what has been reported in the nicotinic acetylcholine receptor (255, 256). These hypotheses can be tested by mutagenesis studies or by examining the pH-dependence of the distribution of conductance states in KirBac1.1.

Polyamine Block

The unfavorable electrostatic environment in the KirBac1.1 cytoplasmic pore (51) is expected to not only affect K^+ conductance, but also polyamine block (79). The data for spermine block of KirBac1.1 [I131C/I138D] in Chapter 3 are from recordings with relatively small currents, which make accurate measurement of the voltage-dependence of block difficult. Larger currents cannot be obtained simply by adding more protein in the reconstitution process, for unknown reasons, but can be achieved using a gain-of-function mutant, V145L (Figure 6.2A). V145L was identified in a yeast complementation screen of KirBac1.1 mutants (307). A single preliminary recording of KirBac1.1 [I138D/V145L], with large currents, shows that the voltage-dependence of spermine block is actually quite steep ($\delta z \sim 4$ (Figure 6.2B) compared to 2.5 as reported in Chapter 3) closer to what has been observed in eukaryotic Kir channels (308). One reason for accurately determining the voltage-dependence of spermine block in KirBac1.1 is that

this may have implications for our understanding of the mechanism of steep voltage dependence. For example, if the steep voltage-dependence of spermine block in eukaryotic Kir channels is due to displacement of K^+ ions occupying the cytoplasmic pore (85), then one might expect spermine block of KirBac1.1 to have a shallow voltage-dependence, since the occupancy of K^+ in the cytoplasmic pore of KirBac1.1 is predicted to be relatively low (51). On the other hand, if spermine block of KirBac1.1 is steeply voltage-dependent, which appears to be the case (Figure 6.2B), this might support the argument that steep voltage-dependence of block is due to displacement of K^+ ions that have a higher occupancy deeper in the pore (i.e. inner cavity and selectivity filter).

An electropositive cytoplasmic pore in KirBac1.1 is also predicted to slow polyamine block rate (79). Indeed, the rate of spermine block in KirBac1.1 [I138D/V145L] appears slow (Figure 6.2A and 6.2C) compared to the strong inward rectifier, Kir2.1, which at 0.1 mM spermine is nearly instantaneous (<1 ms) (79). A slower rate of block is also correlated with an increase in the plateau or residual K^+ current at depolarized (blocked) voltages, which has been attributed to polyamine punchthrough (75, 79). If the blocking rate decreases, the occupancy of the polyamine binding site also decreases such that at a constant rate of polyamine punchthrough, the residual K^+ current increases (79). If polyamine punchthrough is voltage-dependent, then the residual current will also increase with voltage (79). Consistent with these predictions, the plot of relative conductance versus voltage for spermine block of KirBac1.1 [I138D/V145L] shows a significant residual current that appears to increase with voltage, especially in comparison to Ba^{2+} block (Figure 6.2B). However, a complete

data set characterizing the properties of polyamine block in KirBac1.1 [I138D/V145L] is needed to be certain of these interpretations.

In summary, KirBac1.1 is a weak inward rectifier that exhibits key functional differences compared to eukaryotic Kirs channels. The crystal structure of KirBac1.1 along with established functional assays provide a comparative tool for investigating the structural basis of various properties of Kir channel function.

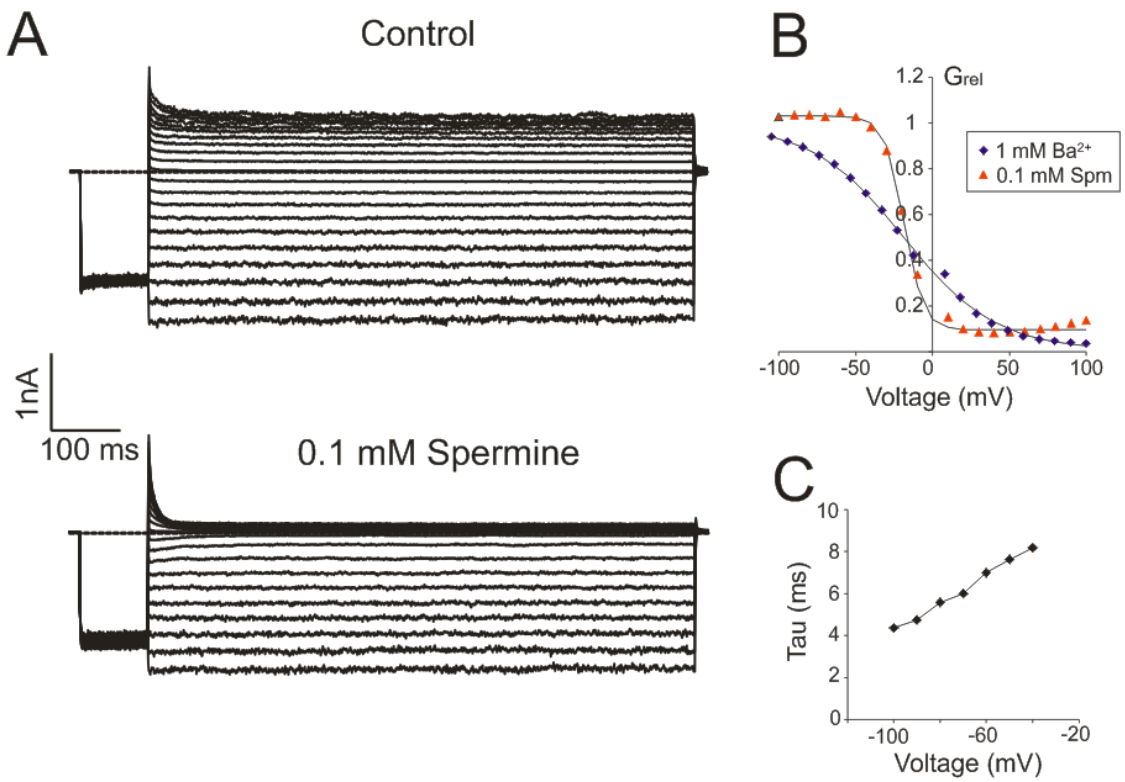

Figure 6.2: Spermine block in KirBac1.1 [I138D/V145L]. (A) Voltage-clamp currents of KirBac1.1 [I138D/V145L] in symmetrical 158 mM KCl, 10 mM KMOPS, pH 7.5 for control and with the addition of 0.1 mM spermine. Voltage-clamp protocol pulses to -80 mV then steps from -100 to +100 mV. (B) Plot of relative conductance versus voltage for Ba^{2+} (trace not shown) and spermine block. Data are fit with a Boltzmann function with the following parameters: for Ba^{2+}, $V_{1/2}$ = -16 mV and δz = 0.9; for spermine, $V_{1/2}$ = -19 mV and δz = 4.0. (C) Time constant (tau) for spermine block versus voltage obtained by fitting traces from (A) in spermine with a simple exponential function.

III. THE MOLECULAR "BOWSTRING" IN KCSA

IIIA. MECHANISM FOR REDUCED CATION SELECTIVITY IN THE ABSENCE OF K^+ IN E71A KCSA

The E71A mutant in KcsA disrupts a H-bond interaction behind the selectivity filter, analogous to a conserved salt bridge in Kir channels. Mutations of this salt bridge in Kir channels consistently reduce K^+-selectivity (118-120). The results discussed in Chapter 4 demonstrate that the E71A mutant in KcsA also reduces K^+-selectivity, by maintaining a conductive selectivity filter, in the absence of K^+ and presence of Na^+ (Chapter 4). Although the reduction in K^+ selectivity in E71A is subtle (i.e. Na^+ is still much less permeable through the channel compared to K^+ or Rb^+), it highlights the importance of the H-bond network behind the filter in tuning cation selectivity in KcsA as in eukaryotic Kir channels.

Similar to KcsA, KirBac1.1 has an E106-D115 H-bond interaction instead of a R-E salt bridge behind the selectivity filter (Figure 6.3A). However, both WT KirBac1.1 and the E106A mutant show relatively higher Na^+ flux in the absence of K^+ compared to WT KcsA, similar to E71A KcsA (Figure 6.3B). This is consistent with the fact that the H-bond network behind the filter in KirBac1.1 appears to be less extensive compared to KcsA with W67 and W68 replaced by F102 and F103 (Figure 6.3A). What other notable differences are present behind the filter between KirBac1.1 and KcsA? Interestingly, H124 at the top of TM2 (equivalent to R89 in KcsA) is positioned next to F102 of the adjacent subunit (Figure 6.3C). WT KirBac1.1 is insensitive to treatment with the positively-charged cysteine-modifying reagent, MTSEA (KirBac1.1 contains no native

cysteines), but H124C is inhibited by MTSEA (Figure 6.3D). One possible explanation for this result is that a positive charge at position 124 inhibits the channel by interacting with F102 (Figure 6.3C). Protonation of H124 may be the mechanism by which KirBac1.1 is inhibited by low pH, and future studies should test whether H124C is insensitive to low pH. Moreover, consistent with the mechanism in KcsA, engineering of this interaction between position 124 and F102 may be conferring an inactivation-like phenotype in KirBac1.1. It may be worthwhile to characterize the functional effects of H124C (MTSEA modified or unmodified) on selectivity, gating, and conductance (e.g. does this mutation alter $^{22}Na^+$ flux?), or test the presence of a putative cation-pi interaction between H124 and F102 using fluorinated unnatural amino acids.

The data in Chapter 4 establish a mechanistic link in KcsA between inactivation and selectivity. There is a correlation between inactivation and selectivity in many Kv and Kir channels, and the broader question is whether this mechanism established in KcsA is applicable to other K^+ channels, such as Kv channels, that exhibit C-type inactivation. In the Kv1.5 mutant, R487V, which reduces C-type inactivation (266), and in Kv3 channels (117), which exhibit minimal inactivation, there is higher conductance to Na^+ or NMG^+ in the absence of K^+. Similarly, mutation of the "bowstring" salt bridge in Kir1.1 abolishes a C-type inactivated-like state and reduces K^+/Rb^+ selectivity (265). These examples of non-inactivating channels showing reduced K^+-selectivity may all be the result of the mechanism that we report in KcsA. Conversely, Shaker channels and Kv2.1 show reduced selectivity for K^+ over Na^+ when progressing into inactivated states (114, 115). Thus, this mechanism is clearly not applicable in all cases since there are

examples of both inactivating and non-inactivating phenotypes being correlated with reduced K^+-selectivity.

The general applicability of this mechanism is also tempered by the fact that Kv channels have no equivalent E71-D80 interaction behind the filter. However, other H-bond interactions behind the filter may play a similar role; D80 is part of a H-bond network in KcsA involving W67, W68 and Y78, which is conserved among Kv channels (309). In Kv2.1, mutations of D378 (equivalent to D80 in KcsA) and Y376 (Y78 in KcsA), which are thought to disrupt this H-bond network, reduce selectivity and destabilize the open state (309, 310). Thus, there is evidence in other K^+ channels that disruption of the H-bond network behind the selectivity filter has coupled effects on selectivity and gating, and structural studies in these channels will be needed to further test the applicability of the mechanism established for KcsA.

IIIB. MECHANISM FOR REDUCED CATION SELECTIVITY IN THE PRESENCE OF K^+ IN E71A KCSA

Although WT KcsA remains conductive to Na^+ in the presence of K^+, the E71A mutant is still more permeable to Na^+ than the WT channel, as seen in $^{22}Na^+$ flux assays and Na^+ punchthrough experiments (Chapter 4). One hypothesis for the structural basis of this effect is that the conformation of the selectivity filter of the "flipped" E71A structure (20) (Chapter 4) is less K^+-selective. A filter with reduced K^+-selectivity would be the result of reduced selective partitioning of K^+ over Na^+, or lowering of the energy barriers for Na^+ conduction. One test of this hypothesis, would be to calculate the free energy

profile for K^+ versus Na^+ through the "flipped" selectivity filter when occupied with K^+ ions, as previously done with WT KcsA (110, 111) (Chapter 1 IIIA). Based on the theories presented in Chapter 1 IIIA and IIIB, a number of structural differences in the E71A "flipped" structure could explain this reduced selectivity. First, the backbone carbonyls of V76 are flipped away from the pore axis. These carbonyls participate in forming the coordination sites, S2 and S3—S2 being the most K-selective (102)—and the flipped conformation could lower the coordination number of these sites (124) or permit water to enter the filter (125, 128), either of which is predicted to reduce selective partitioning of K^+ over Na^+. A second possibility is that E71 makes a direct electrostatic contribution to the free energy profile of the filter and that mutation of this residue to an alanine alters this contribution. Thirdly, altered distribution and occupancy of K^+ ions in the filter may change the energy barriers associated with Na^+ translocation through the pore, since it has been shown that electrostatic repulsion from K^+ ions in the filter creates a large energetic barrier to Na^+ permeation (111).

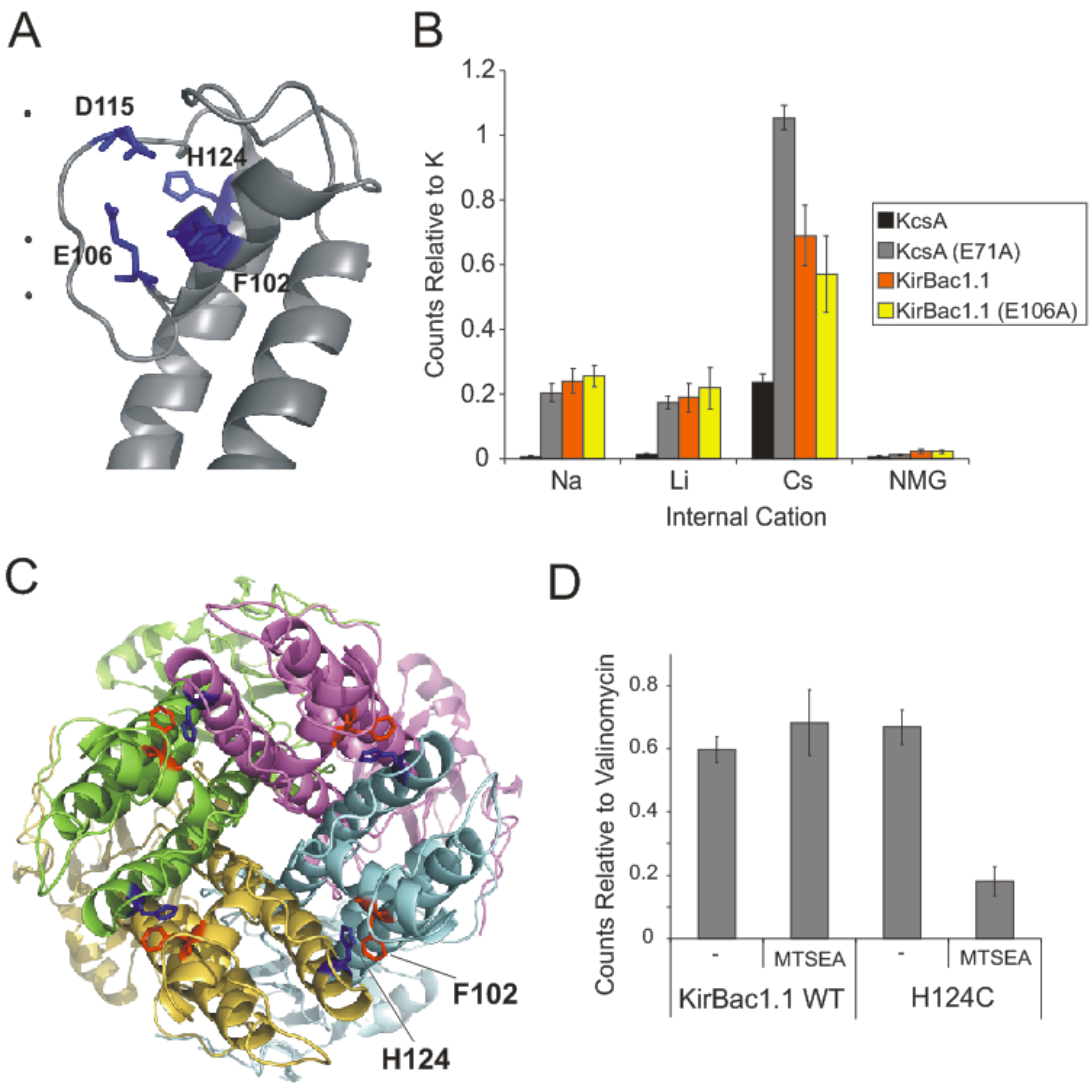

Figure 6.3 Role of the H-bond network behind the selectivity filter on KirBac1.1 function. (A) Crystal structure of KirBac1.1 (1P7B) showing stick side chains of E106, D115, F102, and H124, which are equivalent to E71, D80, W67 and R89 in KcsA. (B) $^{86}Rb^{+}$ uptake counts with different intra-liposomal cations normalized to uptake with K^{+} as the intra-liposomal cation. The data for KcsA are taken from Chapter 4 for comparison with KirBac1.1 (n=3, +/- s.e.m.). (C) Top view of KirBac1.1 tetramer (1P7B) showing stick side chains of H124 (blue) and F102 (red). (D) $^{86}Rb^{+}$ uptake counts normalized to

uptake in valinomycin for WT KirBac1.1 and the H124C mutant with and without MTSEA treatment in liposomes composed of 3:1 POPE:POPG (n=3, +/- s.e.m.). For MTSEA modification, samples were treated with 0.1 mM MTSEA for 30 min. prior to flux experiment.

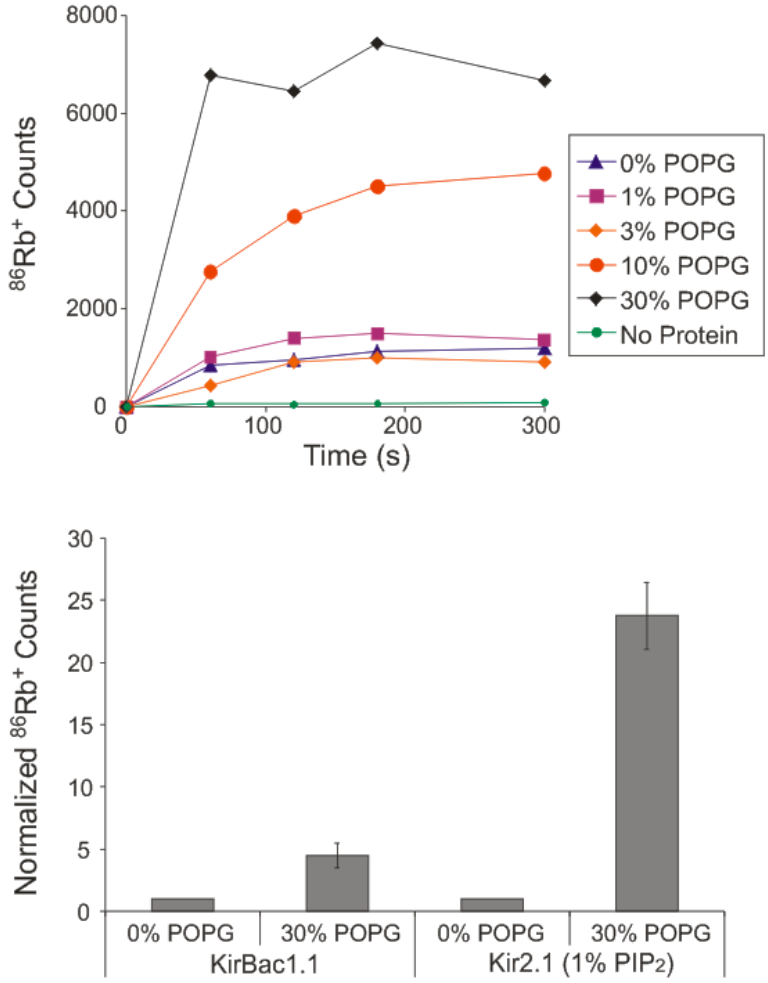

Figure 6.4 KirBac1.1 is active in POPE-only liposomes and weakly activated by POPG. (A) Representative time course of $^{86}Rb^+$ uptake of KirBac1.1 in liposomes with POPE-only and increasing % POPG. (B) Average of $^{86}Rb^+$ uptake in KirBac1.1 in liposomes without and with 25% POPG (n=3, +/- s.e.m.). The data are normalized to uptake in 0% POPG. Also shown is data from Figure 6.5 of Kir2.1 dependence on POPG.

IV. ANIONIC PHOSPHOLIPID REQUIREMENTS IN KIR CHANNELS

IVA. THE PIP_2 BINDING SITE IN EUKARYOTIC KIR CHANNELS

PIP_2 binding sites in eukaryotic Kir channels have been extensively investigated by functional mutagenesis studies (197, 199) and MD simulations using homology structures of Kir6.2 based on KirBac structures (44, 45) (Chapter 1 IIIC). Lipid binding assays have been limited to using cytoplasmic fragments of these channels (Chapter 1 IIIC). Recombinantly expressed and purified human Kir2.1 and Kir2.2 channels have an absolute requirement for membrane PIP_2, and activation occurs through direct interactions without the need for intermediary proteins as reported in Chapter 5. The capability to purify eukaryotic Kir channels now opens the possibility for lipid binding assays that can directly test interactions between PIP_2 and full-length channels. One approach is to use lipid-spotted membranes (205) to assay the binding of Kir2.1 and Kir2.2 to different PIPs and various other lipids. Mutants targeting residues that reduce PIP_2 sensitivity can then be tested, with the expectation that some may disrupt binding to PIPs, while others may have no effect, which might suggest that these mutations alter gating or transduction of the PIP_2 signal. Another approach is to extract lipids that may co-purify with the channel proteins and identify them using TLC, as previously done for KcsA (228). The channels may need to be purified with fewer washes to identify weakly-bound lipids, or the extracted lipids may be detected with mass spectrometry if only trace amounts are present. Broadly speaking, the next steps in elucidating the PIP_2 binding site

in eukaryotic Kir channels is to follow the approaches that have been used to study anionic phospholipid interactions with KcsA: lipid binding assays (228), fluorescence quenching by brominated lipids (227), and MD simulations (231) with crystal structure models of eukaryotic Kir channels, such as Kir2.2 (56).

IVB. STRUCTURAL BASIS OF THE SECONDARY ANIONIC PHOSPHOLIPID REQUIREMENT IN KIR2.1 AND KIR2.2

In addition to PIP_2, Kir2.1 and Kir2.2 have a secondary anionic phospholipid requirement that is non-specific, requires ~100x more lipid than the primary PIP_2 requirement, and increases both open probability and unitary conductance (Chapter 5). Mutagenesis of extracellular-facing residues, K117 and K120 in Kir2.1, exclude the possibility that this secondary requirement occurs through charge-based headgroup interactions at the extracellular side of the channel (Chapter 5). Rather, consistent with the fact that anionic phospholipids are predominantly localized to the inner leaflet of eukaryotic plasma membranes (Chapter 1 IVA), mutagenesis studies suggest that the secondary requirement is likely to be mediated by intracellular charged residues (Chapter 5). As detailed above (Chapter 6 IIIB), this hypothesis can be further tested by lipid binding assays and mutagenesis of basic residues near the intracellular interface.

Activation through the secondary requirement increases Kir2.1 unitary conductance. This could occur through two general mechanisms: 1) anionic phospholipids have a surface-charge effect that concentrates K^+ near the membrane, or 2) anionic phospholipids alter the structure and energetics of the pore. The first mechanism

is unlikely to be the case, since a surface charge effect of acidic residues in Kir2.1 on unitary conductance has been shown to only be significant at low bulk K^+ concentrations (~5-40 mM) (311). I used ~150 mM KCl in all my patch-clamp recordings, which is expected to shield most of the negative charge from the anionic lipids, so that these lipids do not concentrate K^+ near the pore. Furthermore, if anionic phospholipids are interacting with basic residues on the intracellular side of the channel, these are also likely to screen the negative charge of the lipid headgroups. A surface charge mechanism could be tested by recording Kir2.1 single channel currents in symmetrical 150 mM KCl with addition of high concentrations of non-permeant cations, such as NMG^+, on either side of the membrane; if a surface charge effect is present, the increase in unitary conductance due to POPG should be decreased by this non-permeant ion.

It seems more likely that anionic phospholipids are increasing Kir2.1 unitary conductance by altering the structure or energetics of the channel pore. Robertson et al (51) showed that all Kir channels have an "excess" of basic residues facing out towards the membrane at the intracellular interface. The electrostatic contribution of these residues to the channel pore is overall energetically unfavorable for K^+, and cancelling this unfavorable contribution requires binding of at least 2 PIP_2 molecules to each subunit (8 per channel) to screen these positively-charged residues (51). This is more lipid molecules than predicted for PIP_2 activation (3-4 PIP_2 lipids per channel) (184), and PIP_2 has no effect on the unitary conductance of Kir channels (182). One hypothesis is that the secondary requirement for anionic phospholipids in Kir2.1 satisfies this theoretically-predicted requirement to achieve a pore that energetically favors K^+ binding

and conduction. Indeed, this would also explain why increasing POPG increases Kir2.1 unitary conductance because anionic phospholipids are shielding these basic residues, making the channel pore more electronegative. In the study by Robertson et al, cytoplasmic interfacial basic residues in Kir1.1 and Kir2.1 make a stronger electropositive contribution to the pore than they do in KirBac1.1, Kir3.1 and Kir6.2. Consistent with this prediction, I have found that, unlike Kir2.1, KirBac1.1 remains active in POPE-only membranes and is only weakly activated by POPG (Figure 6.4). If anionic phospholipids do not increase the unitary conductance of Kir3.1 and Kir6.2 as effectively as Kir2.1, this would provide further evidence for this hypothesis. This mechanism, however, does not account for the effect of anionic phospholipids on channel gating, and there is likely another mechanism by which anionic phospholipids and PIP_2 increase channel open probability.

IVC. MULTI-MODE LIPID REGULATION OF KIR CHANNELS

Our findings illustrate novel features of how K^+ channels are regulated by the membrane environment, including by those lipids that make up the bulk of the membrane (i.e. anionic phospholipids). In Kir2.1 and Kir2.2, multiple lipids regulate channel activity through at least two distinct regulatory modes (Chapter 5). The model that I propose for dual-mode lipid regulation of Kir2.1 or Kir2.2 channels is shown as a schematic in Figure 6.5. Two binding sites in the channel represent the two regulatory modes: the primary mode, which is activated by squares, and the secondary mode, which is activated by circles (Figure 6.5A, box). The secondary mode is activated by all anionic

phospholipids; thus, PIP, PIP_2, PIP_3, and PG, all have a circle shape. However, PIP_2 appears to be more effective than PG in activating the secondary mode (Chapter 5, Figure 5.8), presumably because it is more negatively charged. Thus, PIP_2 and PIP_3, the more highly charged species, are represented with full circles as the most effective agonists of the secondary mode; PIP and PG are represented with partial circles as less effective agonists (Figure 6.5A, box). By contrast, the primary mode is specific to PIP_2 (large square), whereas PIP and PIP_3 (smaller squares) are weak partial agonists and anionic phospholipids that are not phosphatidylinositol phosphates (PIPs) such as PG (triangle) are completely ineffective as agonists. Thus, when sufficient anionic lipid is present to activate the secondary mode, the level of channel activity is dependent on which lipid (PIP_2- high activity, other PIPs- low activity, PG- no activity) is present to act at the primary mode (Figure 6.5A).

Figure 6.5B illustrates how phosphatidylinositol mono-phosphate (PIP) can either activate or inhibit channel activity under different lipid backgrounds. On a 1% PIP_2 background, PIP activates the channel by acting on the secondary mode, but activation is weak because PIP also competes with PIP_2 at the primary mode as a partial agonist. On a 1% PIP_2/25% PG background where both regulatory modes are nearly fully activated, PIP inhibits channel activity by competing with PIP_2. In the plasma membrane of mammalian cells, $PI(4,5)P_2$ and PI(4)P are the predominant phosphatidylinositol phosphate species, and present in variable but approximately equal amounts with estimates up to ~1 mole% of total phospholipids (164, 177). Thus, these two PIPs are

predicted to competitively act on the primary mode and may even contribute to activation at the secondary mode in a cellular environment.

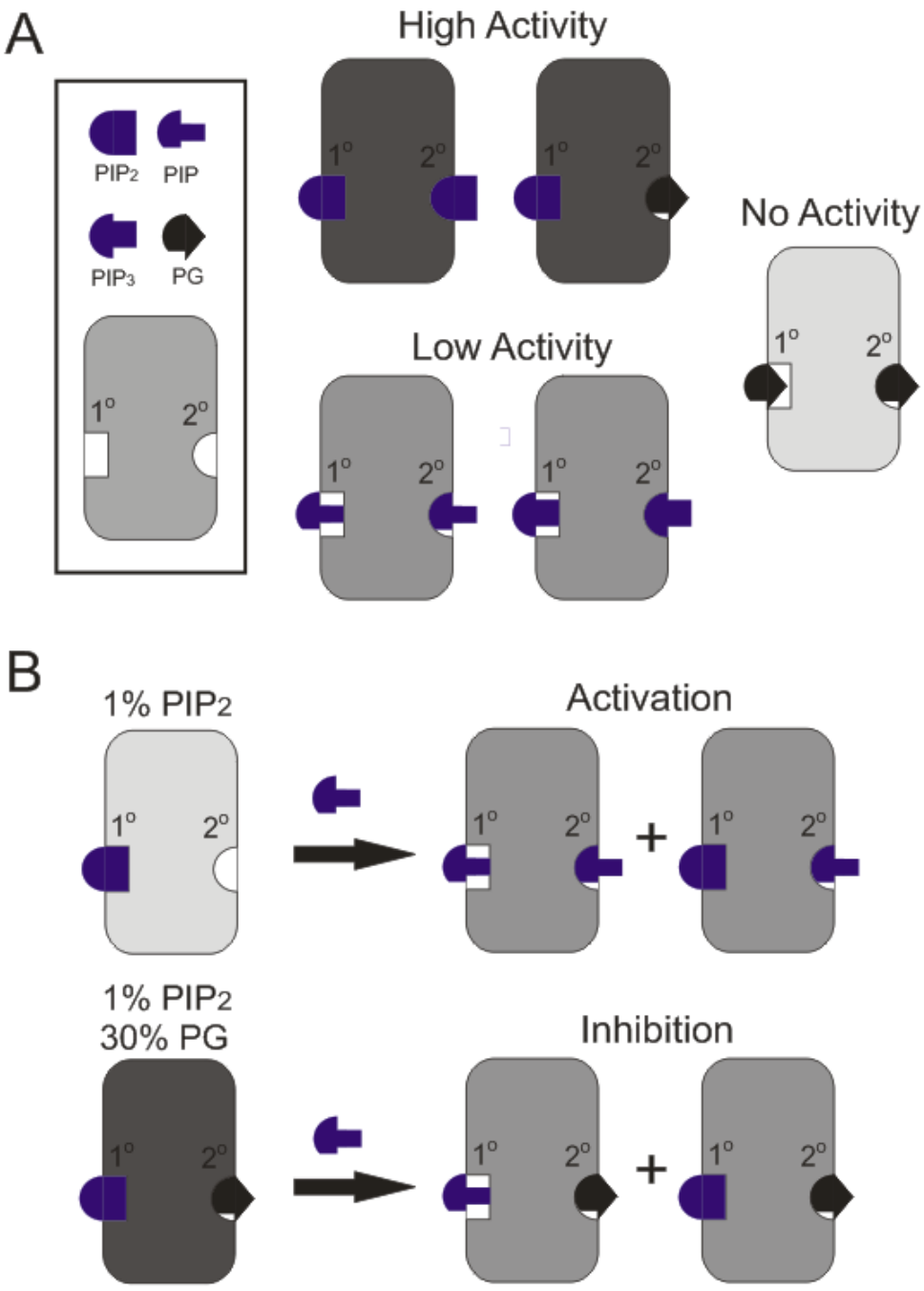

Figure 6.5 Schematic for dual-mode regulation of Kir2.1. (A) *Inside box*: Cartoon of Kir2.1 channel showing two lipid binding sites, which represent the primary and

secondary modes of lipid regulation. Symbols above represent lipids as indicated (PIP-phosphatidylinositol monophosphate, PIP_2- phosphatidylinositol 4,5-bisphosphate, PIP_3-phosphatidylinositol 3,4,5-triphosphate). *Right*: Actions of various lipid modulators, which result in high activity (dark gray), low activity (medium gray), or no activity (light gray). These differences depend on which modulator is acting on the primary mode. (B) Scenarios where PIP (at 10%) can either activate or inhibit Kir2.1 activity. *Above*: Addition of PIP on a 1% PIP_2 background activates Kir2.1. PIP activates via the secondary mode and competitively inhibits via the primary mode. The degree of channel activation is dependent on how effectively PIP competes with PIP_2. *Below*: Addition of PIP on a 1% PIP_2/30% PG background inhibits Kir2.1. PIP competitively inhibits via the primary mode.

V. CONCLUDING REMARKS

One unifying feature of the experiments presented in this thesis is the use of purified, reconstituted channels. The vast majority of electrophysiological studies of Kir channels and ion channels have historically been performed in native tissues or by heterologous expression in mammalian cell lines. With the discovery of prokaryotic channels, such as KirBac1.1, which are easily expressed in *E. coli*, and the recent development of methods to purify human Kir channels from *S. cerevisiae* (288), it is now realistic to study the biochemistry of full length Kir channels. Our findings demonstrate two advantageous features of using purified, reconstituted Kir channels: 1) the identical channel protein may be used for functional studies and crystal structure determination, and 2) the lipid dependence of channel activity can be quantitatively determined in liposomes of defined composition. Thus, I established KirBac1.1 as one structural model of Kir channels, determined a structural mechanism by which KcsA selects for K^+ over Na^+ conduction, and identified a novel mode of lipid regulation by anionic phospholipids in Kir2.1 and Kir2.2. The expectation is that more Kir channel proteins, as well as channels from other families, will soon be purified to undergo similar studies.

This work examined multiple inward rectifying potassium channels that are distantly related: bacterial and human channels. The similarities and differences in their functional and structural properties not only inform structure-function relationships, but raise new hypotheses about when and how these properties may have evolved. The fact that KirBac channels and eukaryotic Kir channels are structurally related suggests that the evolution of functional properties such as steep voltage-dependent block by polyamines

or specific binding and modulation by PIP_2 were already present among bacterial homologues. Sequence alignment of all KirBac channels from KirBac1.1 to KirBac8.1 (248) shows that all of these proteins contain a neutral residue (isoleucine, alanine or serine) at the rectification controller position. KirBac1.1 exhibits steep voltage-dependent block by spermine only when I138 is mutated to an aspartate (Chapter 3). Thus, these bacterial channels are all likely to resemble eukaryotic weak inward rectifiers. Although the functional role of KirBacs is unclear, genetic deletion of KirBac6.1 from cyanobacterium *Synechocystis*, the organism from which it was first identified, slows growth in low K^+ media (307), suggesting that KirBac channels are important for mediating K^+ uptake in bacteria—a function that would not require strong inward rectification. The large cytoplasmic domain, which forms the long pore putatively important for strong inward rectification, may have evolved as a consequence of the cytoplasmic domain providing ligand control in KirBacs. On this structural background, sensitivity to Mg^{2+} and polyamine block subsequently arose in eukaryotic Kir channels with just a single amino acid change to an aspartate or glutamate at the rectification controller position. Strong inward rectification likely evolved in eukaryotes in order to control excitability in action potential-generating cells.

The molecular “bowstring”, which is an R-E salt bridge in all eukaryotic Kir channels, is present as a D-E H-bond interaction in KirBac1.1, KirBac2.1 and KirBac3.1 (248). My preliminary experiments suggest that human Kir2.1 is similar to KcsA in that Na^+ movement through this channel is nearly undetectable by flux assay (data not shown) unlike KirBac1.1. The evolution of the salt bridge in eukaryotic Kir channels may have

served to tighten the selectivity of these channels against Na^+ permeation compared to KirBac channels.

Finally, the qualitatively opposite effect of PIP_2 modulation of eukaryotic Kir channels and KirBac1.1 raises the interesting hypothesis that membrane lipids drove the evolution of channel structure and function. PIP_2 and other phosphatidylinositol phosphates are typically absent in prokaryotic membranes (Chapter 1 IVA), an environment in which KirBac1.1 is active (52) (Chapter 3). The sensitivity of KirBac1.1 to inhibition by PIP_2 may have been a by-product of the evolution of regulatory domains for soluble ligands such as ATP. In eukaryotic membranes, where $PI(4,5)P_2$ is one of the most abundant PIPs and is almost exclusively localized to the plasma membrane (Chapter 1 IVA), Kir channels could not retain the same dependence on PIP_2, since KirBac1.1 would be almost completely inhibited at cellular PIP_2 levels (53) (Chapter 5, Figure 5.1B). Rather, either because Kir channels needed to be silenced during trafficking in intracellular organelles or activated by localized changes in plasma membrane PIP_2 (177, 312), eukaryotic Kir channels evolved an absolute requirement for PIP_2 by relatively minor changes in channel sequence and structure, such as the addition of three residues in the TM-cytoplasmic linker (194) (Chapter 6 IB). As multiple ion channels are regulated by PIP_2 (148), it is possible that this same pattern and potential evolutionary mechanism is present between other channels and their prokaryotic counterparts.

In a similar vein, the secondary requirement for anionic phospholipids may have evolved only in certain eukaryotic Kir channels. Kir2.1 and Kir2.2 require anionic phospholipids for activity (Chapter 5), whereas KirBac1.1 does not and is only weakly

activated by PG (Figure 6.4). The secondary requirement appears to be mediated by channel-lipid interactions at the intracellular interface, which is consistent with the fact that anionic phospholipids are predominantly localized to the inner leaflet of eukaryotic cell membranes (Chapter 1 IVA). In prokaryotic membranes, anionic phospholipids are often localized to the outer leaflet (Chapter 1 IVA), consistent with KcsA having an absolute requirement for anionic phospholipids mediated by channel-lipid interactions on the extracellular side of the channel (Chapter 1 IVE). The evolution of an absolute requirement for anionic phospholipids in Kir2.1 and Kir2.2 that is not present in KirBac1.1 may have been driven by the differential localization and dynamic regulation of anionic phospholipids in eukaryotic compared to prokaryotic cell membranes.

REFERENCES

1. Hille, B. 2001. Ion Channels of Excitable Membranes. Sinauer Associates, Inc., Sunderland, MA. 462-468.

2. Ryan, D., M. da Silva, T. Soong, B. Fontaine, M. Donaldson, A. Kung, W. Jongjaroenprasert, M. Liang, D. Khoo, J. Cheah, S. Ho, H. Bernstein, R. Maciel, R. J. Brown, and L. Ptácek. 2010. Mutations in potassium channel Kir2.6 cause susceptibility to thyrotoxic hypokalemic periodic paralysis. Cell 140:88-98.

3. Hassinen, M., V. Paajanen, and M. Vornanen. 2008. A novel inwardly rectifying K+ channel, Kir2.5, is upregulated under chronic cold stress in fish cardiac myocytes. J Exp Biol 211:2162-2171.

4. Kubo, Y., J. P. Adelman, D. E. Clapham, L. Y. Jan, A. Karschin, Y. Kurachi, M. Lazdunski, C. G. Nichols, S. Seino, and C. A. Vandenberg. 2005. International Union of Pharmacology. LIV. Nomenclature and molecular relationships of inwardly rectifying potassium channels. Pharmacol.Rev. 57:509-526.

5. Gutman, G. A., K. G. Chandy, J. P. Adelman, J. Aiyar, D. A. Bayliss, D. E. Clapham, M. Covarriubias, G. V. Desir, K. Furuichi, B. Ganetzky, M. L. Garcia, S. Grissmer, L. Y. Jan, A. Karschin, D. Kim, S. Kuperschmidt, Y. Kurachi, M. Lazdunski, F. Lesage, H. A. Lester, D. McKinnon, C. G. Nichols, I. O'Kelly, J. Robbins, G. A. Robertson, B. Rudy, M. Sanguinetti, S. Seino, W. Stuehmer, M. M. Tamkun, C. A. Vandenberg, A. Wei, H. Wulff, and R. S. Wymore. 2003. International Union of Pharmacology. XLI. Compendium of voltage-gated ion channels: potassium channels. Pharmacol.Rev. 55:583-586.

6. Anumonwo, J., and A. Lopatin. 2010. Cardiac strong inward rectifier potassium channels. J Mol Cell Cardiol 48:45-54.

7. Zhang, H., T. Flagg, and C. Nichols. 2010. Cardiac sarcolemmal K(ATP) channels: Latest twists in a questing tale! J Mol Cell Cardiol 48:71-75.

8. Koster, J. C., M. A. Permutt, and C. G. Nichols. 2005. Diabetes and insulin secretion: the ATP-sensitive K+ channel (K ATP) connection. Diabetes 54:3065-3072.

9. Simon, D., F. Karet, J. Rodriguez-Soriano, J. Hamdan, A. DiPietro, H. Trachtman, S. Sanjad, and R. Lifton. 1996. Genetic heterogeneity of Bartter's syndrome revealed by mutations in the K+ channel, ROMK. Nat Genet 14:152-156.

10. Plaster, N., R. Tawil, M. Tristani-Firouzi, S. Canún, S. Bendahhou, A. Tsunoda, M. Donaldson, S. Iannaccone, E. Brunt, R. Barohn, J. Clark, F. Deymeer, A. J. George, F. Fish, A. Hahn, A. Nitu, C. Ozdemir, P. Serdaroglu, S. Subramony, G. Wolfe, Y. Fu, and L. Ptácek. 2001. Mutations in Kir2.1 cause the developmental and episodic electrical phenotypes of Andersen's syndrome. Cell 105:511-519.

11. Gloyn, A., E. Pearson, J. Antcliff, P. Proks, G. Bruining, A. Slingerland, N. Howard, S. Srinivasan, J. Silva, J. Molnes, E. Edghill, T. Frayling, I. Temple, D. Mackay, J. Shield, Z. Sumnik, A. van Rhijn, J. Wales, P. Clark, S. Gorman, J. Aisenberg, S. Ellard, P. Njølstad, F. Ashcroft, and A. Hattersley. 2004. Activating mutations in the gene encoding the ATP-sensitive potassium-channel subunit Kir6.2 and permanent neonatal diabetes. N Engl J Med 350:1838-1849.

12. Donaldson, M., J. Jensen, M. Tristani-Firouzi, R. Tawil, S. Bendahhou, W. Suarez, A. Cobo, J. Poza, E. Behr, J. Wagstaff, P. Szepetowski, S. Pereira, T. Mozaffar, D. Escolar, Y. Fu, and L. Ptácek. 2003. PIP2 binding residues of Kir2.1 are common targets of mutations causing Andersen syndrome. Neurology 60:1811-1816.

13. Masia, R., J. C. Koster, S. Tumini, F. Chiarelli, C. Colombo, C. G. Nichols, and F. Barbetti. 2007. An ATP-binding mutation (G334D) in KCNJ11 is associated with a sulfonylurea-insensitive form of developmental delay, epilepsy, and neonatal diabetes. Diabetes 56:328-336.

14. Koster, J., H. Kurata, D. Enkvetchakul, and C. Nichols. 2008. DEND mutation in Kir6.2 (KCNJ11) reveals a flexible N-terminal region critical for ATP-sensing of the KATP channel. Biophys J 95:4689-4697.

15. Doyle, D., J. Morais Cabral, R. Pfuetzner, A. Kuo, J. Gulbis, S. Cohen, B. Chait, and R. MacKinnon. 1998. The structure of the potassium channel: molecular basis of K+ conduction and selectivity. Science 280:69-77.

16. Kuo, A. L., J. M. Gulbis, J. F. Antcliff, T. Rahman, E. D. Lowe, J. Zimmer, J. Cuthbertson, F. M. Ashcroft, T. Ezaki, and D. A. Doyle. 2003. Crystal structure of the potassium channel KirBac1.1 in the closed state. Science 300:1922-1926.

17. Schrempf, H., O. Schmidt, R. Kummerlen, S. Hinnah, D. Muller, M. Betzler, T. Steinkamp, and R. Wagner. 1995. A prokaryotic potassium ion channel with two predicted transmembrane segments from Streptomyces lividans. EMBO J. 14:5170-5178.

18. Meuser, D., H. Splitt, R. Wagner, and H. Schrempf. 1999. Exploring the open pore of the potassium channel from Streptomyces lividans. FEBS Lett. 462:447-452.

19. LeMasurier, M., L. Heginbotham, and C. Miller. 2001. KcsA: it's a potassium channel. J.Gen.Physiol 118:303-314.

20. Cordero-Morales, J. F., L. G. Cuello, Y. X. Zhao, V. Jogini, D. M. Cortes, B. Roux, and E. Perozo. 2006. Molecular determinants of gating at the potassium-channel selectivity filter. Nature Structural & Molecular Biology 13:311-318.

21. Guy, H., and S. Durell. 1995. Structural models of Na+, Ca2+, and K+ channels. Soc Gen Physiol Ser 50:1-16.

22. Durell, S., and H. Guy. 1996. Structural model of the outer vestibule and selectivity filter of the Shaker voltage-gated K+ channel. Neuropharmacology 35:761-773.

23. Zhou, Y., J. H. Morais-Cabral, A. Kaufman, and R. MacKinnon. 2001. Chemistry of ion coordination and hydration revealed by a K+ channel-Fab complex at 2.0 A resolution. Nature 414:43-48.

24. Heginbotham, L., Z. Lu, T. Abramson, and R. MacKinnon. 1994. Mutations in the K+ channel signature sequence. Biophys J 66:1061-1067.

25. HODGKIN, A., and R. KEYNES. 1955. The potassium permeability of a giant nerve fibre. J Physiol 128:61-88.

26. Roux, B., and R. MacKinnon. 1999. The cavity and pore helices in the KcsA K+ channel: electrostatic stabilization of monovalent cations. Science 285:100-102.

27. Roux, B., S. Bernèche, and W. Im. 2000. Ion channels, permeation, and electrostatics: insight into the function of KcsA. Biochemistry 39:13295-13306.

28. Blunck, R., J. F. Cordero-Morales, L. G. Cuello, E. Perozo, and F. Bezanilla. 2006. Detection of the opening of the bundle crossing in KcsA with fluorescence lifetime spectroscopy reveals the existence of two gates for ion conduction. J.Gen.Physiol 128:569-581.

29. Jiang, Y., A. Lee, J. Chen, M. Cadene, B. Chait, and R. MacKinnon. 2002. The open pore conformation of potassium channels. Nature 417:523-526.

30. Thompson, A. N., D. J. Posson, P. V. Parsa, and C. M. Nimigean. 2008. Molecular mechanism of pH sensing in KcsA potassium channels. Proc.Natl.Acad.Sci.U.S.A 105:6900-6905.

31. Loussouarn, G., E. N. Makhina, T. Rose, and C. G. Nichols. 2000. Structure and dynamics of the pore of inwardly rectifying K(ATP) channels. J.Biol.Chem. 275:1137-1144.

32. Capener, C. E., I. H. Shrivastava, K. M. Ranatunga, L. R. Forrest, G. R. Smith, and M. S. P. Sansom. 2000. Homology modeling and molecular dynamics simulation studies of an inward rectifier potassium channel. Biophysical Journal 78:2929-2942.

33. Minor, D. J., S. Masseling, Y. Jan, and L. Jan. 1999. Transmembrane structure of an inwardly rectifying potassium channel. Cell 96:879-891.

34. Miller, C. 1995. The charybdotoxin family of K+ channel-blocking peptides. Neuron 15:5-10.

35. MacKinnon, R., S. L. Cohen, A. Kuo, A. Lee, and B. T. Chait. 1998. Structural conservation in prokaryotic and eukaryotic potassium channels. Science 280:106-109.

36. Lu, Z., and R. MacKinnon. 1997. Purification, characterization, and synthesis of an inward-rectifier K+ channel inhibitor from scorpion venom. Biochemistry 36:6936-6940.

37. Durell, S. R., and H. R. Guy. 2001. A family of putative Kir potassium channels in prokaryotes. BMC.Evol.Biol. 1:14.

38. Hejtmancik, J., X. Jiao, A. Li, Y. Sergeev, X. Ding, A. Sharma, C. Chan, I. Medina, and A. Edwards. 2008. Mutations in KCNJ13 cause autosomal-dominant snowflake vitreoretinal degeneration. Am J Hum Genet 82:174-180.

39. Nishida, M., and R. MacKinnon. 2002. Structural basis of inward rectification: cytoplasmic pore of the G protein-gated inward rectifier GIRK1 at 1.8 A resolution. Cell 111:957-965.

40. Schulte, U., H. Hahn, M. Konrad, N. Jeck, C. Derst, K. Wild, S. Weidemann, J. Ruppersberg, B. Fakler, and J. Ludwig. 1999. pH gating of ROMK (K(ir)1.1) channels: control by an Arg-Lys-Arg triad disrupted in antenatal Bartter syndrome. Proc Natl Acad Sci U S A 96:15298-15303.

41. Schulze, D., T. Krauter, H. Fritzenschaft, M. Soom, and T. Baukrowitz. 2003. Phosphatidylinositol 4,5-bisphosphate (PIP2) modulation of ATP and pH sensitivity in Kir channels - A tale of an active and a silent PIP2 site in the N terminus. Journal of Biological Chemistry 278:10500-10505.

42. Decher, N., V. Renigunta, M. Zuzarte, M. Soom, S. Heinemann, K. Timothy, M. Keating, J. Daut, M. Sanguinetti, and I. Splawski. 2007. Impaired interaction between the slide helix and the C-terminus of Kir2.1: a novel mechanism of Andersen syndrome. Cardiovasc Res 75:748-757.

43. Antcliff, J. F., S. Haider, P. Proks, M. S. Sansom, and F. M. Ashcroft. 2005. Functional analysis of a structural model of the ATP-binding site of the KATP channel Kir6.2 subunit. EMBO J. 24:229-239.

44. Haider, S., A. I. Tarasov, T. J. Craig, M. S. Sansom, and F. M. Ashcroft. 2007. Identification of the PIP2-binding site on Kir6.2 by molecular modelling and functional analysis. EMBO J. 26:3749-3759.

45. Stansfeld, P., R. Hopkinson, F. Ashcroft, and M. Sansom. 2009. PIP(2)-binding site in Kir channels: definition by multiscale biomolecular simulations. Biochemistry 48:10926-10933.

46. Domene, C., A. Grottesi, and M. Sansom. 2004. Filter flexibility and distortion in a bacterial inward rectifier K+ channel: simulation studies of KirBac1.1. Biophys J 87:256-267.

47. Grottesi, A., C. Domene, B. Hall, and M. S. Sansom. 2005. Conformational dynamics of M2 helices in KirBac channels: helix flexibility in relation to gating via molecular dynamics simulations. Biochemistry 44:14586-14594.

48. Domene, C., S. Vemparala, M. L. Klein, C. Venien-Bryan, and D. A. Doyle. 2006. Role of aromatic localization in the gating process of a potassium channel. Biophys.J. 90:L01-L03.

49. Domene, C., M. L. Klein, D. Branduardi, F. L. Gervasio, and M. Parrinello. 2008. Conformational changes and gating at the selectivity filter of potassium channels. J.Am.Chem.Soc. 130:9474-9480.

50. Hellgren, M., L. Sandberg, and O. Edholm. 2006. A comparison between two prokaryotic potassium channels (KirBac1.1 and KcsA) in a molecular dynamics (MD) simulation study. Biophys.Chem. 120:1-9.

51. Robertson, J., L. Palmer, and B. Roux. 2008. Long-pore electrostatics in inward-rectifier potassium channels. J Gen Physiol 132:613-632.

52. Enkvetchakul, D., J. Bhattacharyya, I. Jeliazkova, D. K. Groesbeck, C. A. Cukras, and C. G. Nichols. 2004. Functional characterization of a prokaryotic Kir channel. J.Biol.Chem. 279:47076-47080.

53. Enkvetchakul, D., I. Jeliazkova, and C. G. Nichols. 2005. Direct modulation of Kir channel gating by membrane phosphatidylinositol 4,5-bisphosphate. J.Biol.Chem. 280:35785-35788.

54. Nishida, M., M. Cadene, B. T. Chait, and R. MacKinnon. 2007. Crystal structure of a Kir3.1-prokaryotic Kir channel chimera. EMBO J. 26:4005-4015.

55. Clarke, O., A. Caputo, A. Hill, J. Vandenberg, B. Smith, and J. Gulbis. 2010. Domain reorientation and rotation of an intracellular assembly regulate conduction in Kir potassium channels. Cell 141:1018-1029.

56. Tao, X., J. Avalos, J. Chen, and R. MacKinnon. 2009. Crystal structure of the eukaryotic strong inward-rectifier K+ channel Kir2.2 at 3.1 A resolution. Science 326:1668-1674.

57. Pegan, S., C. Arrabit, W. Zhou, W. Kwiatkowski, A. Collins, P. A. Slesinger, and S. Choe. 2005. Cytoplasmic domain structures of Kir2.1 and Kir3.1 show sites for modulating gating and rectification. Nat.Neurosci. 8:279-287.

58. Katz, B. 1949. Les constantes electriques de la membrane du muscle. Arch. Sci. Physiol. 3:285-299.

59. Lopatin, A. N., E. N. Makhina, and C. G. Nichols. 1995. The Mechanism of Inward Rectification of Potassium Channels - Long-Pore Plugging by Cytoplasmic Polyamines. Journal of General Physiology 106:923-955.

60. Hagiwara, S., S. Miyazaki, and N. Rosenthal. 1976. Potassium current and the effect of cesium on this current during anomalous rectification of the egg cell membrane of a starfish. J Gen Physiol 67:621-638.

61. Lopatin, A. N., and C. G. Nichols. 1996. [K+] dependence of open-channel conductance in cloned inward rectifier potassium channels (IRK1, Kir2.1). Biophys.J. 71:682-694.

62. Armstrong, C. 1971. Interaction of tetraethylammonium ion derivatives with the potassium channels of giant axons. J Gen Physiol 58:413-437.

63. Vandenberg, C. 1987. Inward rectification of a potassium channel in cardiac ventricular cells depends on internal magnesium ions. Proc Natl Acad Sci U S A 84:2560-2564.

64. Matsuda, H., A. Saigusa, and H. Irisawa. 1987. Ohmic conductance through the inwardly rectifying K channel and blocking by internal Mg2+. Nature 325:156-159.

65. Saigusa, A., and H. Matsuda. 1988. Outward currents through the inwardly rectifying potassium channel of guinea-pig ventricular cells. Jpn J Physiol 38:77-91.

66. Silver, M., and T. DeCoursey. 1990. Intrinsic gating of inward rectifier in bovine pulmonary artery endothelial cells in the presence or absence of internal Mg2+. J Gen Physiol 96:109-133.

67. Silver, M., M. Shapiro, and T. DeCoursey. 1994. Effects of external Rb+ on inward rectifier K+ channels of bovine pulmonary artery endothelial cells. J Gen Physiol 103:519-548.

68. Lopatin, A. N., E. N. Makhina, and C. G. Nichols. 1994. Potassium Channel Block by Cytoplasmic Polyamines As the Mechanism of Intrinsic Rectification. Nature 372:366-369.

69. Ficker, E., M. Taglialatela, B. A. Wible, C. M. Henley, and A. M. Brown. 1994. Spermine and spermidine as gating molecules for inward rectifier K+ channels. Science 266:1068-1072.

70. Guo, D., and Z. Lu. 2000. Pore block versus intrinsic gating in the mechanism of inward rectification in strongly rectifying IRK1 channels. J Gen Physiol 116:561-568.

71. Lu, Z., and R. MacKinnon. 1994. Electrostatic tuning of Mg2+ affinity in an inward-rectifier K+ channel. Nature 371:243-246.

72. Shyng, S., T. Ferrigni, and C. G. Nichols. 1997. Control of rectification and gating of cloned KATP channels by the Kir6.2 subunit. J.Gen.Physiol 110:141-153.

73. Guo, D., Y. Ramu, A. M. Klem, and Z. Lu. 2003. Mechanism of rectification in inward-rectifier K+ channels. J.Gen.Physiol 121:261-275.

74. Pearson, W. L., and C. G. Nichols. 1998. Block of the Kir2.1 channel pore by alkylamine analogues of endogenous polyamines. J.Gen.Physiol 112:351-363.

75. Guo, D., and Z. Lu. 2000. Mechanism of IRK1 channel block by intracellular polyamines. J Gen Physiol 115:799-814.

76. Xie, L., S. John, and J. Weiss. 2002. Spermine block of the strong inward rectifier potassium channel Kir2.1: dual roles of surface charge screening and pore block. J Gen Physiol 120:53-66.

77. Kurata, H. T., L. R. Phillips, T. Rose, G. Loussouarn, S. Herlitze, H. Fritzenschaft, D. Enkvetchakul, C. G. Nichols, and T. Baukrowitz. 2004. Molecular basis of inward rectification: polyamine interaction sites located by combined channel and ligand mutagenesis. J.Gen.Physiol 124:541-554.

78. Shin, H. G., Y. Xu, and Z. Lu. 2005. Evidence for sequential ion-binding loci along the inner pore of the IRK1 inward-rectifier K+ channel. J Gen Physiol 126:123-135.

79. Kurata, H. T., W. W. Cheng, C. Arrabit, and P. A. N. C. G. Slesinger. 2007. The Role of the Cytoplasmic Pore in Inward Rectification of Kir2.1 Channels. Journal of General Physiology In print.

80. Kubo, Y., and Y. Murata. 2001. Control of rectification and permeation by two distinct sites after the second transmembrane region in Kir2.1 K+ channel. J Physiol 531:645-660.

81. Yang, J., Y. Jan, and L. Jan. 1995. Control of rectification and permeation by residues in two distinct domains in an inward rectifier K+ channel. Neuron 14:1047-1054.

82. Taglialatela, M., B. Wible, R. Caporaso, and A. Brown. 1994. Specification of pore properties by the carboxyl terminus of inwardly rectifying K+ channels. Science 264:844-847.

83. Taglialatela, M., E. Ficker, B. Wible, and A. Brown. 1995. C-terminus determinants for Mg2+ and polyamine block of the inward rectifier K+ channel IRK1. EMBO J 14:5532-5541.

84. Guo, D., and Z. Lu. 2003. Interaction mechanisms between polyamines and IRK1 inward rectifier K+ channels. J.Gen.Physiol 122:485-500.

85. Xu, Y., H. Shin, S. Szép, and Z. Lu. 2009. Physical determinants of strong voltage sensitivity of K(+) channel block. Nat Struct Mol Biol 16:1252-1258.

86. Kurata, H. T., L. J. Marton, and C. G. Nichols. 2006. The polyamine binding site in inward rectifier K+ channels. J.Gen.Physiol 127:467-480.

87. Kurata, H., K. Diraviyam, L. Marton, and C. Nichols. 2008. Blocker protection by short spermine analogs: refined mapping of the spermine binding site in a Kir channel. Biophys J 95:3827-3839.

88. Kurata, H., E. Zhu, and C. Nichols. 2010. Locale and chemistry of spermine binding in the archetypal inward rectifier Kir2.1. J Gen Physiol 135:495-508.

89. Chang, H., S. Yeh, and R. Shieh. 2003. The effects of spermine on the accessibility of residues in the M2 segment of Kir2.1 channels expressed in Xenopus oocytes. J Physiol 553:101-112.

90. Woodhull, A. 1973. Ionic blockage of sodium channels in nerve. J Gen Physiol 61:687-708.

91. Hille, B., and W. Schwarz. 1978. Potassium channels as multi-ion single-file pores. J Gen Physiol 72:409-442.

92. Spassova, M., and Z. Lu. 1998. Coupled ion movement underlies rectification in an inward-rectifier K+ channel. J.Gen.Physiol 112:211-221.

93. Kline, R., I. Cohen, R. Falk, and J. Kupersmith. 1980. Activity-dependent extracellular K+ fluctuations in canine Purkinje fibres. Nature 286:68-71.

94. Lopatin, A. N., and C. G. Nichols. 2001. Inward rectifiers in the heart: an update on I(K1). J.Mol.Cell Cardiol. 33:625-638.

95. Neyton, J., and C. Miller. 1988. Potassium blocks barium permeation through a calcium-activated potassium channel. J Gen Physiol 92:549-567.

96. Neyton, J., and C. Miller. 1988. Discrete Ba2+ block as a probe of ion occupancy and pore structure in the high-conductance Ca2+ -activated K+ channel. J Gen Physiol 92:569-586.

97. Lockless, S. W., M. Zhou, and R. MacKinnon. 2007. Structural and thermodynamic properties of selective ion binding in a K+ channel. PLoS Biol. 5:e121.

98. Jensen, M., D. Borhani, K. Lindorff-Larsen, P. Maragakis, V. Jogini, M. Eastwood, R. Dror, and D. Shaw. 2010. Principles of conduction and hydrophobic gating in K+ channels. Proc Natl Acad Sci U S A 107:5833-5838.

99. Nimigean, C. M., and C. Miller. 2002. Na+ block and permeation in a K+ channel of known structure. J.Gen.Physiol 120:323-335.

100. Morais-Cabral, J. H., Y. Zhou, and R. MacKinnon. 2001. Energetic optimization of ion conduction rate by the K+ selectivity filter. Nature 414:37-42.

101. Aqvist, J., and V. Luzhkov. 2000. Ion permeation mechanism of the potassium channel. Nature 404:881-884.

102. Bernèche, S., and B. Roux. 2001. Energetics of ion conduction through the K+ channel. Nature 414:73-77.

103. Luzhkov, V., and J. Aqvist. 2001. K(+)/Na(+) selectivity of the KcsA potassium channel from microscopic free energy perturbation calculations. Biochim Biophys Acta 1548:194-202.

104. Noskov, S., S. Bernèche, and B. Roux. 2004. Control of ion selectivity in potassium channels by electrostatic and dynamic properties of carbonyl ligands. Nature 431:830-834.

105. Bezanilla, F., and C. M. Armstrong. 1972. Negative conductance caused by entry of sodium and cesium ions into the potassium channels of squid axons. J.Gen.Physiol 60:588-608.

106. EISENMAN, G. 1962. Cation selective glass electrodes and their mode of operation. Biophys J 2:259-323.

107. Gouaux, E., and R. Mackinnon. 2005. Principles of selective ion transport in channels and pumps. Science 310:1461-1465.

108. Noskov, S., and B. Roux. 2006. Ion selectivity in potassium channels. Biophys Chem 124:279-291.

109. Noskov, S., and B. Roux. 2007. Importance of hydration and dynamics on the selectivity of the KcsA and NaK channels. J Gen Physiol 129:135-143.

110. Egwolf, B., and B. Roux. 2010. Ion Selectivity of the KcsA Channel: A Perspective from Multi-Ion Free-Energy Landscapes. J Mol Biol.

111. Thompson, A., I. Kim, T. Panosian, T. Iverson, T. Allen, and C. Nimigean. 2009. Mechanism of potassium-channel selectivity revealed by Na(+) and Li(+) binding sites within the KcsA pore. Nat Struct Mol Biol 16:1317-1324.

112. Grabe, M., D. Bichet, X. Qian, Y. Jan, and L. Jan. 2006. K+ channel selectivity depends on kinetic as well as thermodynamic factors. Proc Natl Acad Sci U S A 103:14361-14366.

113. Ludwig, A., X. Zong, M. Jeglitsch, F. Hofmann, and M. Biel. 1998. A family of hyperpolarization-activated mammalian cation channels. Nature 393:587-591.

114. Starkus, J. G., L. Kuschel, M. D. Rayner, and S. H. Heinemann. 1997. Ion conduction through C-type inactivated Shaker channels. J.Gen.Physiol 110:539-550.

115. Kiss, L., J. LoTurco, and S. J. Korn. 1999. Contribution of the selectivity filter to inactivation in potassium channels. Biophys.J. 76:253-263.

116. Wang, Z., J. Hesketh, and D. Fedida. 2000. A high-Na(+) conduction state during recovery from inactivation in the K(+) channel Kv1.5. Biophys J 79:2416-2433.

117. Wang, Z., N. Wong, Y. Cheng, S. Kehl, and D. Fedida. 2009. Control of voltage-gated K+ channel permeability to NMDG+ by a residue at the outer pore. J Gen Physiol 133:361-374.

118. Dibb, K. M., T. Rose, S. Y. Makary, T. W. Claydon, D. Enkvetchakul, R. Leach, C. G. Nichols, and M. R. Boyett. 2003. Molecular basis of ion selectivity, block, and rectification of the inward rectifier Kir3.1/Kir3.4 K(+) channel. J.Biol.Chem. 278:49537-49548.

119. Yang, J., M. Yu, Y. N. Jan, and L. Y. Jan. 1997. Stabilization of ion selectivity filter by pore loop ion pairs in an inwardly rectifying potassium channel. Proc Natl Acad Sci U S A 94:1568-1572.

120. Sackin, H., M. Nanazashvili, H. Li, L. Palmer, and D. Walters. 2010. A conserved arginine near the filter of Kir1.1 controls Rb/K selectivity. Channels (Austin) 4.

121. Yi, B., Y. Lin, Y. Jan, and L. Jan. 2001. Yeast screen for constitutively active mutant G protein-activated potassium channels. Neuron 29:657-667.

122. Bichet, D., Y. Lin, C. Ibarra, C. Huang, B. Yi, Y. Jan, and L. Jan. 2004. Evolving potassium channels by means of yeast selection reveals structural elements important for selectivity. Proc Natl Acad Sci U S A 101:4441-4446.

123. Bichet, D., M. Grabe, Y. Jan, and L. Jan. 2006. Electrostatic interactions in the channel cavity as an important determinant of potassium channel selectivity. Proc Natl Acad Sci U S A 103:14355-14360.

124. Bostick, D., and C. r. Brooks. 2007. Selectivity in K+ channels is due to topological control of the permeant ion's coordinated state. Proc Natl Acad Sci U S A 104:9260-9265.

125. Varma, S., and S. Rempe. 2007. Tuning ion coordination architectures to enable selective partitioning. Biophys J 93:1093-1099.

126. Bostick, D., K. Arora, and C. r. Brooks. 2009. K+/Na+ selectivity in toy cation binding site models is determined by the 'host'. Biophys J 96:3887-3896.

127. Shi, N., S. Ye, A. Alam, L. Chen, and Y. Jiang. 2006. Atomic structure of a Na+- and K+-conducting channel. Nature 440:570-574.

128. Roux, B. 2010. Exploring the ion selectivity properties of a large number of simplified binding site models. Biophys J 98:2877-2885.

129. Varma, S., D. Sabo, and S. Rempe. 2008. K+/Na+ selectivity in K channels and valinomycin: over-coordination versus cavity-size constraints. J Mol Biol 376:13-22.

130. Fowler, P., K. Tai, and M. Sansom. 2008. The selectivity of K+ ion channels: testing the hypotheses. Biophys J 95:5062-5072.

131. Almers, W., and C. Armstrong. 1980. Survival of K+ permeability and gating currents in squid axons perfused with K+-free media. J Gen Physiol 75:61-78.

132. Gomez-Lagunas, F. 1997. Shaker B K+ conductance in Na+ solutions lacking K+ ions: a remarkably stable non-conducting state produced by membrane depolarizations. J.Physiol 499 (Pt 1):3-15.

133. Melishchuk, A., A. Loboda, and C. M. Armstrong. 1998. Loss of shaker K channel conductance in 0 K+ solutions: role of the voltage sensor. Biophys.J. 75:1828-1835.

134. Khodakhah, K., A. Melishchuk, and C. M. Armstrong. 1997. Killing K channels with TEA+. Proc.Natl.Acad.Sci.U.S.A 94:13335-13338.

135. Loboda, A., A. Melishchuk, and C. Armstrong. 2001. Dilated and defunct K channels in the absence of K+. Biophys.J. 80:2704-2714.

136. Valiyaveetil, F. I., M. Leonetti, T. W. Muir, and R. MacKinnon. 2006. Ion selectivity in a semisynthetic K+ channel locked in the conductive conformation. Science 314:1004-1007.

137. Valiyaveetil, F., M. Sekedat, R. Mackinnon, and T. Muir. 2004. Glycine as a D-amino acid surrogate in the K(+)-selectivity filter. Proc Natl Acad Sci U S A 101:17045-17049.

138. Ye, S., Y. Li, and Y. Jiang. 2010. Novel insights into K(+) selectivity from high-resolution structures of an open K(+) channel pore. Nat Struct Mol Biol 17:1019-1023.

139. Heginbotham, L., E. Odessey, and C. Miller. 1997. Tetrameric stoichiometry of a prokaryotic K+ channel. Biochemistry 36:10335-10342.

140. Cortes, D., and E. Perozo. 1997. Structural dynamics of the Streptomyces lividans K+ channel (SKC1): oligomeric stoichiometry and stability. Biochemistry 36:10343-10352.

141. Krishnan, M. N., J. P. Bingham, S. H. Lee, P. Trombley, and E. Moczydlowski. 2005. Functional role and affinity of inorganic cations in stabilizing the tetrameric structure of the KcsA K+ channel. J.Gen.Physiol 126:271-283.

142. Irizarry, S. N., E. Kutluay, G. Drews, S. J. Hart, and L. Heginbotham. 2002. Opening the KcsA K+ channel: tryptophan scanning and complementation analysis lead to mutants with altered gating. Biochemistry 41:13653-13662.

143. Jiang, Y., and R. MacKinnon. 2000. The barium site in a potassium channel by x-ray crystallography. J Gen Physiol 115:269-272.

144. Wang, S., Y. Alimi, A. Tong, C. G. Nichols, and D. Enkvetchakul. 2008. Differential roles of blocking ions on KirBac1.1 tetramer stability. J.Biol.Chem.

145. Krishnan, M. N., P. Trombley, and E. G. Moczydlowski. 2008. Thermal stability of the K+ channel tetramer: cation interactions and the conserved threonine residue at the innermost site (S4) of the KcsA selectivity filter. Biochemistry 47:5354-5367.

146. Lu, T., A. Y. Ting, J. Mainland, L. Y. Jan, P. G. Schultz, and J. Yang. 2001. Probing ion permeation and gating in a K+ channel with backbone mutations in the selectivity filter. Nat.Neurosci. 4:239-246.

147. Yellen, G. 2001. Keeping K+ completely comfortable. Nat Struct Biol 8:1011-1013.

148. Suh, B. C., and B. Hille. 2008. PIP2 is a necessary cofactor for ion channel function: how and why? Annu Rev Biophys 37:175-195.

149. Suh, B., L. Horowitz, W. Hirdes, K. Mackie, and B. Hille. 2004. Regulation of KCNQ2/KCNQ3 current by G protein cycling: the kinetics of receptor-mediated signaling by Gq. J Gen Physiol 123:663-683.

150. Zhang, H., L. Craciun, T. Mirshahi, T. Rohács, C. Lopes, T. Jin, and D. Logothetis. 2003. PIP(2) activates KCNQ channels, and its hydrolysis underlies receptor-mediated inhibition of M currents. Neuron 37:963-975.

151. Sackmann, E. 1995. Biological Membranes. Architecture and Function. Elsevier Science B. V., Amsterdam.

152. Harwood, J. L. The Lipid Handbook. Chapman & Hall, London.

153. Dowhan, W., M. Bogdanov, and E. Mileykovskaya. 2008. Biochemistry of Lipids, Lipoproteins and Membranes. Elsevier, Amsterdam.

154. Tanford, C. 1980. The Hydrophobic Effect: Formation of Micelles and Biological Membranes. Wiley, New York.

155. Ohtsuka, T., M. Nishijima, and Y. Akamatsu. 1993. A somatic cell mutant defective in phosphatidylglycerophosphate synthase, with impaired phosphatidylglycerol and cardiolipin biosynthesis. J Biol Chem 268:22908-22913.

156. Vance, J., and R. Steenbergen. 2005. Metabolism and functions of phosphatidylserine. Prog Lipid Res 44:207-234.

157. Raetz, C., and W. Dowhan. 1990. Biosynthesis and function of phospholipids in Escherichia coli. J Biol Chem 265:1235-1238.

158. Awasthi, Y., T. Chuang, T. Keenan, and F. Crane. 1971. Tightly bound cardiolipin in cytochrome oxidase. Biochim Biophys Acta 226:42-52.

159. Robinson, N., F. Strey, and L. Talbert. 1980. Investigation of the essential boundary layer phospholipids of cytochrome c oxidase using Triton X-100 delipidation. Biochemistry 19:3656-3661.

160. Zinser, E., C. Sperka-Gottlieb, E. Fasch, S. Kohlwein, F. Paltauf, and G. Daum. 1991. Phospholipid synthesis and lipid composition of subcellular membranes in the unicellular eukaryote Saccharomyces cerevisiae. J Bacteriol 173:2026-2034.

161. Xu, Y., Y. Ramu, and Z. Lu. 2008. Removal of phospho-head groups of membrane lipids immobilizes voltage sensors of K+ channels. Nature 451:826-829.

162. Colbeau, A., J. Nachbaur, and P. Vignais. 1971. Enzymic characterization and lipid composition of rat liver subcellular membranes. Biochim Biophys Acta 249:462-492.

163. Behnia, R., and S. Munro. 2005. Organelle identity and the signposts for membrane traffic. Nature 438:597-604.

164. Nasuhoglu, C., S. Feng, J. Mao, M. Yamamoto, H. Yin, S. Earnest, B. Barylko, J. Albanesi, and D. Hilgemann. 2002. Nonradioactive analysis of

phosphatidylinositides and other anionic phospholipids by anion-exchange high-performance liquid chromatography with suppressed conductivity detection. Anal Biochem 301:243-254.

165. Ikeda, M., A. Kihara, and Y. Igarashi. 2006. Lipid asymmetry of the eukaryotic plasma membrane: functions and related enzymes. Biol Pharm Bull 29:1542-1546.

166. Verkleij, A., R. Zwaal, B. Roelofsen, P. Comfurius, D. Kastelijn, and L. van Deenen. 1973. The asymmetric distribution of phospholipids in the human red cell membrane. A combined study using phospholipases and freeze-etch electron microscopy. Biochim Biophys Acta 323:178-193.

167. Rothman, J., and E. Kennedy. 1977. Asymmetrical distribution of phospholipids in the membrane of Bacillus megaterium. J Mol Biol 110:603-618.

168. McLaughlin, S., and D. Murray. 2005. Plasma membrane phosphoinositide organization by protein electrostatics. Nature 438:605-611.

169. Nishizuka, Y. 1986. Studies and perspectives of protein kinase C. Science 233:305-312.

170. Ghosh, S., J. Strum, V. Sciorra, L. Daniel, and R. Bell. 1996. Raf-1 kinase possesses distinct binding domains for phosphatidylserine and phosphatidic acid. Phosphatidic acid regulates the translocation of Raf-1 in 12-O-tetradecanoylphorbol-13-acetate-stimulated Madin-Darby canine kidney cells. J Biol Chem 271:8472-8480.

171. Bevers, E., P. Comfurius, and R. Zwaal. 1983. Changes in membrane phospholipid distribution during platelet activation. Biochim Biophys Acta 736:57-66.

172. Fadok, V., D. Voelker, P. Campbell, J. Cohen, D. Bratton, and P. Henson. 1992. Exposure of phosphatidylserine on the surface of apoptotic lymphocytes triggers specific recognition and removal by macrophages. J Immunol 148:2207-2216.

173. Fadok, V., D. Bratton, D. Rose, A. Pearson, R. Ezekewitz, and P. Henson. 2000. A receptor for phosphatidylserine-specific clearance of apoptotic cells. Nature 405:85-90.

174. Simons, K., and E. Ikonen. 1997. Functional rafts in cell membranes. Nature 387:569-572.

175. van Meer, G., and K. Simons. 1986. The function of tight junctions in maintaining differences in lipid composition between the apical and the basolateral cell surface domains of MDCK cells. EMBO J 5:1455-1464.

176. Schuck, S., and K. Simons. 2004. Polarized sorting in epithelial cells: raft clustering and the biogenesis of the apical membrane. J Cell Sci 117:5955-5964.

177. Hilgemann, D. W. 2007. Local PIP(2) signals: when, where, and how? Pflugers Arch 455:55-67.

178. van Meer, G. 2005. Cellular lipidomics. EMBO J 24:3159-3165.

179. Brown, H. A., and R. C. Murphy. 2009. Working towards an exegesis for lipids in biology. Nat Chem Biol 5:602-606.

180. Fan, Z., and J. C. Makielski. 1997. Anionic phospholipids activate ATP-sensitive potassium channels. Journal of Biological Chemistry 272:5388-5395.

181. Gribble, F., P. Proks, B. Corkey, and F. Ashcroft. 1998. Mechanism of cloned ATP-sensitive potassium channel activation by oleoyl-CoA. J Biol Chem 273:26383-26387.

182. Shyng, S. L., and C. G. Nichols. 1998. Membrane phospholipid control of nucleotide sensitivity of KATP channels. Science 282:1138-1141.

183. Leung, Y. M., W. Z. Zeng, H. H. Liou, C. R. Solaro, and C. L. Huang. 2000. Phosphatidylinositol 4,5-bisphosphate and intracellular pH regulate the ROMK1 potassium channel via separate but interrelated mechanisms. J.Biol.Chem. 275:10182-10189.

184. Xie, L. H., S. A. John, B. Ribalet, and J. N. Weiss. 2008. Phosphatidylinositol-4,5-bisphosphate (PIP2) regulation of strong inward rectifier Kir2.1 channels: multilevel positive cooperativity. J.Physiol 586:1833-1848.

185. Rohacs, T., J. Chen, G. D. Prestwich, and D. E. Logothetis. 1999. Distinct specificities of inwardly rectifying K(+) channels for phosphoinositides. J.Biol.Chem. 274:36065-36072.

186. Huang, C. L., S. Y. Feng, and D. W. Hilgemann. 1998. Direct activation of inward rectifier potassium channels by PIP2 and its stabilization by G beta gamma. Nature 391:803-806.

187. Rohacs, T., C. Lopes, T. Mirshahi, T. Jin, H. Zhang, and D. E. Logothetis. 2002. Assaying phosphatidylinositol bisphosphate regulation of potassium channels. Methods Enzymol. 345:71-92.

188. Rohács, T., C. Lopes, T. Jin, P. Ramdya, Z. Molnár, and D. Logothetis. 2003. Specificity of activation by phosphoinositides determines lipid regulation of Kir channels. Proc Natl Acad Sci U S A 100:745-750.

189. Rapedius, M., M. Soom, E. Shumilina, D. Schulze, R. Schonherr, C. Kirsch, F. Lang, S. J. Tucker, and T. Baukrowitz. 2005. Long chain CoA esters as competitive antagonists of phosphatidylinositol 4,5-bisphosphate activation in Kir channels. Journal of Biological Chemistry 280:30760-30767.

190. Schulze, D., M. Rapedius, T. Krauter, and T. Baukrowitz. 2003. Long-chain acyl-CoA esters and phosphatidylinositol phosphates modulate ATP inhibition of KATP channels by the same mechanism. J Physiol 552:357-367.

191. Manning Fox, J. E., C. G. Nichols, and P. E. Light. 2004. Activation of adenosine triphosphate-sensitive potassium channels by acyl coenzyme A esters involves multiple phosphatidylinositol 4,5-bisphosphate-interacting residues. Mol.Endocrinol. 18:679-686.

192. Deeney, J., M. Prentki, and B. Corkey. 2000. Metabolic control of beta-cell function. Semin Cell Dev Biol 11:267-275.

193. Larsson, O., J. Deeney, R. Bränström, P. Berggren, and B. Corkey. 1996. Activation of the ATP-sensitive K+ channel by long chain acyl-CoA. A role in

modulation of pancreatic beta-cell glucose sensitivity. J Biol Chem 271:10623-10626.

194. D'Avanzo, N., W. W. L. Cheng, S. Wang, D. Enkvetchakul, and C. G. Nichols. 2010. Lipids driving protein structure? Evolutionary adaptations in Kir channels. Channels 4:139-141.

195. Enkvetchakul, D., I. Jeliazkova, J. Bhattacharyya, and C. G. Nichols. 2007. Control of inward rectifier K channel activity by lipid tethering of cytoplasmic domains. J.Gen.Physiol 130:329-334.

196. Baukrowitz, T., U. Schulte, D. Oliver, S. Herlitze, T. Krauter, S. J. Tucker, J. P. Ruppersberg, and B. Fakler. 1998. PIP2 and PIP as determinants for ATP inhibition of K-ATP channels. Science 282:1141-1144.

197. Shyng, S. L., C. A. Cukras, J. Harwood, and C. G. Nichols. 2000. Structural determinants of PIP(2) regulation of inward rectifier K(ATP) channels. J.Gen.Physiol 116:599-608.

198. Zhang, H. L., C. He, X. X. Yan, T. Mirshahi, and D. E. Logothetis. 1999. Activation of inwardly rectifying K+ channels by distinct PtdIns(4,5)P-2 interactions. Nature Cell Biology 1:183-188.

199. Lopes, C. M., H. Zhang, T. Rohacs, T. Jin, J. Yang, and D. E. Logothetis. 2002. Alterations in conserved Kir channel-PIP2 interactions underlie channelopathies. Neuron 34:933-944.

200. Soom, M., R. Schonherr, Y. Kubo, C. Kirsch, R. Klinger, and S. H. Heinemann. 2001. Multiple PIP2 binding sites in Kir-2.1 inwardly rectifying potassium channels. Febs Letters 490:49-53.

201. Cukras, C. A., I. Jeliazkova, and C. G. Nichols. 2002. Structural and functional determinants of conserved lipid interaction domains of inward rectifying Kir6.2 channels. J.Gen.Physiol 119:581-591.

202. Cukras, C. A., I. Jeliazkova, and C. G. Nichols. 2002. The role of NH2-terminal positive charges in the activity of inward rectifier KATP channels. J.Gen.Physiol 120:437-446.

203. Ashcroft, F. M. 2005. ATP-sensitive potassium channelopathies: focus on insulin secretion. J.Clin.Invest 115:2047-2058.

204. Enkvetchakul, D., G. Loussouarn, E. Makhina, S. L. Shyng, and C. G. Nichols. 2000. The kinetic and physical basis of K(ATP) channel gating: toward a unified molecular understanding. Biophys.J. 78:2334-2348.

205. Wang, C., K. Wang, W. Wang, Y. Cui, and Z. Fan. 2002. Compromised ATP binding as a mechanism of phosphoinositide modulation of ATP-sensitive K+ channels. FEBS Lett 532:177-182.

206. Sui, J., K. Chan, and D. Logothetis. 1996. Na+ activation of the muscarinic K+ channel by a G-protein-independent mechanism. J Gen Physiol 108:381-391.

207. Logothetis, D., Y. Kurachi, J. Galper, E. Neer, and D. Clapham. 1987. The beta gamma subunits of GTP-binding proteins activate the muscarinic K+ channel in heart. Nature 325:321-326.

208. Hilgemann, D. W., and R. Ball. 1996. Regulation of cardiac Na+,Ca2+ exchange and K-ATP potassium channels by PIP2. Science 273:956-959.

209. Sui, J., J. Petit-Jacques, and D. Logothetis. 1998. Activation of the atrial KACh channel by the betagamma subunits of G proteins or intracellular Na+ ions depends on the presence of phosphatidylinositol phosphates. Proc Natl Acad Sci U S A 95:1307-1312.

210. Loussouarn, G., L. J. Pike, F. M. Ashcroft, E. N. Makhina, and C. G. Nichols. 2001. Dynamic sensitivity of ATP-sensitive K(+) channels to ATP. J.Biol.Chem. 276:29098-29103.

211. Thierfelder, S., B. Doepner, C. Gebhardt, H. Hirche, and K. Benndorf. 1994. ATP-sensitive K+ channels in heart muscle cells first open and subsequently close at maintained anoxia. FEBS Lett 351:365-369.

212. Ho, I., and R. Murrell-Lagnado. 1999. Molecular mechanism for sodium-dependent activation of G protein-gated K+ channels. J Physiol 520 Pt 3:645-651.

213. Rosenhouse-Dantsker, A., J. Sui, Q. Zhao, R. Rusinova, A. Rodríguez-Menchaca, Z. Zhang, and D. Logothetis. 2008. A sodium-mediated structural switch that controls the sensitivity of Kir channels to PtdIns(4,5)P(2). Nat Chem Biol 4:624-631.

214. Logothetis, D., and H. Zhang. 1999. Gating of G protein-sensitive inwardly rectifying K+ channels through phosphatidylinositol 4,5-bisphosphate. J Physiol 520 Pt 3:630.

215. Enkvetchakul, D., and C. G. Nichols. 2003. Gating mechanism of KATP channels: function fits form. J.Gen.Physiol 122:471-480.

216. Ribalet, B., S. John, L. Xie, and J. Weiss. 2005. Regulation of the ATP-sensitive K channel Kir6.2 by ATP and PIP(2). J Mol Cell Cardiol 39:71-77.

217. MacGregor, G. G., K. Dong, C. G. Vanoye, L. Q. Tang, G. Giebisch, and S. C. Hebert. 2002. Nucleotides and phospholipids compete for binding to the C terminus of K-ATP channels. Proceedings of the National Academy of Sciences of the United States of America 99:2726-2731.

218. Proks, P., and F. Ashcroft. 2009. Modeling K(ATP) channel gating and its regulation. Prog Biophys Mol Biol 99:7-19.

219. Trapp, S., P. Proks, S. Tucker, and F. Ashcroft. 1998. Molecular analysis of ATP-sensitive K channel gating and implications for channel inhibition by ATP. J Gen Physiol 112:333-349.

220. Drain, P., L. Li, and J. Wang. 1998. KATP channel inhibition by ATP requires distinct functional domains of the cytoplasmic C terminus of the pore-forming subunit. Proc Natl Acad Sci U S A 95:13953-13958.

221. Koster, J. C., Q. Sha, S. Shyng, and C. G. Nichols. 1999. ATP inhibition of KATP channels: control of nucleotide sensitivity by the N-terminal domain of the Kir6.2 subunit. J.Physiol 515 (Pt 1):19-30.

222. Alekseev, A., M. Kennedy, B. Navarro, and A. Terzic. 1997. Burst kinetics of co-expressed Kir6.2/SUR1 clones: comparison of recombinant with native ATP-sensitive K+ channel behavior. J Membr Biol 159:161-168.

223. Coulter, K., F. Périer, C. Radeke, and C. Vandenberg. 1995. Identification and molecular localization of a pH-sensing domain for the inward rectifier potassium channel HIR. Neuron 15:1157-1168.

224. McNicholas, C., G. MacGregor, L. Islas, Y. Yang, S. Hebert, and G. Giebisch. 1998. pH-dependent modulation of the cloned renal K+ channel, ROMK. Am J Physiol 275:F972-981.

225. Rosenhouse-Dantsker, A., E. Leal-Pinto, D. Logothetis, and I. Levitan. 2010. Comparative analysis of cholesterol sensitivity of Kir channels: role of the CD loop. Channels (Austin) 4:63-66.

226. Heginbotham, L., L. Kolmakova-Partensky, and C. Miller. 1998. Functional reconstitution of a prokaryotic K+ channel. Journal of General Physiology 111:741-749.

227. Marius, P., M. Zagnoni, M. E. Sandison, J. M. East, H. Morgan, and A. G. Lee. 2008. Binding of anionic lipids to at least three nonannular sites on the potassium channel KcsA is required for channel opening. Biophys.J. 94:1689-1698.

228. Valiyaveetil, F. I., Y. F. Zhou, and R. Mackinnon. 2002. Lipids in the structure, folding, and function of the KcsA K+ channel. Biochemistry 41:10771-10777.

229. Lee, A. 2003. Lipid-protein interactions in biological membranes: a structural perspective. Biochim Biophys Acta 1612:1-40.

230. Williamson, I., S. Alvis, J. East, and A. Lee. 2003. The potassium channel KcsA and its interaction with the lipid bilayer. Cell Mol Life Sci 60:1581-1590.

231. Deol, S. S., C. Domene, P. J. Bond, and M. S. Sansom. 2006. Anionic phospholipid interactions with the potassium channel KcsA: simulation studies. Biophys J 90:822-830.

232. Demmers, J., A. van Dalen, B. de Kruijff, A. Heck, and J. Killian. 2003. Interaction of the K+ channel KcsA with membrane phospholipids as studied by ESI mass spectrometry. FEBS Lett 541:28-32.

233. Alvis, S., I. Williamson, J. East, and A. Lee. 2003. Interactions of anionic phospholipids and phosphatidylethanolamine with the potassium channel KcsA. Biophys J 85:3828-3838.

234. Marius, P., S. Alvis, J. East, and A. Lee. 2005. The interfacial lipid binding site on the potassium channel KcsA is specific for anionic phospholipids. Biophys J 89:4081-4089.

235. Williamson, I., S. Alvis, J. East, and A. Lee. 2002. Interactions of phospholipids with the potassium channel KcsA. Biophys J 83:2026-2038.

236. Lee, A. 2004. How lipids affect the activities of integral membrane proteins. Biochim Biophys Acta 1666:62-87.

237. LeMasurier, M., L. Heginbotham, and C. Miller. 2001. KcsA: it's a potassium channel. J Gen Physiol 118:303-314.

238. Thompson, A. N., I. Kim, T. D. Panosian, T. M. Iverson, T. W. Allen, and C. M. Nimigean. 2009. Mechanism of potassium channel selectivity revealed by Na+ and Li+ binding sites inside the KcsA pore. Nat Struct Mol Biol in press.

239. Woodhull, A. M. 1973. Ionic blockage of sodium channels in nerve. J Gen Physiol 61:687-708.

240. Nimigean, C. M., and C. Miller. 2002. Na+ block and permeation in a K+ channel of known structure. J Gen Physiol 120:323-335.

241. Otwinowski, Z., and W. Minor. 1997. Processing of X-ray Diffraction Data Collected in Oscillation Mode. Methods in Enzymology 276:307-326.

242. Collaborative Computational Project, N. 1994. The CCP4 Suite: Programs for protein crystallography. Acta Crystallographica Section D Biological Crystallography 50:760-763.

243. Emsley, P., and K. Cowtan. 2004. Coot: model-building tools for molecular graphics. Acta Crystallogr D Biol Crystallogr 60:2126-2132.

244. Murshudov, G. N., A. A. Vagin, and E. J. Dodson. 1997. Refinement of macromolecular structures by the maximum-likelihood method. Acta Crystallogr D Biol Crystallogr 53:240-255.

245. Painter, J., and E. A. Merritt. 2006. Optimal description of a protein structure in terms of multiple groups undergoing TLS motion. Acta Crystallogr D Biol Crystallogr 62:439-450.

246. Kuo, A., C. Domene, L. N. Johnson, D. A. Doyle, and C. Venien-Bryan. 2005. Two different conformational states of the KirBac3.1 potassium channel revealed by electron crystallography. Structure. 13:1463-1472.

247. Haider, S., S. Khalid, S. J. Tucker, F. M. Ashcroft, and M. S. Sansom. 2007. Molecular dynamics simulations of inwardly rectifying (Kir) potassium channels: a comparative study. Biochemistry 46:3643-3652.

248. Sun, S., J. H. Gan, J. J. Paynter, and S. J. Tucker. 2006. Cloning and functional characterization of a superfamily of microbial inwardly rectifying potassium channels. Physiol Genomics 26:1-7.

249. Chakrapani, S., J. F. Cordero-Morales, and E. Perozo. 2007. A Quantitative Description of KcsA Gating II: Single-Channel Currents. J.Gen.Physiol 130:479-496.

250. Cuello, L. G., J. G. Romero, D. M. Cortes, and E. Perozo. 1998. pH-dependent gating in the Streptomyces lividans K+ channel. Biochemistry 37:3229-3236.

251. Splitt, H., D. Meuser, I. Borovok, M. Betzler, and H. Schrempf. 2000. Pore mutations affecting tetrameric assembly and functioning of the potassium channel KcsA from Streptomyces lividans. FEBS Lett. 472:83-87.

252. Molina, M. L., F. N. Barrera, A. M. Fernandez, J. A. Poveda, M. L. Renart, J. A. Encinar, G. Riquelme, and J. M. Gonzalez-Ros. 2006. Clustering and coupled gating modulate the activity in KcsA, a potassium channel model. J.Biol.Chem. 281:18837-18848.

253. Mazzanti, M., R. Assandri, A. Ferroni, and D. DiFrancesco. 1996. Cytoskeletal control of rectification and expression of four substates in cardiac inward rectifier K+ channels. FASEB J 10:357-361.

254. Oishi, K., K. Omori, H. Ohyama, K. Shingu, and H. Matsuda. 1998. Neutralization of aspartate residues in the murine inwardly rectifying K+ channel IRK1 affects the substate behaviour in Mg2+ block. J Physiol 510 (Pt 3):675-683.

255. Cymes, G. D., Y. Ni, and C. Grosman. 2005. Probing ion-channel pores one proton at a time. Nature 438:975-980.

256. Cymes, G. D., and C. Grosman. 2008. Pore-opening mechanism of the nicotinic acetylcholine receptor evinced by proton transfer. Nat.Struct.Mol.Biol. 15:389-396.

257. Loussouarn, G., L. R. Phillips, R. Masia, T. Rose, and C. G. Nichols. 2001. Flexibility of the Kir6.2 inward rectifier K(+) channel pore. Proc.Natl.Acad.Sci.U.S.A 98:4227-4232.

258. Lu, T., L. Wu, J. Xiao, and J. Yang. 2001. Permeant ion-dependent changes in gating of Kir2.1 inward rectifier potassium channels. J.Gen.Physiol 118:509-522.

259. Heginbotham, L., M. LeMasurier, L. Kolmakova-Partensky, and C. Miller. 1999. Single streptomyces lividans K(+) channels: functional asymmetries and sidedness of proton activation. J.Gen.Physiol 114:551-560.

260. Domene, C., D. A. Doyle, and C. Venien-Bryan. 2005. Modeling of an ion channel in its open conformation. Biophys.J. 89:L01-L03.

261. Domene, C., S. Vemparala, S. Furini, K. Sharp, and M. L. Klein. 2008. The role of conformation in ion permeation in a K+ channel. J.Am.Chem.Soc. 130:3389-3398.

262. Vemparala, S., C. Domene, and M. L. Klein. 2008. Interaction of anesthetics with open and closed conformations of a potassium channel studied via molecular dynamics and normal mode analysis. Biophys.J. 94:4260-4269.

263. Ader, C., R. Schneider, S. Hornig, P. Velisetty, E. M. Wilson, A. Lange, K. Giller, I. Ohmert, M. F. Martin-Eauclaire, D. Trauner, S. Becker, O. Pongs, and M. Baldus. 2008. A structural link between inactivation and block of a K+ channel. Nat.Struct.Mol.Biol. 15:605-612.

264. Giorgetti, A., P. Carloni, P. Mistrik, and V. Torre. 2005. A homology model of the pore region of HCN channels. Biophys.J. 89:932-944.

265. Sackin, H., M. Nanazashvili, H. Li, L. Palmer, and D. Walters. 2009. An intersubunit salt bridge near the selectivity filter stabilizes the active state of Kir1.1. Biophys J 97:1058-1066.

266. Wang, Z., X. Zhang, and D. Fedida. 2000. Regulation of transient Na+ conductance by intra- and extracellular K+ in the human delayed rectifier K+ channel Kv1.5. J Physiol 523 Pt 3:575-591.

267. Berneche, S., and B. Roux. 2002. The ionization state and the conformation of Glu-71 in the KcsA K(+) channel. Biophys.J. 82:772-780.

268. Cordero-Morales, J. F., L. G. Cuello, Y. Zhao, V. Jogini, D. M. Cortes, B. Roux, and E. Perozo. 2006. Molecular determinants of gating at the potassium-channel selectivity filter. Nat Struct Mol Biol 13:311-318.

269. Cordero-Morales, J. F., V. Jogini, A. Lewis, V. Vasquez, D. M. Cortes, B. Roux, and E. Perozo. 2007. Molecular driving forces determining potassium channel slow inactivation. Nat.Struct.Mol.Biol. 14:1062-1069.

270. Cuello, L. G., V. Jogini, D. M. Cortes, and E. Perozo. 2010. Structural mechanism of C-type inactivation in K(+) channels. Nature 466:203-208.

271. Chakrapani, S., J. F. Cordero-Morales, and E. Perozo. 2007. A quantitative description of KcsA gating I: macroscopic currents. J Gen Physiol 130:465-478.

272. Chakrapani, S., J. F. Cordero-Morales, and E. Perozo. 2007. A quantitative description of KcsA gating II: single-channel currents. J Gen Physiol 130:479-496.

273. Thompson, A. N., D. J. Posson, P. V. Parsa, and C. M. Nimigean. 2008. Molecular mechanism of pH sensing in KcsA potassium channels. Proc Natl Acad Sci U S A 105:6900-6905.

274. Vales, E., and M. Raja. 2010. The "flipped" state in E71A-K+-channel KcsA exclusively alters the channel gating properties by tetraethylammonium and phosphatidylglycerol. J Membr Biol 234:1-11.

275. Rotem, D., A. Mason, and H. Bayley. 2010. Inactivation of the KcsA potassium channel explored with heterotetramers. J Gen Physiol 135:29-42.

276. Choi, H., and L. Heginbotham. 2004. Functional influence of the pore helix glutamate in the KcsA K+ channel. Biophys J 86:2137-2144.

277. Singh, D., A. Rosenhouse-Dantsker, C. Nichols, D. Enkvetchakul, and I. Levitan. 2009. Direct regulation of prokaryotic Kir channel by cholesterol. J Biol Chem 284:30727-30736.

278. Cuello, L., V. Jogini, D. Cortes, and E. Perozo. 2010. Structural mechanism of C-type inactivation in K(+) channels. Nature 466:203-208.

279. Lockless, S. W., M. Zhou, and R. MacKinnon. 2007. Structural and thermodynamic properties of selective ion binding in a K+ channel. PLoS Biol 5:e121.

280. Valiyaveetil, F. I., M. Leonetti, T. W. Muir, and R. Mackinnon. 2006. Ion selectivity in a semisynthetic K+ channel locked in the conductive conformation. Science 314:1004-1007.

281. López-Barneo, J., T. Hoshi, S. Heinemann, and R. Aldrich. 1993. Effects of external cations and mutations in the pore region on C-type inactivation of Shaker potassium channels. Receptors Channels 1:61-71.

282. Baukrowitz, T., and G. Yellen. 1995. Modulation of K+ current by frequency and external [K+]: a tale of two inactivation mechanisms. Neuron 15:951-960.

283. Domene, C., and S. Furini. 2009. Dynamics, energetics, and selectivity of the low-K+ KcsA channel structure. J Mol Biol 389:637-645.

284. Ma, H. P., S. Saxena, and D. G. Warnock. 2002. Anionic phospholipids regulate native and expressed epithelial sodium channel (ENaC). J Biol Chem 277:7641-7644.

285. Schmidt, D., Q. Jiang, and R. MacKinnon. 2006. Phospholipids and the origin of cationic gating charges in voltage sensors. Nature 444:775-779.

286. Suh, B., T. Inoue, T. Meyer, and B. Hille. 2006. Rapid chemically induced changes of PtdIns(4,5)P2 gate KCNQ ion channels. Science 314:1454-1457.

287. Long, S. B., X. Tao, E. B. Campbell, and R. MacKinnon. 2007. Atomic structure of a voltage-dependent K+ channel in a lipid membrane-like environment. Nature 450:376-U373.

288. D'Avanzo, N., W. Cheng, X. Xia, L. Dong, P. Savitsky, C. Nichols, and D. Doyle. 2010. Expression and purification of recombinant human inward rectifier K(+) (KCNJ) channels in Saccharomyces cerevisiae. Protein Expr Purif.

289. Cheng, W. W., D. Enkvetchakul, and C. G. Nichols. 2009. KirBac1.1: it's an inward rectifying potassium channel. J Gen Physiol 133:295-305.

290. Liu, G., C. Derst, G. Schlichthörl, S. Heinen, G. Seebohm, A. Brüggemann, W. Kummer, R. Veh, J. Daut, and R. Preisig-Müller. 2001. Comparison of cloned Kir2 channels with native inward rectifier K+ channels from guinea-pig cardiomyocytes. J Physiol 532:115-126.

291. Marius, P., M. Zagnoni, M. E. Sandison, J. M. East, H. Morgan, and A. G. Lee. 2008. Binding of anionic lipids to at least three nonannular sites on the potassium channel KcsA is required for channel opening. Biophysical Journal 94:1689-1698.

292. Saarikangas, J., H. Zhao, and P. Lappalainen. 2010. Regulation of the actin cytoskeleton-plasma membrane interplay by phosphoinositides. Physiol Rev 90:259-289.

293. Yamaji-Hasegawa, A., and M. Tsujimoto. 2006. Asymmetric distribution of phospholipids in biomembranes. Biol Pharm Bull 29:1547-1553.

294. Lopaschuk, G., and J. Russell. 1991. Myocardial function and energy substrate metabolism in the insulin-resistant JCR:LA corpulent rat. J Appl Physiol 71:1302-1308.

295. Han, X., D. Abendschein, J. Kelley, and R. Gross. 2000. Diabetes-induced changes in specific lipid molecular species in rat myocardium. Biochem J 352 Pt 1:79-89.

296. Han, X., J. Yang, K. Yang, Z. Zhao, D. Abendschein, and R. Gross. 2007. Alterations in myocardial cardiolipin content and composition occur at the very earliest stages of diabetes: a shotgun lipidomics study. Biochemistry 46:6417-6428.

297. Chi, Y., and R. Gupta. 1998. Alterations in heart and kidney membrane phospholipids in hypertension as observed by 31P nuclear magnetic resonance. Lipids 33:1023-1030.

298. Hamplová, B., V. Pelouch, O. Nováková, J. Skovránek, B. Hucín, and F. Novák. 2004. Phospholipid composition of myocardium in children with normoxemic and hypoxemic congenital heart diseases. Physiol Res 53:557-560.

299. Stokes, C., and J. Hawthorne. 1987. Reduced phosphoinositide concentrations in anterior temporal cortex of Alzheimer-diseased brains. J Neurochem 48:1018-1021.

300. Wells, K., A. Farooqui, L. Liss, and L. Horrocks. 1995. Neural membrane phospholipids in Alzheimer disease. Neurochem Res 20:1329-1333.

301. Han, X., D. Holtzman, and D. J. McKeel. 2001. Plasmalogen deficiency in early Alzheimer's disease subjects and in animal models: molecular characterization using electrospray ionization mass spectrometry. J Neurochem 77:1168-1180.

302. Hilgemann, D. 2004. Biochemistry. Oily barbarians breach ion channel gates. Science 304:223-224.

303. Suh, B., and B. Hille. 2005. Regulation of ion channels by phosphatidylinositol 4,5-bisphosphate. Curr Opin Neurobiol 15:370-378.

304. D'Avanzo, N., W. W. L. Cheng, S. Wang, D. Enkvetchakul, and C. G. Nichols. 2010. Lipids driving protein structure? Evolutionary adaptations in Kir channels. 4.

305. Bichet, D., F. Haass, and L. Jan. 2003. Merging functional studies with structures of inward-rectifier K(+) channels. Nat Rev Neurosci 4:957-967.

306. Zhang, Y., J. Robertson, D. Gray, and L. Palmer. 2004. Carboxy-terminal determinants of conductance in inward-rectifier K channels. J Gen Physiol 124:729-739.

307. Paynter, J., I. Andres-Enguix, P. Fowler, S. Tottey, W. Cheng, D. Enkvetchakul, V. Bavro, Y. Kusakabe, M. Sansom, N. Robinson, C. Nichols, and S. Tucker. 2010. Functional complementation and genetic deletion studies of KirBac channels: activatory mutations highlight gating-sensitive domains. J Biol Chem.

308. Lu, Z. 2004. Mechanism of rectification in inward-rectifier K+ channels. Annu.Rev.Physiol 66:103-129.

309. Chapman, M., M. Blanke, H. Krovetz, and A. VanDongen. 2006. Allosteric effects of external K+ ions mediated by the aspartate of the GYGD signature sequence in the Kv2.1 K+ channel. Pflugers Arch 451:776-792.

310. Chapman, M., H. Krovetz, and A. VanDongen. 2001. GYGD pore motifs in neighbouring potassium channel subunits interact to determine ion selectivity. J Physiol 530:21-33.

311. D'Avanzo, N., H. Cho, I. Tolokh, R. Pekhletski, C. Gray, S. Goldman, and P. Backx. 2005. Conduction through the inward rectifier potassium channel, Kir2.1, is increased by negatively charged extracellular residues. J Gen Physiol 125:493-503.

312. Shen, W., X. Tian, M. Day, S. Ulrich, T. Tkatch, N. Nathanson, and D. Surmeier. 2007. Cholinergic modulation of Kir2 channels selectively elevates dendritic excitability in striatopallidal neurons. Nat Neurosci 10:1458-1466.

APPENDIX

PUBLICATIONS

1. Kurata, H. T., W. W. L. Cheng, C. Arrabit, P. A. Slesinger, and C. G. Nichols. 2007. The role of the cytoplasmic pore in inward rectification of Kir2.1 channels. J Gen Physiol. 130:145-55.
2. Cheng, W. W. L., A. Tong, T. P. Flagg, and C. G. Nichols. 2008. Random assembly of SUR subunits in K(ATP) channel complexes. Channels (Austin). 2:34-8.
3. Cheng, W. W. L., D. Enkvetchakul, and C. G. Nichols. 2009. KirBac1.1: it's an inward rectifying potassium channel. J Gen Physiol. 133:295-305.
4. D'Avanzo, N., W. W. L. Cheng, X. Xia, L. Dong, P. Savitsky, C. G. Nichols, and D. A. Doyle. 2010. Expression and purification of recombinant human inward rectifier K+ (KCNJ) channels in Saccharomyces cerevisiae. Protein Expr Purif. 71:115-21.
5. D'Avanzo, N., W. W. L. Cheng, S. Wang, D. Enkvetchakul, and C. G. Nichols. 2010. Lipids driving protein structure? Evolutionary adaptations in Kir channels. Channels (Austin). 4:139-141.
6. Paynter, J. J., I. Andres-Enguix, P. W. Fowler, S. Tottey, W. W. L. Cheng, D. Enkvetchakul, V. N. Bavro, Y. Kusakabe, M. S. Sansom, N. J. Robinson, C. G. Nichols, and S. J. Tucker. 2010. Functional complementation and genetic deletion studies of KirBac channels: activatory mutations highlight gating-sensitive domains. J Biol Chem. 285(52): 40754-40761.

7. Cheng, W. W. L., N. D'Avanzo, D. A. Doyle, and C. G. Nichols. 2010. Direct and specific activation of human inward rectifier K+ channels by membrane phosphatidylinositol 4,5-bisphosphate. J Biol Chem. 285(48): 37129-37132.
8. Cheng, W. W. L., N. D'Avanzo, D. A. Doyle, and C. G. Nichols. 2010. Dual-mode phospholipid regulation human inward rectifying potassium channels. Biophys J. 100(3): 620-628.
9. Kurata H. T., W. W. L. Cheng, and C. G. Nichols. 2011. Polyamine block of inward rectifying potassium channels. Methods in Molecular Biology. 720:113-126.
10. Cheng, W. W. L., J. G. McCoy, A. N. Thompson, C. G. Nichols, and C. M. Nimigean. 2010. Mechanism for selectivity-inactivation coupling in KcsA potassium channels. Proceedings of the National Academy of Sciences. 108(13): 5272-5277.